Alma Mater Studiorum - Università di Bologna

DOTTORATO DI RICERCA IN

SCIENZE E TECNOLOGIE DELLA SALUTE

Ciclo 36

Settore Concorsuale: 09/G2 - BIOINGEGNERIA

Settore Scientifico Disciplinare: ING-INF/06 – BIOINGEGNERIA ELETTRONICA E INFORMATICA

TOWARD ELECTROCARDIOGRAM ACQUISITION VIA A NOVEL WEARABLE DEVICE AND ANALYSIS VIA ARTIFICIAL INTELLIGENCE

Presentata da: Luca Neri

Coordinatore Dottorato

Igor Diemberger

Supervisore

Claudio Borghi

Co-supervisore

Henry R. Halperin

Esame finale anno 2024

“Believe you can, and you’re halfway there.”

Theodore Roosevelt (26th U.S. President)

Abstract

This Ph.D. project was part of a collaboration between the University of Bologna, AccYouRate S.p.A., and Johns Hopkins University to develop new wearable devices, and in particular, a smart t-shirt, in combination with signal processing and artificial intelligence algorithms applied to the electrocardiogram (ECG).

The ECG is a simple, economical, standardized clinical test to assess heart functionality and disease. This "old" method is now attracting new interest due to the evolution of acquisition, processing, and data extraction techniques. Wearables and artificial intelligence are the actors in this field of research that combine the different expertise between medicine and engineering.

Much ongoing research is tackling new aspects of ECG-related technology and applications, such as wearables and artificial intelligence algorithms. More in detail, the combination of wearables and artificial intelligence shows the potential to enhance healthcare, extract novel information from patients, and reduce costs. The evolution of technology and new sensor applications generates many devices that can help improve disease diagnosis and patients' health. These devices allow the acquisition, processing, and transmission of patient's physiological signals and parameters (e.g., pulse rate, ECG signals, body position, body temperature, blood pressure) to hospitals or specialized centers to perform diagnostic monitoring and remote treatments. Moreover, the rise of artificial intelligence applications and their connection with large volumes of medical data shows the potential to augment the patient's data analysis by discovering new features and insights.

This Ph.D. thesis aims to enhance a novel "smart t-shirt" by developing new algorithms applied to the ECG for signal processing, disease detection, and prediction and testing its performance compared to gold standard devices to understand its potential and possible limitations.

Firstly, the project focuses on the review of current literature. The main findings highlight the preponderant use of 1 to 3 leads ECGs in combination with artificial intelligence and wearables for cardiovascular applications, even if sleep apnea and mental health have gained interest in recent

years, in addition to other minor applications. The most significant limitations are the relatively low use of wearables for research purposes due to the preference for publicly available databases and the lack of standardization in using performance measurements to compare research results.

The second part of the thesis describes the development of a novel algorithm for QRS complex detection, which is part of the waveforms that compose the ECG. Due to the importance of the QRS complex detection for ECG analysis and feature extraction, we modified the gold standard, the Pan-Tompkins algorithm, to obtain a more efficient and more accurate solution that can better serve wearable and mobile applications. We tested the novel algorithm on different publicly available datasets and confirmed the superiority of this tool.

The third part of the thesis is centered on an innovative artificial intelligence algorithm for predicting sudden cardiac arrest. Using a new dataset, a deep learning model was developed that could predict which patient would suffer a cardiac arrest. The promising results are valid with both 12 leads and single-lead ECG.

The fourth part of the thesis shows the results of a clinical trial to evaluate the signals collected with a smart t-shirt. The comparison with a gold standard Holter monitor revealed the features and limitations of the smart t-shirt to address future development and improvements.

In conclusion, the Ph.D. project highlighted the advantages and limitations of combining wearable devices with artificial intelligence when acquiring and analyzing the ECG. Future research will be dedicated to improving wearables ECG signal acquisition and artificial intelligence algorithms and collecting more specific and high-quality datasets.

Content

1. Introduction

1.1 The Electrocardiogram and the Heart

The electrocardiogram (ECG or EKG) is a fundamental tool in modern medicine and cardiology, allowing healthcare professionals to assess the electrical activity of the heart. This chapter describes cardiac electrophysiology as the basis of the ECG and explores the intricate relationship between this diagnostic tool and the heart's physiology.

1.1.1 Basic Cardiac Physiology

Before delving into the ECG, it is essential to comprehend the heart's structure and function [1,2]. The human heart is a muscular organ, roughly the size of a clenched fist, located in the chest cavity slightly to the left. The heart generates the pressure to propel blood through the body. This continuous flow of blood is vital for delivering oxygen and nutrients to various tissues and organs.

The heart is divided into four chambers (Figure 1.1): two atria (left and right) and two ventricles (left and right). These chambers work in a coordinated manner to maintain blood circulation. The atria receive blood returning from the body and lungs, while the ventricles pump blood to the body and lungs.

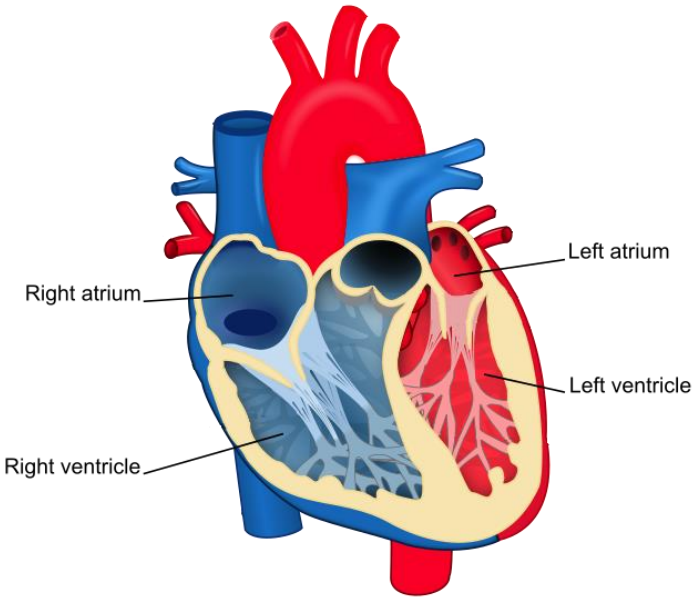

Figure 1.1. Heart diagram (modified version of the image from: ZooFari, CC, BY 3.0, via Wikimedia Commons)

To coordinate myocardial contraction, the heart features an intrinsic electrical system. This system initiates electrical impulses, causing the heart muscle to contract rhythmically.

1.1.2 Basic Cardiac Electrophysiology

The heartbeat is driven by a sequence of electrical events that occur in the heart. The primary components of this electrical system include:

Sinoatrial Node (SA Node): Often referred to as the heart's natural pacemaker, the SA node is a small cluster of specialized cells located in the right atrium. It generates electrical impulses at a regular rate, typically around 60-100 times per minute, initiating each heartbeat.

Atria Conduction: The electrical impulses generated by the SA node travel through the atria, causing them to contract and push blood into the ventricles.

Atrioventricular Node (AV Node): The AV node is between the atria and ventricles. It delays the electrical impulses to allow the ventricles time to fill with blood from the atria.

Ventricular Conduction: After passing through the AV node, the electrical impulses are conducted through specialized fibers in the ventricles, resulting in their contraction and the ejection of blood into the pulmonary artery and aorta.

Repolarization: Following each contraction, the heart muscle cells must reset, or repolarize, before they can contract again.

1.1.3 The Electrocardiogram

The ECG is a graphical representation of the heart's electrical activity over time, recorded from voltage changes on the body's surface. A typical ECG waveform consists of several distinct components (Figure 1.2):

P-Wave: Represents atrial depolarization, the electrical stimulation that triggers atrial contraction.

QRS Complex: Reflects ventricular depolarization, the electrical events associated with ventricular contraction.

T-Wave: Marks ventricular repolarization, the return of the ventricles to their resting state.

ST Segment: Represents the interval between ventricular depolarization and repolarization.

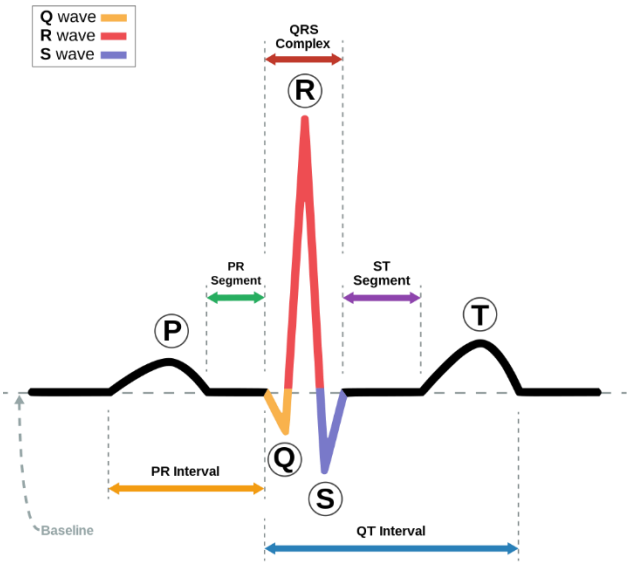

Figure 1.2. Characteristic waveform of the electrocardiogram during sinus rhythm (image from: Agateller -Anthony Atkielski-, CC, BY 3.0, via Wikimedia Commons)

1.1.3.1 The Standard 12 Leads

There are 12 standard leads in a typical ECG (Figure 1.3), which are divided into three groups:

- Bipolar Limb Leads (I, II, III): These leads measure electrical activity between two limb electrodes. Lead I - the right and left arms, Lead II - the right leg and left arm, and Lead III - the right leg and left leg.
- Augmented Unipolar Limb Leads (aVR, aVL, aVF): These leads record electrical activity between one limb electrode and a virtual central point generated from the leads I, II, III. aVR looks at the right arm, aVL at the left arm, and aVF at the left leg.
- Precordial (Chest) Leads (V1-V6): These leads are placed in the chest and record electrical activity in the horizontal plane, between different point in chest and the virtual central point generated from the leads I, II, III. V1 closest to the right side of the heart and V6 on the left side of the heart.

Each lead provides a unique view of the heart's electrical activity, which helps doctors diagnose various heart conditions.

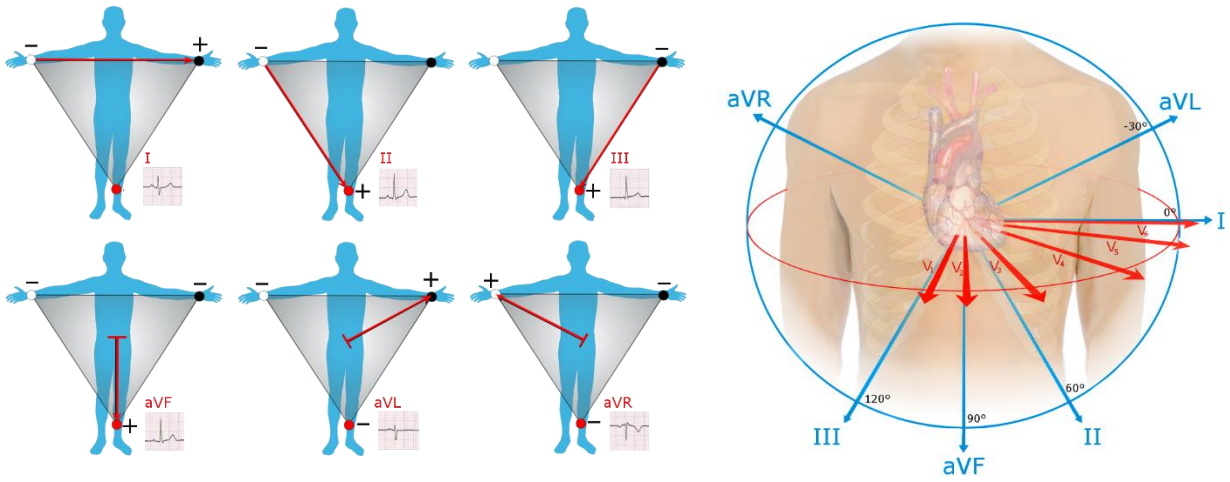

Figure 1.3. The 12 leads of a standard electrocardiogram (image from: Jul059, CC, BY 3.0, via Wikimedia Commons)

1.1.3.2 Interpreting the Electrocardiogram

Interpreting an ECG involves assessing the shapes, durations, and amplitudes of these waveforms and provides valuable insights into heart health and guides treatment decisions. Clinicians analyze various aspects, such as heart rate, rhythm regularity, and the presence of any abnormalities or deviations from the norm. In fact, ECG is invaluable for diagnosing a wide range of cardiac conditions, including arrhythmias, ischemia (insufficient blood flow to the heart muscle), myocardial infarctions (heart attacks), and conduction disorders.

1.1.3.3 Clinical Applications of the ECG

The ECG plays a crucial role in clinical medicine:

Diagnosis: primary tool for detecting heart conditions, often serving as a starting point for further evaluation.

Risk Assessment: helps to assess the risk of future cardiac events and guides preventive measures.

Monitoring: Continuous monitoring allows for the detection of intermittent arrhythmias.

Treatment Guidance: assists in guiding the selection and adjustment of medications and interventions.

Research: ECG data contributes to ongoing research in cardiology and electrophysiology.

1.2 Artificial Intelligence and Wearables: Empowering the Electrocardiogram

The synergy and integration of Artificial Intelligence (AI) and wearable technology into healthcare has revolutionized the way to monitor and understand the heart's electrical activity. It is transforming the field of cardiology, offering new insights into heart health and early detection of cardiac abnormalities.

1.2.1 Wearable Technology and Continuous Monitoring

Wearable devices, such as smart t-shirts, smartwatches and fitness trackers, have become increasingly popular [3–7]. They offer remote continuous monitoring of various health parameters, including heart rate and rhythm. These devices are equipped with sensors that collect data from the wearer's body, making it possible to track changes in heart activity throughout the day. They can alert users to potential heart rhythm irregularities, prompting them to seek medical attention if necessary. This immediate feedback empowers individuals to take proactive steps towards better heart health. Cardiologists can remotely access ECG data, track changes over time, and make adjustments to treatment plans as needed. This telehealth approach enhances patient care, reduces hospital visits, and improves overall health outcomes.

1.2.2 AI-Powered ECG Analysis

AI algorithms have elevated the capabilities of ECG analysis [8–10]. By processing vast amounts of ECG data, AI can detect subtle abnormalities that might be missed by human observers. This technology allows for:

Early Detection: identify irregular heart rhythms, such as atrial fibrillation, often before symptoms manifest. Early detection enables timely intervention and reduces the risk of complications.

Personalized Risk Assessment: assess an individual's risk of developing heart conditions based on their unique ECG patterns and other health data. This personalized risk assessment guides preventive strategies.

Predictive Analytics: predict heart events, such as arrhythmias or heart attacks, by analyzing historical ECG data and patient health records.

Drug Development: accelerates drug discovery and development by simulating the effects of pharmaceutical compounds on heart function, reducing the time and cost of bringing new treatments to market.
Rehabilitation: offer rehabilitation solutions, guiding patients through personalized exercise regimens and monitoring their progress.

1.2.3 Privacy and Ethical Considerations

While AI and wearables offer tremendous potential, they also raise important ethical and privacy concerns. Safeguarding sensitive health data and ensuring responsible AI use are paramount. Regulations and standards must evolve to protect patient privacy while harnessing the benefits of these technologies.

1.3 Aims and Outline of the Project

The aim of the project was to elevate the understanding of electrocardiogram enhancement through wearables and AI as a tool to improve diseases prediction and diagnosis. For that, the first objective was to investigate the current state of the art of this research field. Then, the project focused on developing new algorithms for ECG signal processing and ECG analysis through AI algorithm, and evaluation of monitoring capabilities of a novel wearable device.

The thesis starts with a literature review of the published knowledge about the use of the electrocardiogram in combination with wearables and AI for disease detection and prediction. The review created the ground base for this work, and it described the current limitations and future directions.

The work was divided into three research areas to reach the thesis objectives.: the development of an accurate and efficient QRS detection algorithm, the development of an AI model to predict the occurrence of cardiac arrest, and the clinical study to evaluate and validate the smart t-shirt with a gold standard device.

For the QRS detection algorithm:

• To develop and validate a reliable algorithm to detect the QRS complex and permit its use on wearable and mobile applications. The gold standard Pan-Tompkins algorithm was taken as reference of which the new algorithm is a modified version. (Chapter 3).

For the AI model to predict the occurrence of cardiac arrest:

• To develop and assess a deep learning model capabilities as a screening tool for the prediction of cardiac arrest by processing the information of ECG recorded before the event in combination with other patient's data (Chapter 4).

For the clinical study to evaluate and validate the smart t-shirt with a gold standard device:

• To validate the smart t-shirt developed in collaboration with AccYouRate. A clinical study was conducted to compare the signal quality of the smart t-shirt with a Holter monitor (Chapter 5).

Limitations and conclusions are wrapping up the research findings and future steps in the development of ECG-AI for wearable applications (Chapter 6, 7).

2. Electrocardiogram Monitoring Wearable Devices and Artificial-Intelligence Enabled Diagnostic Capabilities: A Review

from the manuscript:

Electrocardiogram Monitoring Wearable Devices and Artificial-Intelligence Enabled Diagnostic Capabilities: A Review

L. Neri, M. T. Oberdier, K.C.J. van Abeelen, L. Menghini, E. Tumarkin, H. Tripathi, S. Jaipalli, A. Orro, N. Paolocci, I. Gallelli, M. Dall'Olio, A. Beker, R.T. Carrick, C. Borghi, and H. R. Halperin

Published in: *Sensors 2023, 23(10), 4805; https://doi.org/10.3390/s23104805*

2.1Abstract

Worldwide, population aging and unhealthy lifestyles have increased the incidence of high-risk health conditions such as cardiovascular diseases, sleep apnea, and other conditions. Recently, to facilitate early identification and diagnosis, efforts have been made in the research and development of new wearable devices to make them smaller, more comfortable, more accurate, and increasingly compatible with artificial intelligence technologies. These efforts can pave the way to longer and continuous health monitoring of different biosignals, including the real-time detection of diseases, thus providing more timely and accurate predictions of health events that can drastically improve the healthcare management of patients. Most recent reviews focus on a specific category of disease, the use of artificial intelligence in 12-lead electrocardiograms, or on wearable technology. However, we present recent advances in the use of electrocardiogram signals acquired with wearable devices or from publicly available databases and the analysis of such signals with artificial intelligence methods to detect and predict diseases. As expected, most of the available research focused on heart diseases, sleep apnea, and other emerging areas, such as mental stress. From a methodological point of view, although traditional statistical methods and machine learning are still widely used, we observe an increasing use of more advanced deep learning methods, specifically architectures that can handle the complexity of biosignal data. These deep learning methods typically include convolutional and recurrent neural networks. Moreover, when proposing new artificial intelligence methods, we observe that the prevalent choice is to use publicly available databases rather than collecting new data.

2.2 Introduction

The electrocardiogram (ECG) is among the most commonly utilized clinical tests for patient monitoring and assessment because it is easy to acquire and provides extensive information about patients' cardiac health [3]. Instead, continuous, real-time, remote monitoring allows for more rigorous oversight of patients’ conditions, even compared to in-hospital observation. Wearable devices to address monitoring are now a prominent focus of industry [3–7,11], which in turn

provides strong motivation to apply artificial intelligence (AI) algorithms to ECG signals for automated disease detection and prediction [10,12–15].

Therefore, this review focuses on wearable medical devices for ECG acquisition followed by AI analysis (ECG-AI) to predict and detect specific diseases (Figure 2.1).

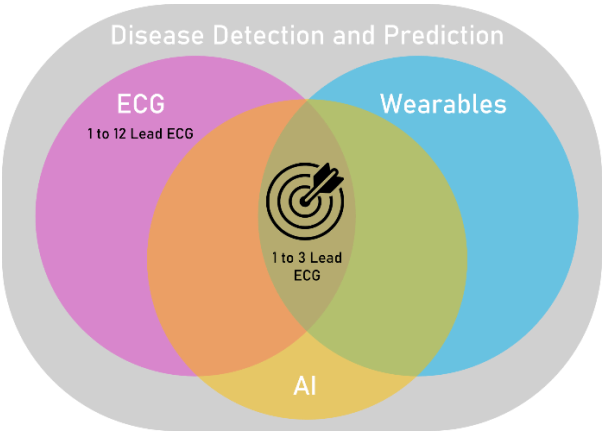

Figure 2.1. The synergy of ECG recording wearable devices and artificial intelligence algorithms enables disease detection and prediction.

We mainly focused on published results obtained with single-lead ECG systems, which are widely used in ambulatory monitoring but are not comfortable to wear for long periods. The use of single-lead ECG has the potential to give important diagnostic information on the user's health [3,7] but also has some limitations compared to the standard 12-lead ECG [11].

We examined publications on ECG signals and AI technology applied to wearable and mobile devices for predicting and detecting diseases. Most of the included papers are related to CVD, followed by, in order of number of published studies, the other three groups: 1) sleep apnea, 2) mental health and epilepsy, and 3) other applications such as hyperglycemia and hypoglycemia (Figure 2.2). While other diseases such as hyperkalemia, hypokalemia, and acute pulmonary embolism are addressed in literature related to ECG-AI, these studies were not included here because they generally use 12-lead ECGs and do not focus on wearable applications.

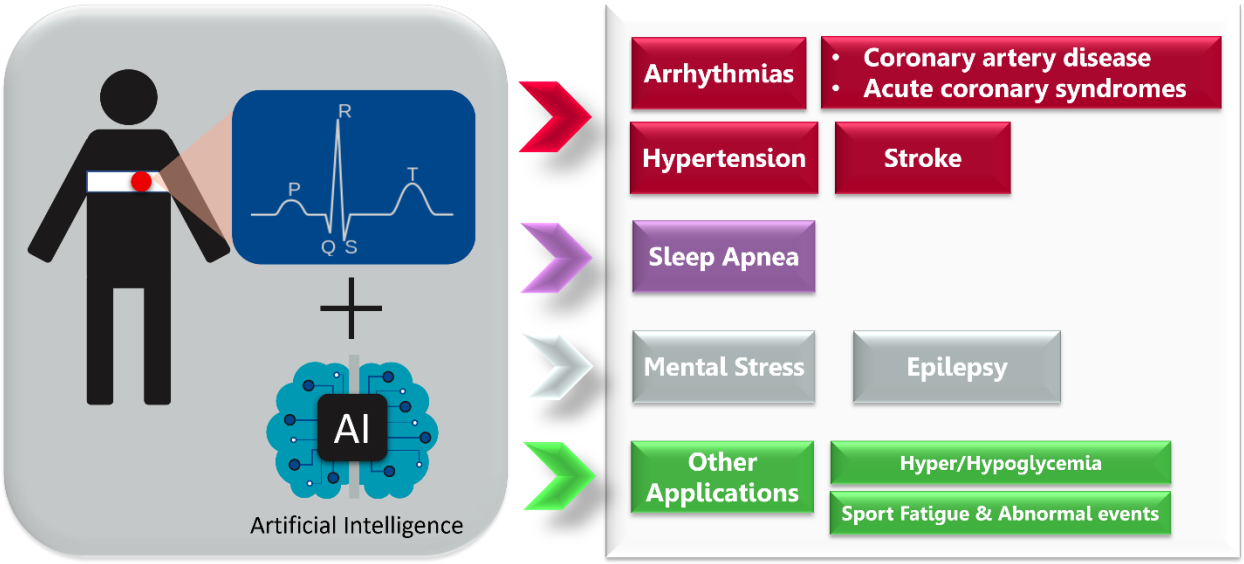

Figure 2.2. Main areas of electrocardiography- and artificial intelligence-based medical application reviewed in the present work.

2.3 Cardiovascular System

2.3.1 Diseases

ECG-based monitoring technologies with disease detection and prediction capabilities have been developed [16–22]. This section summarizes significant advancements related to two broad categories of cardiac conditions, namely arrhythmias and coronary artery disease.

2.3.1.1 Arrhythmias

Cardiac arrhythmia is an abnormal rhythm of the heartbeat [23]. The electrical pathway of a normal cardiac contraction has a characteristic electrical pattern on an ECG recording, comprised of a "P" wave (indicating atrial depolarization), followed by a "QRS" complex (indicating ventricular depolarization), and a "T" wave (indicating ventricular repolarization). A typical ECG is shown in Figure 2.3.

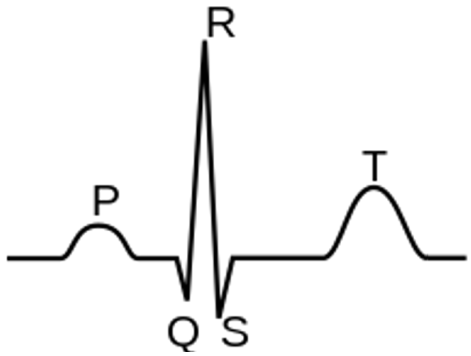

Figure 2.3. Components of a normal electrocardiogram include P- and T-waves and the QRS complex.

Perturbations in the ECG may indicate underlying pathophysiologic changes. Common conditions that can be discerned from ECG changes include various arrhythmias. The most common type of irregular arrhythmia is atrial fibrillation (AF), which is characterized by disorganized electrical impulses of the atrium. AF increases the risk of stroke by up to 17% annually in high-risk individuals [24]. In addition, AF with sustained ventricular rates greater than 110 beats per minute can lead to cardiomyopathy, heart failure (HF), and sudden cardiac death if not adequately treated [25]. The worldwide prevalence of AF was estimated at approximately 46 million individuals in 2016 [26], with up to one-third of these individuals being asymptomatic and thus unaware they have AF while also being at increased risk of stroke.

In addition to AF, there are other arrhythmias for which wearable ECG devices are amenable including premature atrial contraction, premature ventricular contraction (PVC), atrial flutter, atrioventricular reentrant tachycardia, atrioventricular nodal reentrant tachycardia, and first-, second-, or third-degree heart block. Several recent papers demonstrated wearable technology capable of identifying premature atrial contractions or PVCs with over 97% accuracy [21,22,27,28]. A class of malignant arrhythmias has a high risk of progression to cardiac arrest or even death [29]. Examples of malignant rhythms include ventricular tachycardia and ventricular fibrillation.

2.3.1.2 Coronary Artery Disease

Coronary artery disease is the insidious buildup of cholesterol plaques within the walls of the arteries of the heart, eventually leading to narrowing of the blood vessels [30]. When the narrowing of blood vessels surpasses a critical threshold (often described as a narrowing of greater than 70%

of the inner lumen of the artery), symptoms such as exertional chest pain (angina), exertional shortness of breath, and decreased exercise tolerance can occur. Coronary artery disease accounts for the vast majority of cardiac-related deaths [31]. A diagnosis of coronary heart disease generally requires a history and physical exam, a stress test, and observation of ECG changes suggestive of cardiac ischemia.

Various ECG changes are associated with acute and chronic ischemia. For instance, the presence of Q waves in any lead other than the right-sided leads (i.e., aVR and V1, occasionally in III) is often pathognomonic for prior infarction and non-viable myocardium [32]. On the other hand, chronically inverted T waves and ST depressions are generally described as non-specific ECG patterns and are difficult to interpret on their own, requiring additional context. However, in the correct clinical setting, these changes can be dynamic where they appear while the patient has active symptoms and normalize when they resolve. Such dynamic changes indicate significant coronary artery disease that needs to be aggressively investigated because the sudden development of ST-segment elevation associated with symptoms suggests an evolving coronary artery occlusion and subsequent myocardial impairment. Such patients need to be examined then treated immediately. Future work to develop ECG-AI wearables for real-time detection of acute ischemia will likely improve outcomes.

2.3.2 Wearables

ECG-AI has been combined with wearable devices to investigate various cardiac pathologies, including AF, stroke, cardiac arrest, and heart failure. In fact, arrhythmia monitoring is among the most popular applications of wearable devices in medicine. However, wearable devices are limited in their ability to detect arrhythmias other than AF [11,33], particularly ventricular tachycardia or ventricular fibrillation, which is why wearable technologies capable of accurately detecting either ventricular tachycardia or ventricular fibrillation were limited in the literature.

Overall, there are a limited number of studies involving wearables. Some studies use commercially available wearables to explore the implementation of ECG-AI. For example, devices such as the Amazfit Band 1S (PPG and single-lead ECG) [34], the HealthyPiV3 biosensors [35], or Polar H7 HR monitor [36] have been utilized. A few research groups have even built their own wearable ECG recording prototypes [37–39].

The Food and Drug Administration (FDA) recently approved a single-lead ECG smartwatch proven to detect AF in the general population [40]. Another device developed for AF monitoring and detection includes a single-lead wireless ECG patch worn over the chest, which provides real-time ECG monitoring using cloud-based data analysis and data sharing with medical providers [17]. Similarly, a custom wrist-based wearable ECG recorder was compared to the standard 12-lead configuration via a prospective, registration-only, single-center study for detection of AF [41]. Although a small dataset based on a relatively low number of patients was used, a sensitivity and specificity of 99.4% and 99.8%, respectively, were reported. The wrist-based device's convenience and ease of use was highlighted as an attractive modality for arrhythmia detection in the general population. Lastly, a single-lead ECG chest belt that transmits data to a cloud service for analysis was described, and a sensitivity and specificity of 100% and 95.4%, respectively, were reported [42]. The study included a user experience questionnaire, showing that 77% of participants preferred the chest belt to a standard 3-lead Holter monitor. Additional studies detecting AF have been performed using commercially-available heart rate monitors and ECG systems [34–36,43–45].

2.3.3 Algorithms

2.3.3.1 Arrhythmia

Due to their ubiquitous availability, most ECG-AI research has been performed using public databases such as the PhysioNet [46] MIT-BIH Arrhythmia database [47,48] while only a few research groups have independently acquired data from patients. Curated and publicly available datasets include physician annotations that provide reference for ECG-AI algorithm training (Table 2.1).

Machine learning (ML) and deep learning (DL) have both been extensively applied to ECG data to detect arrhythmias. Despite being relatively less performing, ML is utilized for arrhythmia detection due to some of the limitations of DL including resource-intensive hyper-parameters to find the optimal network configuration and the challenges in understanding the rules underlying trained prediction models [49]. However, DL has shown modest improvements over ML for arrhythmia detection. The varying sample resolutions could pose a challenge for these techniques, but it was shown that it is possible to accurately detect arrythmias using down sampled ECG data [50].

ML approaches often include the use of decision tree ensembles such as Random Forest [17,51] or support vector machines (SVMs) [44,52] for arrhythmia classification. Multi-stage and multi-level classification systems derive local features of atrial and ventricular activity through a combination of SVMs and decision trees and global features from the raw ECG recording, ultimately leading to classification through linear SVMs. Further, a rotated linear-kernel SVM has been proposed in which two SVM classifiers are trained, one on the global dataset and the other on a patient-dependent dataset obtaining two different discriminant hyperplanes. The final hyperplane, obtained by rotating the first hyperplane by a specific amount towards the second hyperplane, resulted in an improved sensitivity [53]. Similarly, this ML method has been used with a classifier of de-correlated Lorenz plots of inter-beat intervals [36], and with another classifier built on features extracted through pre-processing methods from density Poincaré plots that represented the ECG segments [27]. Alternatively, the use of SVMs through a semi-supervised learning method was demonstrated [54], while the hybrid framework effectively combined the advantages of ensemble learning and evolutionary computation to maximize arrhythmia classification accuracy [55].

With regard to DL approaches, convolutional neural network (CNN) architecture was applied to arrhythmia [56–58] and AF classifications [28,59]. Other architectures of interest for AF classification include a deep densely connected neural network based on 12-lead ECG [19], a feedforward neural network based on features encompassing R-R intervals [60] and another based on the Lightweight Fusing Transformer [21]. Hybrid constructions have also been presented, frequently involving an architecture based on a CNN and Long Short-Term Memory (LSTM) [61–64], as well as an extension to SVM with predictions from a CNN [45]. With a similar premise to the rotated linear-kernel SVM [53], a study has proposed a Generic CNN suitable for all individuals, and a Tuned Dedicated CNN as obtained by finetuning the previous model with respect to a specific individual [65]. Another approach of interest is multi-scale (MS) CNNs to improve feature extraction and classification from ECG data [66]. Additionally, a global hybrid multi-scale convolutional neural network (Acc 99.84%) was proposed as an advanced alternative to other MS-based approaches through their hybrid multi-scale convolution module [67].

Previous research has also designed lightweight DL models using cloud-based applications to efficiently classify ECG data. These approaches utilize fused Recurrent Neural Networks (RNN) layers instead of standard RNN layers [43]. The application of compression [48,68] and conversion

techniques (Acc 99.60%) [69], and model-hardware co-optimization [70] to reduce the model's size in terms of computational parameters, resulted in lower memory consumption and inference time. Other techniques to accelerate arrhythmia detection include real-time data compression, signal processing, and data transmission [71–73]. Alternatively, ECG data may be compressed to enable real-time AF classification [74,75].

In addition to directly processing ECG data, some studies focused on its two-dimensional representation, which can be used for feature extraction and/or classification. Examples of these representations include spectrograms [35] and iris spectrograms [76]. Alternatively, the ECG signal may be transformed into an electrocardiomatrix, which is a two-dimensional representation that includes the rhythm and shape of the QRS complex [77]. A beat-interval-texture CNN was then used to process the electrocardiomatrix. In this architecture, there are four different layers: the first two layers perform low-level feature extraction, and the two subsequent layers perform high-level feature extraction using three types of convolution filters (beat, interval, and texture). Next, a feature attention layer weighs the identified features concerning the arrhythmia classes and uses such weighted features for classification.

Deep metric learning for PVC detection has also been demonstrated [22]. Such learning methods combine the mechanisms of metric learning for effective feature extraction in which the features are processed with K-Nearest Neighbors for binary classification. In comparing ML and DL, the former may use the ECG to define summary features that provide physiologic insight, whereas the latter automatically extracts discriminating information from complete waveforms [78]. ML and DL may complement one another, as demonstrated by the multiview fusion classification model in which both summary and deep features from ECG signals were fused [61]. However, DL may independently offer some physiologic information via gradient-weighted class activation mapping, which can highlight the relative contributions of temporal regions of the ECG signal that most contribute to the AI-obtained classification [77].

Table 2.1. Summary of ECG-based AI algorithms applied to arrhythmias.

Authors (Year)	Specific Application	ECG System (Sampling Frequency)	AI Algorithm/Method	Database/Dataset	Performance (%)				
					Acc	Sen	Spe	AUC	F1
Jeon et al. (2020) [43]	General arrhythmias	**2-lead ECG patch [Samsung S-Patch 2] (256 Hz)**	Recurrent Neural Networks	MIT-BIH Arrhythmia Wearable device: S-Patch 2	99.80	-	-	-	-
Plawiak et al. (2020) [55]	General arrhythmias	-	Deep Genetic Ensemble of Classifiers	MIT-BIH Arrhythmia	99.37	94.62	99.66	-	-
Panganiban et al. (2021) [35]	General arrhythmias	**2-lead ECG [HealthyPiV3 biosensors] (n.s.)**	CNN	MIT-BIH Atrial Fibrillation, PAF Prediction Challenge, PTB Diagnostic ECG, Challenge 2015 Training Set, Fantasia, and PAF Prediction Challenge. ECG signals collected for this study	98.73	96.83	99.21	-	96.83
Alqudah et al. (2021) [76]	General arrhythmias	-	CNN	IEEE DataPort MIT-BIH Arrhythmia	99.13	99.31	99.81	-	-
Yildirim et al. (2018) [56]	General arrhythmias	-	CNN	MIT-BIH Arrhythmia	95.20	93.52	99.61	-	92.45
Bazi et al. (2020) [44]	General arrhythmias	**Wireless 3-lead ECG sensor [Shimmer Sensing (100, 200 Hz)**	SVM	12-lead Tech-Patient CARDIO ECG simulator Wearable device: Shimmer Sensing MIT-BIH Arrhythmia	95.10	95.80	-	-	-
Lee et al. (2022) [48]	General arrhythmias	-	CNN	ECG from patients at the Korea University Anam Hospital in Seoul, Korea	97.90	98.30	97.60	99.70	97.70
Itzhak et al. (2022) [50]	General arrhythmias	-	Random Forest	Annotated Holter ECG database acquired at the University of Virginia Heart Station	93.30	91.30	81.30	95.30	90.60
Li et al. (2018) [65]	General arrhythmias	-	Generic CNN and Tuned Dedicated CNN	MIT-BIH Arrhythmia	96.89	-	-	-	-
Ran et al. (2022) [70]	General arrhythmias	12-lead ECG prototype (500Hz)	Deep CNN	12-lead ECG recordings from three centers of Tongji Hospital	-	89.10	99.70	94.40	91.30
Ribeiro et al. (2022) [69]	General arrhythmias	-	CNN	MIT-BIH Arrhythmia	99.60	98.50	99.80	-	98.80
Hua et al. (2018) [54]	General arrhythmias	-	SVM	MIT-BIH Arrhythmia	98.58	97.70	99.62	-	-
Karthiga et al. (2021) [57]	General arrhythmias	-	CNN	MIT-BIH Arrhythmia	91.92	90.21	95.19	-	90.11
Zhang et al. (2022) [58]	General arrhythmias	-	CNN	MIT-BIH Arrhythmia	98.74	98.11	99.05	-	-
Lee et al. (2021) [77]	General arrhythmias	-	Beat-Interval-Texture-CNN	2017 PhysioNet/Computing in Cardiology Challenge	-	80.73	-	-	81.75

Smisek et al. (2018) [52]	General arrhythmias	-	SVMs-Decision Tree	2017 PhysioNet/Computing in Cardiology Challenge	-	-	-	-	81.00
Shin et al. (2022) [62]	General arrhythmias	-	CNN-Bidirectional Long Short-Term Memory	MIT-BIH Arrhythmia	91.70	92.00	91.00	99.40	92.00
Alqudah et al. (2021) [79]	General arrhythmias	-	CNN	MIT-BIH Arrhythmia	93.80	95.20	97.40	-	93.60
Huang, et al. (2021) [61]	General arrhythmias	-	CNN-LSTM	MIT-BIH Arrhythmia	98.93	96.46	99.33	-	-
Tang et al. (2019) [53]	General arrhythmias	-	SVM	MIT-BIH Arrhythmia	98.90	92.80	99.40	-	92.00
Sakib et al. (2021) [68]	General arrhythmias	-	Deep Learning-based Lightweight Arrhythmia Classification (CNN)	MIT-BIH Supraventricular Arrhythmia MIT-BIH Arrhythmia St Petersburg INCART 12-lead Arrhythmia Sudden Cardiac Death Holter	96.67	-	-	97.96	-
Shao et al. (2020) [17]	AF	**Custom 1-lead ECG patch (250Hz)**	Decision Tree Ensemble	2017 PhysioNet/Computing in Cardiology Challenge MIT-BIH Atrial Fibrillation Simulated ECG signals from generator FLUKE MPS450	99.62	99.61	99.64	-	92.00
Chen et al. (2020) [34]	AF	**PPG & 1-lead ECG [Amazfit Health Band 1S] (250Hz)**	CNN	PPG and single-channel ECG data	94.76	87.33	99.20	-	-
Cai et al. (2020) [19]	AF	12-lead ECG (500 Hz)	Deep Densely connected Neural Network	12-lead ECG 10s recordings collected from multiple hospitals and wearable ECG devices (3 different data sources)	99.35	99.19	99.44	-	-
Cheng et al. (2020) [74]	AF	-	Deep Learning Neural Networks	MIT-BIH Atrial Fibrillation	97.52	97.59	97.40	-	98.02
Fan et al. (2018) [66]	AF	-	Multi-Scale CNN	2017 PhysioNet/Computing in Cardiology Challenge	98.13	93.77	98.77	-	-
Ramesh et al. (2021) [59]	AF	-	CNN	Train: MIT-BIH Normal Sinus Rhythm, MIT-BIH Atrial Fibrillation, MIT-BIH Arrhythmia Test: UMass PPG, acquired from wrist-worn wearable devices	95.50	94.50	96.00	95.30	93.40
Ma et al. (2020) [45]	AF	**SmartVest system (400Hz)**	SVM extended with CNN predictions	Train: MIT-BIH Atrial Fibrillation Test: PhysioNet/Computing in Cardiology Challenge 2017, China Physiological Signal Challenge (CPSC) 2018, 24-h ECG recording (12 h before and 12 h after the radio frequency ablation surgery) collected from an AF patient with the wearable device	99.08	98.67	99.50	-	-
Lown et al. (2020) [36]	AF	1. 12-lead ECG (n.s.) **2. HR monitor [Polar H7 (PH7) HR] (n.s.)**	SVM	MIT-BIH Atrial Fibrillation MIT-BIH Arrhythmia	-	100.0	97.60	-	-

Zhang et al. (2021) [67]	AF	-	Global Hybrid Multi-Scale Convolutional Neural Network	China Physiological Signal Challenge 2018 (12-lead ECG) 2017 PhysioNet/Computing in Cardiology Challenge (single-lead ECG)	99.84	99.65	99.98	-	99.54
Zhang et al. (2020) [75]	AF	-	CNN	MIT-BIH Atrial Fibrillation	96.23	95.92	96.55	-	96.25
Chen et al. (2022) [60]	AF	-	Feedforward Neural Network	2017 PhysioNet/Computing in Cardiology Challenge MIT-BIH Arrhythmia	84.00	84.26	93.23	89.40	-
Mei et al. (2018) [51]	AF	-	Baggin Trees	2017 PhysioNet/Computing in Cardiology Challenge	96.60	83.20	98.60	-	-
Wu et al. (2020) [49]	AF	-	Extreme Gradient Boosting	2017 PhysioNet/Computing in Cardiology Challenge MIT-BIH Atrial Fibrillation MIT-BIH Normal Sinus Rhythm MIT-BIH Arrhythmia	95.47	94.59	96.40	-	95.56
Bashar et al. (2021) [27]	AF, PAC and PVC	-	SVM	Medical Information Mart for Intensive Care (MIMIC) III	97.45	98.99	95.18	-	-
Yu et al. (2021) [22]	PVCs	-	Deep Metric Learning-K-Nearest Neighbors	MIT-BIH Arrhythmia	99.70	97.45	99.87	-	-
Wang (2021) [28]	PVCs	-	CNN with improved Gated Recurrent Unit network	MIT-BIH Arrhythmia China Physiological Signal Challenge 2018	98.30	98.40	98.20	-	-
Meng et al. (2022) [21]	PVC, SPB	-	Lightweight Fussing Transformer with LightConv Attention	The 3rd China Physiological Signal Challenge 2020	99.32	92.44	-	-	93.63
Khan et al. (2020) [37]	CVDs	-	SVM	Cleveland Heart Disease dataset from the UCI repository	93.33	94.29	92.73	-	-
Dami et al. (2021) [80]	CVDs	-	LSTM Deep Belief Network	Four databases: DB1 - KAGGLE heart disease dataset | DB2 - Shahid Beheshti Hospital Research Center | DB3 - Physionet site - Hypertensive patients | DB4 - UCI Heart Disease dataset	88.42	85.13	85.54	-	-
Khan et al. (2020) [81]	CVDs	**Custom 1-lead ECG (n.s.)**	Deep Convolutional Neural Network	UCI machine learning repository, Framingham, and Public Health Dataset	98.20	97.80	92.80	-	95.00
Tan et al. (2021) [64]	CVDs and COVID-19	-	CNN-LSTM	MIT-BIH Arrhythmia	99.29	97.77	99.53	-	-
Mazumder et al. (2021) [63]	VT and VF	-	CNN-LSTM	MIT-BIH Malignant Ventricular Arrhythmia (VFDB) Creighton University Ventricular Tachycardia (CUDB)	-	99.21	99.68	-	-

Notes: Bold type highlights the wearable device when present and used to collect data. The best AI model/algorithm and results when different models/Algorithms, datasets, signals, and events are considered were reported.

Abbreviations: AF = Atrial Fibrillation; CVD = Cardiovascular disease; PAC = Premature Atrio Ventricular Contractions; PVC = premature ventricular contraction; VF = Ventricular Tachycardia; VF = Ventricular Fibrillation; SPB = Supraventricular premature beat; ECG = Electrocardiogram; PPG: Photoplethysmography; n.s. = not specified; HR = Heart Rate; CCN = Convolutional Neural Network; LSTM = Long Short-Term Memory; SVM = Support Vector Machine; Acc = Accuracy; Sen = Sensitivity; Spe = Specificity; AUC = Area Under the Curve of receiver-operating characteristic curves.

2.3.3.2 Other cardiovascular diseases

Other cardiovascular conditions amenable to ECG-AI include myocardial infarction and heart failure (Table 2.2). Particularly with myocardial infarction detection, there has been a shift from ML techniques towards DL techniques [20,39,82] due to higher performances and no handcrafted feature extraction required. DL techniques for myocardial infarction detection include both the application of simple and complex models. Examples of simple DL models include an Artificial Neural Network with only three layers (Acc 99.10%) [83] and CNN [16,20] and LSTM [84] algorithms. More complex DL models include a Deep Belief Network for unsupervised heart rate variability (HRV) feature extraction and selection with LSTM for classification [80], a multi-channel lightweight model for the simultaneous analysis and classification of four ECG leads [85], and a two-dimensional CNN for the classification of ECG waveform snapshots [38]. It is important to notice that the ECG-AI determination of myocardial infarction commonly involves 12-lead data because the different leads represent different projections of the heart's electrical activity, which is necessary to capture region-specific ischemia [16,20,82–85]. However, some algorithms were assessed based on data recorded from wearable single-lead devices [38,39].

The analysis of 12-lead data also enabled the screening of heart failure with reduced ejection fraction (Acc 82.50%) [86]. Following a short-time Fourier transform in combination with a CNN, an interpretable model highlighted the essential regions in the various ECG leads associated with the final classification. In particular, the lateral (aVL, I, −aVR, V5, V6) and anterior leads (V3, V4) greatly impacted heart failure with reduced ejection fraction detection. In contrast, the performance of the inferior leads (II, aVF, III) was relatively poor. The findings also confirmed that a rightward T-wave axis, prolonged QT duration, and prolonged QTc are associated with heart failure and that the T-wave axis is an independent and strong risk factor for cardiac events in the elderly.

Table 2.2. Summary of ECG-based AI algorithms applied to other cardiovascular diseases.

Authors (Year)	Specific Application	ECG System (Sampling Frequency)	AI Algorithm/Method	Database/Dataset	Performance (%)				
					Acc	Sen	Spe	AUC	F1
Gibson et al. (2022) [16]	Myocardial Infarction	-	CNN	Latin America Telemedicine Infarct Network (LATIN)	90.50	86.00	94.50	-	-
Baloglu et al. (2019) [20]	Myocardial Infarction	-	CNN	PTB ECG: MI on standard 12-lead ECG data	99.78	99.80	-	-	-
Cho et al. (2021) [86]	Heart Failure	12-lead ECG [Page Writer Cardiograph - Philips] (500 Hz)	Short-time Fourier transform – CNN combination	ECG from multicenter study	82.50	92.10	82.10	92.90	-
Wasimuddin et al. (2021) [38]	Myocardial Infarction	**Custom 1-lead ECG (n.s.)**	CNN	European ST-T Custom wearable device	99.26	99.27	99.27	-	-
Chowdhury et al. (2019) [39]	Myocardial Infarction-Cardiac Arrest	**Custom 1-lead ECG (500Hz)**	Support Vector Machine	MIT-BIH ST Change Normal subjects and an ECG simulator to simulate abnormal ST-elevated MI situations to test the functionality of the complete system in real-time	97.40	99.10	-	-	98.70
Shahnawaz et al. (2021) [83]	Myocardial Infarction	-	Artificial Neural Network	PTB (PhysioNet)	99.10	100.00	98.10	-	99.00
Sopic, et al. (2018) [82]	Myocardial Infarction	-	Random Forest	PTB (PhysioNet)	80.30	87.95	79.63	-	-
Martin et al. (2021) [84]	Myocardial Infarction	-	Deep Long Short-Term Memory	PTB-XL and PTB (PhysioNet)	79.69	76.59	85.89	-	83.42
Cao et al. (2021) [85]	Myocardial Infarction	-	Multi-Channel Lightweight model	PTB (PhysioNet)	96.65	94.30	97.72	96.71	-

Notes: Bold type highlights the wearable device when present and used to collect data. The best AI model/algorithm and results when different models/Algorithms, datasets, signals, and events are considered were reported.
Abbreviations: n.s. = not specified; CNN = Convolutional Neural Network; Acc = Accuracy; Sen = Sensitivity; Spe = Specificity; AUC = Area Under the Curve of receiver-operating characteristic curves.

2.4 Sleep Apnea

Sleep apnea is a sleep disorder characterized by interruption of breath during sleep [87]. It is divided into two subtypes: central sleep apnea (CSA) and obstructive sleep apnea (OSA). (Figure 2.4). CSA is less prevalent and results from abnormal regulation of breathing in the brainstem respiratory centers, which leads to an absence or diminution of involuntary respiratory effort while asleep [88]. OSA is a highly prevalent sleep-related disorder characterized by repetitive complete obstruction (apnea) or partial obstruction (hypopnea) of the upper airway that results from loss of muscle tone in anatomically susceptible persons [89]. It is estimated that OSA affects almost 1 billion people globally [90], with 425 million adults aged 30-69 years having moderate to severe OSA [91]. CSA is associated with heart failure, renal failure, and acute phases of stroke, while OSA can lead to excessive daytime sleepiness, chronic fatigue, hypertension, stroke, and other cardiovascular disorders. Thus, early and accurate diagnosis of sleep apnea is essential.

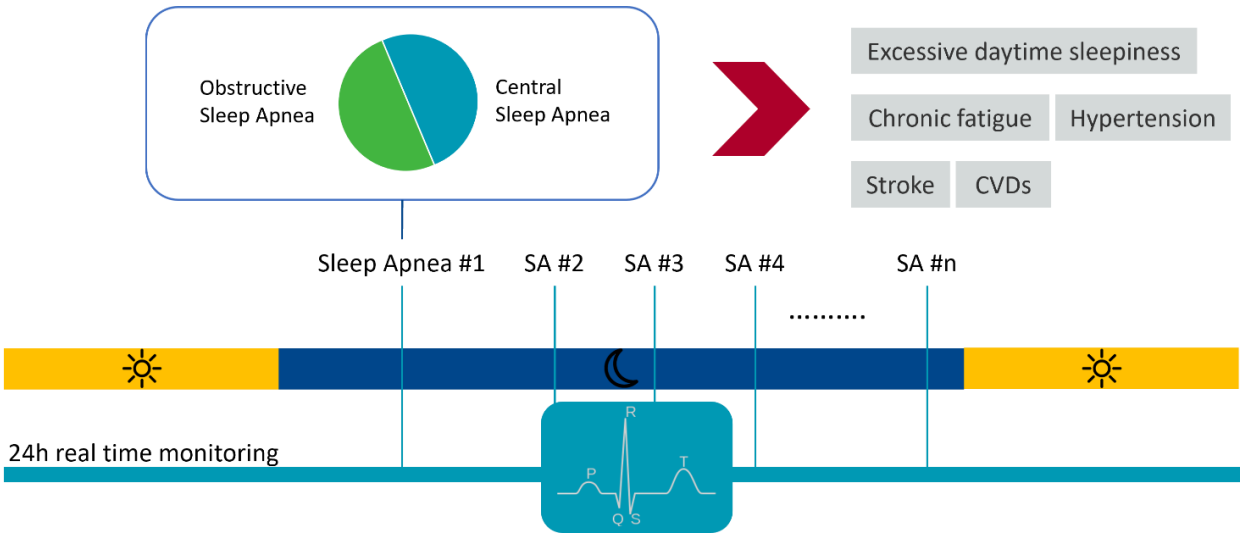

Figure 2.4. Sleep apnea and its consequences relative to diagnostics potentially enabled by continuous real-time ECG monitoring.

Laboratory-based polysomnography has been used as a reference standard for diagnosing OSA. Polysomnography involves the overnight recording of bilateral occipital, central, and frontal electroencephalogram, chin, leg, surface electromyogram, left and right eye electro-oculogram, ECG, pulse-oximetry, airflow, and respiratory effort. Yet, polysomnography is time-consuming,

expensive, and uncomfortable for the patient and requires a trained technician. Therefore, an ECG-AI approach to sleep apnea diagnosis is a potentially convenient and cost-effective alternative [92].

2.4.1 Wearables

To our knowledge, no studies investigated the use of wearable ECG-AI devices for sleep apnea detection. In fact, sleep apnea ECG data analysis has solely relied on existing datasets such as the PhysioNet Apnea-ECG database [93] or by collecting new data based on polysomnography.

2.4.2 Algorithms

When automatically identifying OSA from ECG recordings, DL is preferable over traditional ML because of its ability to automatically learn discriminating features from raw data (Table 2.3). For instance, a CNN using a modified LeNet-5 architecture was compared against five conventional approaches [94]. The superior performance of CNN (Acc 96.00%) for OSA classification was further reinforced by the finding that short-term (30-second) ECG segments were classified into four (normal, mild, moderate, and severe) versus two (normal and OSA) categories [95].

An OSA detection framework based on a multiscale dilation attention CNN and a weighted-loss time-dependent classification model for feature extraction and classification were proposed to fully exploit ECG information via DL [96]. The novelty of multiscale dilation attention-one dimensional CNN lies in the parallel multi-branch structure and dilation operations, which allow the model to explore the feature space efficiently by assigning feature weight with the efficient channel attention module. The classifier addresses the challenges following temporal dependence between ECG segments using a weighted loss function that reduces class imbalance.

Hybrid DL methods have also been proposed in which different methods are combined. Examples are the CNN and LSTM combination with SVM [97], a hybrid three-dimensional CNN-LSTM combination where 20 successive single-segments were analyzed simultaneously to include the time evolution pattern of the ECG [98], and a CNN representation learning model for feature extraction combined with a temporal dependence model for classification [99]. To address the limited ability of classic network architectures in feature extraction, the use of a one-dimensional squeeze-and-excitation residual group network to detect OSA using inter-beat intervals and R-wave and Q-wave amplitude from two-minute ECG signal segments was proposed [100]. The network architecture is a CNN in which the residual group convolutions are included to alleviate

the computational burden whereas the squeeze-and-excitation mechanism manages the importance of the three inputs.

Table 2.3. Summary of ECG-based AI algorithms applied to sleep apnea.

Authors (Year)	ECG System (Sampling Frequency)	AI Algorithm/Method	Database/Dataset	Performance				
				Acc	Sen	Spe	AUC	F1
Bahrami et al. (2022) [98]	-	Hybrid three-dimensional CNN - LSTMs	Apnea-ECG (PhysioNet)	94.95	93.92	95.63	-	93.65
Yang et al. (2021) [100]	-	Squeeze-and-excitation residual group network	Apnea-ECG and UCDDB dataset (PhysioNet)	90.30	87.60	91.90	96.50	87.30
Urtnasan et al. (2020) [95]	-	CNN	Subjects studied with overnight PSG	96.00	-	-	99.00	99.00
Qin et al. (2022) [99]	-	CNN-Representation Learning model and Temporal Dependence model	Apnea-ECG (PhysioNet) In-group database from The Sixth Affiliated Hospital of Sun Yat-sen University	91.10	88.90	92.40	97.00	88.30
Almutairi et al. (2021) [97]	-	CNN-LSTMs and Support Vector Machine	Apnea-ECG (PhysioNet)	90.20	91.24	90.36	-	92.76
Shen et al. (2021) [96]	-	MultiScale Dilation Attention-CNN and Weighted-Loss Time-Dependent	Apnea-ECG (PhysioNet)	89.40	89.80	89.10	96.40	86.60
Wang et al. (2018) [94]	-	CNN	Apnea-ECG and UCDDB dataset (PhysioNet)	87.60	83.10	90.30	95.00	-

Notes: Bold type highlights the wearable device when present and used to collect data. The best AI model/algorithm and results when different models/Algorithms, datasets, signals, and events are considered were reported. Performance is reported per-segment.
Abbreviations: CNN = Convolutional Neural Network; LSTM = Long Short-Term Memory; Acc = Accuracy; Sen = Sensitivity; Spe = Specificity; AUC = Area Under the Curve of receiver-operating characteristic curves.

2.5 Mental Health and Epilepsy

Another field of ECG-AI application is clinical psychophysiology, which has used cardiovascular indicators for decades as proxies of cognitive and emotional processes [101]. The stress response is the most investigated of such processes and is characterized by a set of physiologic changes, including increased heart and respiratory rates, skin conductance, cortisol secretion, and muscular and pupillary dilation [102]. The individual tendency to be either hyper- or hypo-reactive is associated with an increased risk for cardiovascular disease and other somatic and mental health conditions [103–105]. Consequently, clinical psychophysiology aims to identify objective signs and early biomarkers of somatic and mental illness [106] with applications ranging from cardiovascular rehabilitation to clinical monitoring and work-related health and safety [107–109].

The data-gathering approach in this research field commonly entails the psychophysiological assessment, during which study participants are exposed to stressful tasks (e.g., mental arithmetic, cold pressure test, public speech) preceded by a baseline phase and followed by a recovery phase [110] (Figure 2.5). Such an evaluation is most widely implemented in a laboratory setting; however, several variants have been proposed to improve its everyday validity, including virtual-reality-based studies [111] and ambulatory assessments [112].

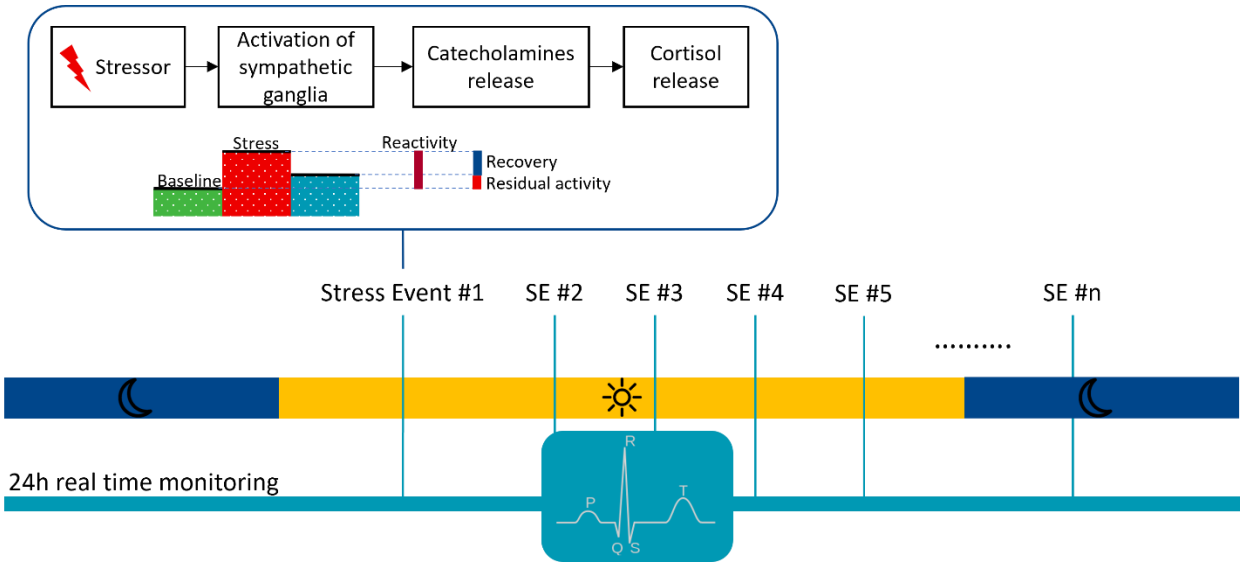

Figure 2.5. Stress response and its physiology relative to diagnostics potentially enabled by continuous, real-time ECG monitoring.

Regardless of the specific focus on stress or emotions, most of the reviewed studies (see Table 2.4) focused on HRV features. HRV is an index of cardiovascular flexibility and adaptability with higher HRV being associated with more effective responsivity to stressors and recovery in stress-free conditions [113]. Moreover, vagal tone is a main determinant of resting-state HRV levels, and it is also associated with a network of structures involved in emotion regulation (e.g., the amygdala) and executive functions (e.g., the prefrontal cortex) [113,114]. Therefore, HRV is among the physiologic indicators of stress, emotions, and other self-regulatory processes [115]. HRV indices in both the time and the frequency domains are widely used for ECG-AI stress detection and emotion recognition [108].

HRV is also implicated in other neuropsychologic conditions such as epilepsy and epileptic seizures, the prediction of which has profound clinical utility [116]. For instance, epileptic patients are characterized by lower high-frequency HRV and overall sympathovagal imbalance [117], and cardio acceleration (tachycardia), with HRV reductions being typical peripheral concomitants of epileptiform electroencephalography (EEG) activity [117,118].

2.5.1 Wearables

Several commercial wearable devices were used to collect ECG data for research involving stress detection and emotion recognition, including the Zephyr BioHarness 3.0 [78,119], T-REX TR100A [120], and “LaPatch” [121]. However, the continued development of public, disease-dedicated databases, such as the PhysioNet Driver stress dataset [122], allows for algorithm development and evaluation without collecting data [123]. Such an approach is mainly used for epilepsy applications, where the condition is monitored and not induced and where the biosignals are directly evaluated from patients to detect and predict event occurrence. In these studies, ECG and EEG data are analyzed together. An additional two studies were reported in which the ECG signal was collected with ad-hoc wearable prototypes alongside other biosignals such as the EEG [124,125].

2.5.2 Algorithms

Various ML and DL approaches are used in psychophysiological research. Conventional ML techniques were adopted for mental fatigue detection and emotion classification [121,123]. In

particular, a wavelet scattering algorithm was successfully applied to extract more complex ECG features than the standard time- and frequency-based features [123].

ML and DL are mainly used for stress detection, as in a study where stress level was estimated through a combination of principal component analysis for feature extraction and SVM for classification [119]. Moreover, a two-branched Deep Learning Neural Network (DNN) based on Deep ECG Net structure was proposed [78]. Two branches are devoted to feature extraction of ECG and respiratory features, respectively, after which they are concatenated for classification. Of interest are the author's visualizations of the network's learning process, which provide insight into the network's decision-making. In a second DNN, training methods were investigated: training from scratch and transfer learning [120]. In the latter method, the pre-trained model parameters were determined following training on one database after which they were adjusted using a second database. Classification performance analyses indicated that the transfer learning application improved the scores of all metrics (Acc 90.19%). ECG-AI algorithms for mental stress and emotion detection are typically trained on signal segments classified as "stressed" vs. "unstressed" based on the experimental phase of the psychophysiological assessment (i.e., stressor versus baseline/recovery) [78,119–121], whereas a study labeled the segments based on self-report measures [121], and other studies ECG activity with changes in criterion variables such as salivary cortisol [119] and expert rating of participants' facial expressions [123] (see Table 2.4).

For seizure detection, two different ML approaches were reported. The application of multivariate statistical process control was demonstrated via a technique that searches for changes in HRV indices that could indicate seizures [124]. Nonetheless, the system had a sensitivity of 85.7% with a false alarm rate of 0.62 times per hour, implying a need for improvement. The use of two singular models were evaluated: the first, based on SVM, to classify EEG signals and the second, based on random forest, to classify ECG signals [125]. The classifiers were used against a multimodal model by integrating the predictions of the two models for seizure detection. Performance evaluation showed that integrating the prediction results of both physiologic signals in the multimodal model increased sensitivity while maintaining the same false alarm rate for two out of three databases. These studies typically used data from long-term pre-surgical monitoring [124–126]. The AI algorithms were then trained and tested against expert annotation of video-recorded EEG segments, which were categorized as during, after, or between seizures. Overall, these studies were characterized by lower heterogeneity in terms of research protocols and reported

algorithm performance metrics compared to stress and emotion recognition studies due to the higher availability of research standards for clinical validation [127].

Studies involving ECG-AI wearables to detect mental health conditions are limited in several ways. First, many studies used small samples with poorly specified or even unspecified inclusion criteria. Such low statistical power limit algorithm performance, reproducibility, and the generalizability of results. Second, signal pre-processing steps, including detection of ECG components, artifact identification, and computation of the ECG features are substantially different among the reviewed studies. Some studies used ECG tracing of 20 seconds or less, which excludes the use of HRV features such as the low frequency power (requires a frequency of 0.04 Hz or oscillations as long as 25 seconds) because signal segments lasting at least 10 times the lower frequency bound (about 4 minutes) have been recommended to provide proper estimates [128].

Table 2.4. Summary of ECG-based AI algorithms applied to mental health and epilepsy.

Authors (Year)	Specific Application	ECG System (Sampling Frequency)	AI Algorithm/ Method	Sample/Database	Protocol/Tasks	Performance (%)				
						Acc	Sen	Spe	AUC	F1
Seo et al. (2019) [78]	Mental stress recognition	Zephyr BioHarness (n.s.)	Deep Neural Network (Deep ECG-Respiration Network)	18 healthy adults	Four randomized 5-min stress tests (math or Stroop) with varying difficulty (easy vs. hard), each followed by 5-min recovery	83.90	-	-	92.00	81.00
Cho et al. (2019) [120]	Stress recognition	Training: None Testing: T-REX TR100A (256 Hz)	Deep Neural Network with transfer learning	Training: Driver stress database on PhysioNet Testing: 17 individuals	Training: 15-min resting, 20-to-60-min driving, 15-min resting Testing: 5-min baseline, 5-min simple math, 5-min recovery, 5-min hard math	90.19	93.00	85.40	93.80	92.20
Betti et al. (2017) [119]	Mental stress monitoring	Zephyr BioHarness (250 Hz)	Support Vector Machine	12 healthy individuals	10-min resting, 15-min stress tests (cold pressure and math), 10-min recovery	86.00	84.00	90.00	-	-
Huang et al. (2018) [121]	Mental fatigue detection	"LaPatch" (250 Hz)	K-Nearest Neighbors and others	29 healthy individuals	10-min resting, 10-min quiz	74.50	-	-	74.00	-
Sepulveda et al. (2021) [123]	Emotion recognition	-	Ensemble Bagged Tree and others	2018 AMIGOS	16 short videos (< 250 sec) and 4 long videos (> 14 min)	90.30	-	-	-	89.50
Yamakawa et al. (2020) [124]	Epileptic seizure prediction	**Custom telemeter based on portable ECG (1 kHz)**	Multivariate Statistical Process Control	Model construction: 15 refractory epilepsy patients Model evaluation: 7 focal epilepsy patients, 7 healthy controls	Patients: 32-to-105-hour ECG and video-EEG monitoring during seated or supine resting Controls: 5-to-11-hour ECG ambulatory monitoring	-	85.70	-	-	-
Vandecasteele et al. (2021) [125]	Multimodal epileptic seizure detection	**1-lead ECG (n.s.)**	Multimodal integrating SVM (EEG) and Random Forest (ECG) predictions	135 focal epilepsy patients from the SeizeIT1, Epilepsiae- Freiburg, and Epilepsiae- Paris	Long-term pre-surgical monitoring	-	92.00	-	-	-

Notes: Bold type highlights the wearable device when present and used to collect data. The best AI model/algorithm and results when different models/Algorithms, datasets, signals, and events are considered were reported.

Abbreviations: ECG = Electrocardiogram; n.s. = not specified; EEG = Electroencephalogram; Sen = Sensitivity; Spe = Specificity; Acc = Accuracy; AUC = Area Under the Curve of receiver-operating characteristic curves.

2.6 Other Applications

Examples of ECG-AI applied to other areas are reported in Table 2.5. Applications include the evaluation of blood sugar and sports medicine.

2.6.1 Wearables

Public databases relating ECG and outcome data are currently available for the most common cardiac conditions such as AF and only a minority is available for other diseases. Therefore, consumer devices such as the Medtronic Zephyr BioPatch™ HP80 [129], and single-lead ECG prototypes [130,131] have been used to collect patient-specific data related to other medical conditions for subsequent AI analysis. However, the number of publicly available datasets for tailored medical applications is increasing [46].

2.6.2 Algorithms

ECG-AI has been successfully used to detect hyperglycemia and hypoglycemia [129,130]. A novel feature extraction method and a ten-layer Artificial Neural Network classifier for the detection of hyperglycemia [130] was proposed, and it achieved an improvement of 53% versus the previous models. A person-specific system including a DL model for each participant, was proposed for the detection of hypoglycemia [129]. Specifically, data recorded from the first few days were used for training, while the rest was used for system evaluation. Two models were investigated: a CNN and a CNN-RNN combination. The CNN module produced a fixed-length ECG to be further processed by the next RNN module.

Another application of ECG-AI is in sports medicine to evaluate fatigue and abnormal health events in real-time. The effectiveness of this approach was demonstrated via a weighted one-class SVM using signals recorded on volunteers undergoing specific tasks [131].

Table 2.5. Summary of other applications of ECG-based AI algorithms.

Authors (Year)	Specific Application	ECG System (Sampling Frequency)	AI Algorithm/Method	Database/Dataset	Performance (%)				
					Acc	Sen	Spe	AUC	F1
Cordeiro, et al. (2021) [130]	Blood Sugar - Hyperglycemia	**Custom 1-lead ECG with Analog AD-8232 (1000 Hz)**	Deep Learning Neural Network	60s ECG, Blood glucose, and other profile information (such as age, gender, height, weight, and heart rate)	-	87.57	85.04	94.53	-
Porumb et al. (2020) [129]	Blood Sugar - Hypoglycemia	**1-lead ECG [Medtronic Zephyr BioPatch™ HP80 (250 Hz)**	Convolutional Neural Networks + Recurrent Neural Networks	ECG signals and actigraphy, recorded continuously during a nominal period of 14 nights for each subject. 8 healthy participants were recruited: 4 hypoglycemic and 4 healthy	90.00	88.30	92.20	-	-
Luo (2020) [131]	Sport - Fatigue & Abnormal Events	**Smart wearable device [based on OpenBCI] (n.s.)**	Weighted one-class SVM	5400 sub-signals from 30 volunteers during 1 hour	93.65	-	-	96.70	-

Notes: Bold type highlights the wearable device when present and used to collect data. The best AI model/algorithm and results when different models/Algorithms, datasets, signals, and events are considered were reported.
Abbreviations: n.s. = not specified; SVM = Support Vector Machine; Acc = Accuracy; Sen = Sensitivity; Spe = Specificity; AUC = Area Under the Curve of receiver-operating characteristic curves.

2.7 General Challenges and Limitations

The clinical reliability of wearable devices is challenged by several factors including the fact that mobile versions collect less data compared to their clinical analogs. An example is the ECG's of wearable devices that are typically single to triple leads while those utilized clinically feature twelve leads. Wearable technologies are also intended to be worn throughout activities of daily living, which results in an increased likelihood of collecting intermittent or noisy data. Further, the real-time effectiveness of corresponding AI algorithms are potentially compromised by processing demands relative to battery capacity, or when the processing is to be done on the cloud, limited connection to wireless networks in rural areas.

Once recorded via wearable devices, data are commonly reviewed by physicians when such information would be valuable and better to understand a patient's history [9]. However, diagnoses and predictions provided by AI algorithms are less readily accepted by clinicians [132] because the basis for these decisions is a black box. That is, an AI algorithm may decide about a particular medical condition, but the inherent lack of physiologic insight makes the reliability of such decisions uncertain by clinical standards. Determinations made by supervised AI algorithms are therefore more likely to be clinically acceptable if more insight into the physiologic mechanism by which they make their predictions can be provided.

Two limitations result from the need to provide physiologic detail. First, defining summary domain-aware features to enable supervised AI reduces the dimensionality of the data and may thus limit prediction potential at the expense of a better physiologic understanding. Indeed, to perform supervised learning and therefore satisfy clinical standards for physiologic understanding, data should be processed to obtain translatable summary features. Regarding ECG analysis, such characteristics may include the R-R interval, QRS width and magnitude, and S-T segment elevation or depression, among others. Nonetheless, this approach relies on knowing what summary features to define and doing so comprehensively. Unfortunately, the definition of translatable characteristics relies on those that are already known via traditional medicine. These characteristics are the most obvious to human interpretation, which thus undermines a main advantage of using AI: the ability to make determinations beyond the threshold of human elucidation. Second, it may also be desirable to perform processing steps such as truncating, filtering, or down-sampling data to make physiologic detail more obvious or optimize input before

initiating an AI algorithm. However, these steps also potentially remove valuable information beyond the level of human interpretation. Towards a compromise of deeper knowledge with some physiologic insight, heat maps that highlight the temporal segment of the ECG most influential in making a classification are valuable [77].

Another challenge facing clinical adoption of AI diagnoses is that there are no standards for defining what level of correctness is sufficient to replace a physician as the primary assessor. Such a threshold is particularly important to consider in the context of AI algorithms being trained by physician specialists because AI diagnoses are then relative to the most expert clinical standard rather than the average [133]. Additionally, this standard assumes that all patients have access to the best physician specialist with whom the AI algorithm is being compared. In fact, many individuals may not have any access at all, especially in real-time. Thus, wearable devices in conjunction with AI algorithms offer far greater monitoring of patients but have a higher standard for diagnostic reliability.

An additional limitation of current AI methods is that algorithm training requires the availability of quality data. In most cases, such datasets need to be large enough to be divided into training and testing sets while also being curated so that most fields are complete and are purged of erroneous information. As shown in this review, many publicly available, condition-specific datasets are emerging. However, developers should keep in mind that each database has its limitations (e.g., not socioeconomically or racially diverse enough) that narrow the database's scope of use. After acceptance of an algorithm, ongoing post-application clinical validation is essential to maintaining confidence in diagnostic or predictive correctness but is more challenging because these data are not curated and may thus be noisy, discontinuous, or otherwise incomplete.

As demonstrated in the tables of this review, there are no standards for defining correctness, and therefore, the direct comparison of various AI methods is often not possible. However, all measures of correctness (total error rate, positive predictive value, accuracy, sensitivity, specificity, AUC, and F1) rely on base variables including true positives, true negatives, false positives, and false negatives [8,134]. The consistent reporting of all base variable values or all measures of correctness would overcome this current limitation.

In general, methods proposed in the literature are not easy to compare due to the different datasets used in the experiments and different research targets. The most promising algorithm for ECG applications is Deep Learning CNN architecture. However, in arrhythmias detection and

classification, it is possible to have a clearer understanding and insight of the algorithms' performances. In fact, arrythmia detection is a common outcome for ECG-AI technology because arrhythmias can be relatively easily identified using one-lead ECG without the need of the standard 12-leads, making these detection techniques easier to transfer and deploy on wearable devices. Unsurprisingly, the most popular application of wearable devices in medicine are arrhythmia detectors/monitors. For the other applications, more research and datasets need to be analyzed. Based on our work, we expect an increase in interest in applications of wearables and ECG-AI in sleep apnea and mental stress. Moreover, new applications of ECG-AI for other conditions, such as hyper/hypoglycemia, will likely see an increase in data and research work as well. Promoting challenges between research groups seems to be the best way to boost the development of the best AI solutions. Examples of such competitions include MIT-BIH Arrhythmia or the 2017 PhysioNet/Computing in Cardiology Challenge.

2.8 Towards the Future

Wearable devices will continue to have an increasing role in personalized healthcare because they enhance accessibility, reliability, and cost effectiveness. Technology advancements that enable this expansion will include devices that acquire more reliable and higher quality signals and those that obtain more signals simultaneously, increasingly approximating clinical diagnostics. In terms of the wearable ECG, high-quality data will be continuously obtained from more reliable and improved sensors with multiple leads [3,7].

In the future, AI algorithms will be trained using an increasing number of larger, curated, condition-specific datasets. Future datasets that are more generalized to include more covariates to capture additional peripheral information are also likely to emerge. Data collected by wearable ECG devices will increasingly be transferred to a cloud for AI processing because the algorithms will be too computationally intensive to be executed locally [4,8].

Prospective wearable ECG-AI devices will normalize the near instantaneous assessment and treatment of certain acute conditions, improving outcomes. These devices and algorithms will also more comprehensively consider whole-body physiology and health by integrating a variety of data

sources simultaneously. Ongoing successes will increase confidence in automated decision making and reinforce its role in personalized healthcare [14,132].

2.9 Conclusions

The ECG contains highly valuable information. Diagnosing and predicting specific clinical conditions, including arrhythmias, coronary artery disease, sleep apnea, mental health, and epilepsy are increasingly enabled via wearable devices that record ECG data and continuously analyze it in real-time using AI algorithms. In this review, we highlighted the current applications, with performances and limitations, of ECG-AI applied to wearable devices for disease detection and prediction. As reported by several other authors, ongoing development of large, curated datasets targeting specific clinical conditions is essential for developing and validating various AI approaches. Because ECG-AI is tailored to specific medical applications, the methods that are most effective for one clinical condition are not necessarily appropriate for application to others. Advancements in this field require a combination of knowledge domains that create a unique expertise. Such technology is leading to a paradigm shift in personalized medicine that is making the diagnosis of many conditions more accessible, reliable, and cost effective.

Abbreviations

Acc, Accuracy; AF, atrial fibrillation; AI, artificial intelligence; CSA, Central sleep apnea; CNN, convolutional neural network; CVD, cardiovascular diseases; DL, deep learning; DNN, deep learning neural network; ECG, electrocardiogram; ECG-AI, Artificial intelligence-enhanced electrocardiography EEG, electroencephalogram;	FDA, food and drug administration; HF, heart failure; HR; heart rate; ML, machine learning; LSTM, Long Short-Term Memory OSA, Obstructive sleep apnea; PPG, photoplethysmography; PVC, premature ventricular contraction; RNN, recurrent neural networks; SVM, support vector machine.

3. Algorithm for Mobile Platform-Based Real-Time QRS Detection

from the manuscript:

Algorithm for Mobile Platform-Based Real-Time QRS Detection

L. Neri, M. T. Oberdier, A. Augello, M. Suzuki, E. Tumarkin, S. Jaipalli, G. A. Geminiani, H. R. Halperin, and C. Borghi

Published in: *Sensors 2023, 23(3), 1625;*

3.1 Abstract

Recent advancements in smart, wearable technologies have allowed the detection of various medical conditions. In particular, continuous collection and real-time analysis of electrocardiogram data have enabled the early identification of pathologic cardiac rhythms. Various algorithms to assess cardiac rhythms have been developed, but these utilize excessive computational power. Therefore, adoption to mobile platforms requires more computationally efficient algorithms that do not sacrifice correctness. This study presents a modified QRS detection algorithm, the AccYouRate Modified Pan–Tompkins (AMPT), which is a simplified version of the well-established Pan–Tompkins algorithm. Using archived ECG data from a variety of publicly avail-able datasets, relative to the Pan–Tompkins, the AMPT algorithm demonstrated improved computational efficiency by 4–20×, while also universally enhancing correctness, both of which favor translation to a mobile platform for continuous, real-time QRS detection.

3.2 Introduction

Continuous collection and real-time analysis of physiologic data are increasingly common due to advances in wearable technologies [6,135]. One of the most commonly acquired signals is the electrocardiogram (ECG), which is a record of the time-varying electrical activity of the heart. The ECG is common for routine cardiac evaluation because it is inexpensive, noninvasive, and provides continuous real-time data of heart physiology. The ECG is particularly valuable for detecting cardiac anomalies such as arrythmias [3,136,137].

Many algorithms have been developed to recognize characteristics of the ECG, and the detection of the QRS complex is fundamental for analysis [138–149] because it is the major landmark that allows the waveform to be segmented into heartbeats for determining the heart rate and its variability [150]. The accurate detection of the QRS signal is also fundamental to more detailed ECG processing [151].

One common method for QRS detection is the Pan–Tompkins algorithm, which was developed prior to the advent of wearable technologies [152]. In our experience, the Pan–

Tompkins algorithm caused real-time processing delays and was suboptimally correct when evaluating publicly available data that simulated signals that would be acquired from mobile platforms and wearable technologies.

Therefore, to better enable real-time QRS detection via mobile platform-based ECG devices, such as wearable technologies with smartphone interfaces, more computationally efficient algorithms are necessary that do not sacrifice (and may even improve) correctness [153–156]. We hypothesized that our modified QRS detection algorithm is more computationally efficient and at least as correct as the established method on which it is based.

3.3 Methods

The Pan-Tomkins algorithm has been modified (known here as the AccYouRate Modified Pan-Tomkins, AMPT) to be more computationally efficient and thus, more amenable to application on a mobile platform. Using archived ECG data from a variety of publicly available ECG datasets, both algorithms were evaluated for computational efficiency and correctness as compared to manually and independently annotated QRS complexes.

3.3.1 Algorithms

The AMPT algorithm differs from the original Pan–Tompkins method in two major ways:

1) The Pan–Tompkins algorithm performs an analysis on two simultaneous signals: the bandpassed signal and the resulting filtered signal. The peaks from each signal are compared on a time basis for correspondence. However, with the AMPT algorithm, the signal peaks and the noise peaks from the bandpassed signal are not calculated and only the final filtered signal is analyzed.
2) The Pan–Tompkins algorithm uses two average RR intervals for search back (one for sinus rhythm and one for arrhythmias), which entails defining the signal and noise peaks, thresholds, and a series of RR limits. The AMPT does not differentiate based on regular or irregular rhythms, and therefore requires fewer computational steps because search back is calculated from a single averaged RR interval.

The AMPT algorithm utilizes the same low- and high-pass filters, derivative, squaring function, and moving window integration as the original Pan–Tompkins method. However, only the filtered signal is used for the AMPT. Thus, for the AMPT algorithm, the set of filtered ECG thresholds is redefined as (corresponding to Equations (17) - (20) of the original Pan-Tompkins manuscript [152]):

$$SPKF = 0.125\ PEAKF + 0.875\ SPKF \quad (1)$$

$$NPKF = 0.125\ PEAKF + 0.875\ NPKF \quad (2)$$

$$THRESHOLD\ F1 = NPKF + 0.25\ (SPKF - NPKF) \quad (3)$$

$$THRESHOLD\ F2 = 0.25\ THRESHOLD\ F1 \quad (4)$$

where PEAKF is the overall peak, SPKF is the running estimate of the signal peak, NPKF is the running estimate of the noise peak, THRESHOLD F1 is the first threshold, and THRESHOLD F2 is the second threshold, consistent with nomenclature from the original Pan–Tompkins paper. Next, when the QRS complex is identified using THRSHOLD F2, the signal peak is redefined as (corresponding to Equation (21) of the original Pan-Tompkins manuscript [152]):

$$SPKF = 0.125\ PEAKF + 0.875\ SPKF \quad (5)$$

Further, the average of the eight most recent sequential RR intervals is redefined as (corresponding to Equation (24) of the original Pan-Tompkins manuscript [152]):

$$RR\ AVERAGE1 = 0.125\ (RRn\text{-}7 + RRn\text{-}6 + \ldots + RRn) \quad (6)$$

where RRn is the most recent RR interval. Then, an RR limit is redefined as (corresponding to Equation (28) of the original Pan-Tompkins manuscript [152]):

$$RR\ MISSED\ LIMIT = 1.66\ RR\ AVERAGE1 \quad (7)$$

The AMPT algorithm also uses the same T-wave identification as the original Pan–Tompkins method.

In summary, from the original Pan–Tompkins manuscript [152][20], the fiducial mark and Equations (12)–(16), (22), (23), (25)–(27), and (29) were not used, the coefficients of Equations (20) and (21) were modified, and RR Average 1 (rather than RR Average 2) was used in Equation (28) for the AMPT algorithm.

The Pan–Tompkins algorithm was obtained as an intact Python code by Pickus from a public software repository and forum [157]. Via line-by-line inspection, this code was confirmed to exactly implement all steps reported in the original Pan–Tompkins manuscript. The first steps of the algorithm, which include the application of a set of filters, are suitable for the specific, previously used sampling rate of 200 Hz.

The AMPT algorithm was custom written in Python, independent of publicly available Pan–Tompkins codes. The AMPT code is available at https://github.com/Accyourate-Group-S-p-A/acy_ampt (accessed on 25 January 2023).

Both the Pan–Tompkins and AMPT codes were executed in Python 3.7 using IDE PyCharm 2019.2.6 Professional Edition and public Python libraries (NumPy, SciPy, Pandas, WFDB, and time). For comparison purposes, all processing took place on the same desktop computer (HP Z840 Workstation (Hewlett Packard, Palo Alto, USA), Processor: Intel Xeon CPU E5-2620 v3–2.40 GHz, 64 GB RAM (Intel, Santa Clara, USA)) which was only running those background programs (in addition to Python and PyCharm) that loaded upon booting into 64-bit Windows 10 Pro (Microsoft, Redmond, USA).

3.3.2 ECG Datasets

To compare algorithms, multiple datasets were downloaded from the PhysioBank ATM [46] and Harvard Dataverse [158] repositories. Records included annotations of QRS complexes that were manually identified throughout all data and adjudicated independently of this project. The datasets were those curated to specifically feature high and low signal qualities [159], normal sinus rhythms [160], arrhythmias [161], paced rhythms (subset of arrhythmias dataset), and telehealth-acquired signals [158]. The sampling attributes of these datasets are shown in Table 3.1.

Table 3.1. Number of beats, number of records, record length, total time, and sampling frequency by dataset.

Dataset	Description	Number of Beats	Number of Records	Record Length (min)	Total Time (min)	Sample Frequency (Hz)
A1	High Quality	72,415	100	10	1000	250
A2	Low Quality	78,618	100	10	1000	360
B1	Normal Sinus Rhythm	48,494	18	30	540	128
B2	Arrhythmias	103,724	44	30	1320	360
C	Paced Rhythm	8923	4	30	120	360
D	TeleHealth	6708	134	0.5	125	500

All the data from the High and Low Quality, Arrhythmias, and Paced Rhythm datasets were utilized. However, only the first thirty minutes of each Normal Sinus Rhythm sample were used because when longer periods were considered, hardware resources became a limiting factor and, thus, computational time did not exclusively reflect algorithm efficiency. Further, from the TeleHealth dataset, 116 samples were excluded because there was a prohibitively small number of reliable ECG waveforms.

Finally, across datasets and across patients within datasets, there was not a consistent lead configuration. Therefore, in cases where multiple ECG recordings were present, those listed first were utilized.

3.3.3 Analysis

Both algorithms were executed with all samples (except the Normal Sinus Rhythm dataset, from which only the first thirty minutes of each tracing were used), and their outputs were compared to the annotations for each dataset. Accurate detection was indicated if the annotated R peak fell within 150 milliseconds of the algorithm-detected R peak, which is consistent with the ANSI/AAMI guidelines [162]. Other classification possibilities were false positive, false negative, and failed detection. These findings were summarized by calculations for correctness including total error rate, sensitivity, positive predictive value, accuracy, and F1, which were mathematically defined as:

$$\text{Total Error Rate} = \frac{\boldsymbol{FN + FP}}{\boldsymbol{TB}} \tag{8}$$

$$\text{Sensitivity} = \frac{\boldsymbol{TP}}{\boldsymbol{TP + FN}} \tag{9}$$

$$\text{Positive Predictive Value} = \frac{\boldsymbol{TP}}{\boldsymbol{TP + FP}} \quad (10)$$

$$\text{Accuracy} = \frac{\boldsymbol{TP}}{\boldsymbol{TP + FP + FN}} \quad (11)$$

$$\text{F1} = \frac{(\boldsymbol{2 * TP})}{\boldsymbol{2 * TP + FP + FN}} \quad (12)$$

where FN is False Negatives (annotated beats that are not detected); FP is False Positives (beats detected not corresponding to an annotated beat); TB is Total Beats (sum of annotated beats); and TP is True Positives (annotated beats that are correctly detected). True negatives are not typically used to calculate the accuracy of QRS detection [134,139]. The processing time of each ECG sample was measured and expressed on the basis of ten seconds of ECG data. A computational efficiency factor was defined as the ratio of times to execute each sample (Pan–Tompkins to AMPT).

For a fair comparison across datasets, the analysis was repeated by resampling all data to 200 Hz. In this way, all ECGs were filtered using the same cut-off frequencies.

3.4 Results

As compared to the Pan–Tompkins algorithm, the AMPT algorithm was computationally more efficient across all datasets (Figure 3.1). For the Pan–Tompkins algorithm, processing times varied from a low of 12.38 milliseconds per ten seconds of ECG data for the TeleHealth dataset to a high of 50.24 milliseconds for the Paced Rhythms dataset, whereas for the AMPT algorithm, the shortest processing time was 1.09 milliseconds per ten seconds of ECG data for the Normal Sinus Rhythm dataset and the longest was 4.56 milliseconds for the Low Quality dataset. As indicated by the efficiency factor and relative to the Pan–Tompkins, the AMPT algorithm improved computational efficiency by a minimum factor of 4.0 for the Low Quality dataset and a maximum of 21.2 for the Paced Rhythms dataset. Intermediate efficiency factors were 8.3, 4.7, 16.4, and 15.8 for the High Quality, TeleHealth, Normal Sinus Rhythms, and Arrhythmias' datasets, respectively.

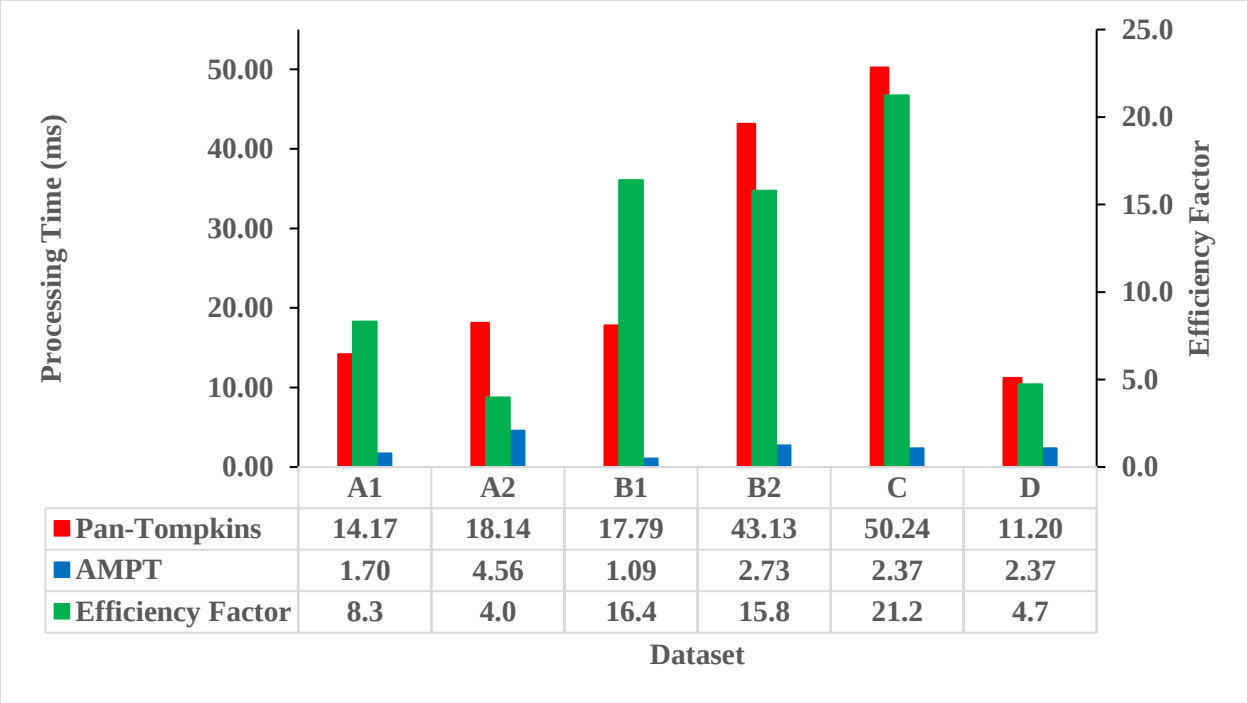

Figure 3.1. Processing times per ten seconds of ECG data for the Pan–Tompkins (red) and AMPT (blue) algorithms with their efficiency factors (green) by dataset. A1 = High Quality, A2 = Low Quality, B1 = Normal Sinus Rhythm, B2 = Arrhythmias, C = Paced Rhythm, and D = TeleHealth datasets.

The AMPT algorithm was also more correct than the Pan–Tompkins algorithm ac-cording to F1 (Figure 3.2). For the Pan–Tompkins algorithm, the F1 had a low of 75.45 for the Paced Rhythms dataset and a high of 99.63 for the High Quality dataset, where-as for the AMPT algorithm, the F1 low was 83.28 for the TeleHealth dataset and the high was 99.81 for the High Quality dataset. From the Pan–Tompkins to the AMPT algorithms, the F1 improvement was highest for the Paced Rhythm dataset with a difference of 20.52%. F1 improvements of 3–5% were also demonstrated with the Low Quality and TeleHealth datasets. Across all other measures including error rate, sensitivity, positive predictive value, and accuracy, and for all datasets, the AMPT algorithm was correct more often than the Pan–Tompkins (Table 3.2).

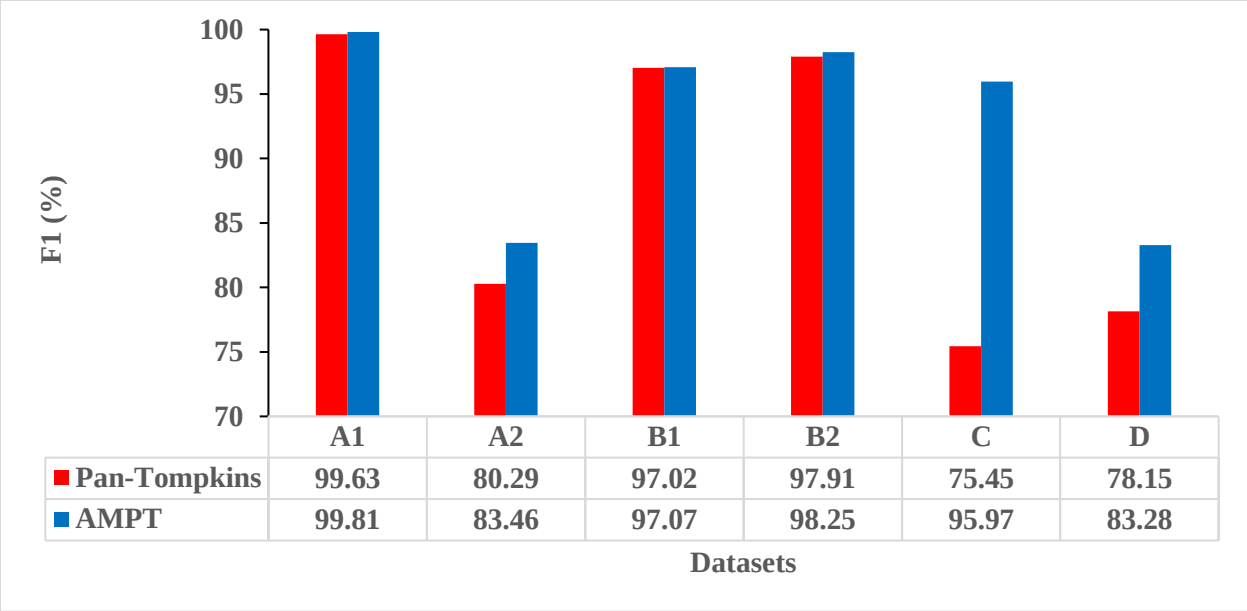

Figure 3.2. F1 correctness for the Pan–Tompkins (red) and AMPT (blue) algorithms by dataset. A1 = High Quality, A2 = Low Quality, B1 = Normal Sinus Rhythm, B2 = Arrhythmias, C = Paced Rhythm, and D = TeleHealth datasets.

Table 3.2. Correctness of the Pan–Tompkins and AMPT algorithms by dataset. A1 = High Quality, A2 = Low Quality, B1 = Normal Sinus Rhythm, B2 = Arrhythmias, C = Paced Rhythm, and D = TeleHealth datasets.

Dataset	Annotated Peaks	Algorithm	True Positives (Beats)	False Positives (Beats)	False Negatives (Beats)	Failed Detection (Beats)	Error Rate (%)	Sensitivity (%)	Positive Predictive Value (%)	Accuracy (%)
A1	72,415	Pan–Tompkins	72,073	191	348	539	0.74	99.51	99.75	99.26
		AMPT	72,267	135	148	283	0.39	99.80	99.82	99.62
A2	78,618	Pan–Tompkins	64,653	11137	14,065	25,202	32.06	80.75	85.12	74.09
		AMPT	64,993	8671	13,639	22,310	28.38	82.06	86.37	78.54
B1	48,494	Pan–Tompkins	45,231	134	2988	3122	6.44	95.08	99.74	94.85
		AMPT	45,301	8	3083	3091	6.37	94.97	99.98	94.96
B2	103,724	Pan–Tompkins	99,783	349	3720	4069	3.92	96.36	99.66	96.09
		AMPT	100,135	144	3380	3524	3.40	96.80	99.83	96.66
C	8923	Pan–Tompkins	6684	2132	2238	4370	48.97	74.93	75.97	64.26
		AMPT	8468	276	454	730	8.18	96.90	95.07	92.81
D	6708	Pan–Tompkins	3218	972	522	1494	40.10	84.92	77.56	68.91
		AMPT	3394	707	334	1041	27.94	90.00	81.04	76.29

Within the Arrhythmia dataset, processing times per ten seconds of ECG data and all measures of correctness varied by sample for the Pan–Tompkins and AMPT algorithms (Tables 3.A1 and 3.A2, respectively (Appendix 3.7)). The efficiency gain was less for samples with high amplitude variability or a large number of arrhythmias, and this was determined qualitatively (Figure 3.A1).

After resampling and reprocessing all data at 200 Hz, the relative performance of each algorithm did not change across datasets. The AMPT algorithm was still computationally more efficient and more correct than the original Pan–Tompkins algorithm (Figures 3.A2 and 3.A3 (Appendix 3.7)). However, the processing times of the resampled data were less than those prior to resampling because there were fewer data points to process.

3.5 Discussion

In evaluating archived and independently annotated ECG data, the AMPT algorithm was both computationally more efficient and more correct than the Pan–Tompkins method. These differences are attributed to the removal of unnecessary, parallel computations, including the double signal analysis for peak detection and one of the two average RR intervals.

Efficiency improvements are dramatic enough to potentially enable the translation of the AMPT algorithm to a mobile platform. However, the AMPT algorithm is relatively less advantageous for processing samples with high amplitude variability or a large number of arrhythmias, as observed by comparing samples with extreme values.

The AMPT algorithm improved F1 correctness by 3–5% for the Low Quality and TeleHealth datasets compared to the Pan–Tompkins, which is significant because these data are most similar to those signals that would be recorded and processed from mobile platforms and wearable technologies. Additionally, with the exception of the sensitivities determined from the Normal Sinus Rhythm dataset, across all dimensions of correctness including total error rate, sensitivity, positive predictive value, accuracy, and F1, the AMPT algorithm outperformed the Pan–Tompkins algorithm for all datasets. Some of the correctness improvements are modest, but they demonstrate that algorithm changes to enhance computational efficiency did not sacrifice accuracy.

AMPT performance was compared to that of Pan–Tompkins; however, it is not possible to directly compare the performance of the AMPT algorithm to other QRS detection algorithms reported in the literature. Inconsistencies in hardware prevent comparison of computational efficiency [139,144–149,155], while non-uniform, and unexplained or selective exclusion of data, variations in the temporal width of the detection window, and discrepancies among sampling rates

make the direct comparison of accuracies not practical [139–143,149,152,155]. Nonetheless, other studies compare their results to those of Pan–Tompkins [139–149,152,155], and most are faster and more accurate across publicly available datasets, which is consistent with our findings. Therefore, the AMPT would likely be competitive with the computational efficiency and accuracy of other algorithms.

In this analysis, all samples and beats from the High Quality, Low Quality, Arrhythmias, and Paced Rhythms datasets were included because complete sets are most representative of patient or consumer data that would be evaluated in real-time (i.e., continuous analysis of data on a beat-to-beat basis without accumulating a backlog of unanalyzed beats). However, only the first thirty minutes of data from the Normal Si-nus Rhythm dataset were studied here because longer periods had excessive computational demands, while thirty minutes per sample was still deemed long enough to determine the relative performance of each algorithm. The exclusion of the TeleHealth samples also does not affect the findings of this study because in most cases, neither algorithm was able to detect the few annotated beats available for analysis in the excluded samples.

The AMPT algorithm was motivated by development of a smart t-shirt that monitors and analyzes a single-lead ECG recording in real-time [163,164]. Initially, the Pan–Tompkins method was utilized with a prototype device; however, there were substantial computational delays and consequent data loss. Therefore, the AMPT algorithm was written to be more computationally efficient, while having improved QRS detection capabilities. In conjunction with the smart t-shirt and on a mobile platform, the AMPT algorithm eliminated the prior delays and data loss and processed the data in real-time without lagging (data not presented).

While demand for computationally efficient ECG analysis algorithms will remain strong due to the need to conserve the energy of battery-powered devices [155], continued advances in mobile device processing speed will diminish the dependency on efficient algorithms to deliver a single ECG analysis outcome. Instead, an efficient QRS detection algorithm will allow for greater complexity of other aspects of parallel ECG analysis such as P- and T-wave analyses [153,154].

This study is limited in that it is a retrospective analysis, and the corresponding patients and pathologies may not represent those of the general population. A more comprehensive future study is necessary to assess the AMPT algorithm’s performance in real-time and with a larger, more diverse patient population. Another limitation is that this study was performed via a desktop computer (rather than on a mobile device) because a consistent platform was necessary to

standardize conditions and enable direct comparison of the algorithms' computational efficiency. Nonetheless, real world application and evaluation will need to feature mobile devices running different operating systems and a variety of other simultaneous applications.

3.6 Conclusion

As compared to the Pan–Tompkins algorithm, the AMPT algorithm demonstrated improved computational efficiency of QRS detection while also enhancing correctness. When applied on a mobile platform, the AMPT algorithm was observed to eliminate processing delays and data loss, which may enable continuous, real-time, QRS detection on a variety of mobile devices. However, these data were not representative of a clinical trial or field test. Additional studies are necessary to move this technology towards continuous, real-time monitoring of patients and recreational users.

3.7 Appendix

Table 3.A1. Processing time per ten seconds of ECG data and correctness of the Pan-Tompkins algorithm for the Arrhythmias dataset (B2) by sample.

Sample	Processing time (ms)	Total (Annotated Beats)	Peaks Detected	True Positives	False Positives	False Negatives	Failed Detection (Beats)	Total Error Rate (%)	Sensitivity (%)	Positive Predictive Value (%)	Accuracy (%)	F1 (%)
100	42.71	2274	2270	2270	0	4	4	0.18	99.82	100.00	99.82	99.91
101	38.71	1874	1866	1865	1	9	10	0.53	99.52	99.95	99.52	99.73
103	39.15	2091	2080	2080	0	11	11	0.53	99.47	100.00	99.47	99.74
105	40.11	2691	2604	2556	48	115	163	6.06	95.69	98.16	95.69	96.91
106	42.18	2098	2016	2016	0	82	82	3.91	96.09	100.00	96.09	98.01
108	40.71	1824	1778	1755	23	59	82	4.50	96.75	98.71	96.75	97.72
109	53.47	2535	2523	2523	0	12	12	0.47	99.53	100.00	99.53	99.76
111	46.44	2133	2121	2118	3	15	18	0.84	99.30	99.86	99.30	99.58
112	45.69	2550	2536	2535	1	15	16	0.63	99.41	99.96	99.41	99.69
113	36.80	1796	1792	1792	0	4	4	0.22	99.78	100.00	99.78	99.89
114	37.58	1890	1426	1384	42	506	548	28.99	73.23	97.05	73.23	83.47
115	39.93	1962	1950	1950	0	10	10	0.51	99.49	100.00	99.49	99.74
116	45.40	2421	2387	2386	1	35	36	1.49	98.55	99.96	98.55	99.25
117	35.67	1539	1532	1532	0	7	7	0.45	99.55	100.00	99.55	99.77
118	44.88	2301	2276	2275	1	25	26	1.13	98.91	99.96	98.91	99.43
119	39.75	2094	1984	1984	0	110	110	5.25	94.75	100.00	94.75	97.30
121	36.72	1876	1859	1859	0	14	14	0.75	99.25	100.00	99.25	99.62
122	38.10	2479	2472	2472	0	6	6	0.24	99.76	100.00	99.76	99.88
123	34.03	1519	1515	1515	0	4	4	0.26	99.74	100.00	99.74	99.87
124	41.84	1634	1606	1606	0	28	28	1.71	98.29	100.00	98.29	99.14
200	44.88	2792	2598	2593	5	197	202	7.23	92.94	99.81	92.94	96.25
201	39.06	2039	1894	1894	0	145	145	7.11	92.89	100.00	92.89	96.31
202	41.12	2146	2117	2117	0	28	28	1.30	98.69	100.00	98.69	99.34
203	50.60	3108	2914	2897	17	175	192	6.18	94.30	99.42	94.30	96.79

205	44.27	2672	2650	2648	2	17	19	0.71	99.36	99.92	99.36	99.64
207	54.98	2385	2170	2152	18	227	245	10.27	90.46	99.17	90.46	94.61
208	47.65	3040	2868	2717	151	317	468	15.39	89.55	94.74	89.55	92.07
209	50.26	3052	3003	3002	1	43	44	1.44	98.59	99.97	98.59	99.27
210	46.52	2685	2580	2574	6	108	114	4.25	95.97	99.77	95.97	97.83
212	45.05	2763	2747	2743	4	18	22	0.80	99.35	99.85	99.35	99.60
213	45.22	3294	3242	3242	0	52	52	1.58	98.42	100.00	98.42	99.20
214	42.10	2297	2255	2253	2	43	45	1.96	98.13	99.91	98.13	99.01
215	52.60	3400	3351	3351	0	36	36	1.06	98.94	100.00	98.94	99.47
219	47.48	2312	2151	2151	0	89	89	3.85	96.03	100.00	96.03	97.97
220	36.98	2069	2044	2044	0	25	25	1.21	98.79	100.00	98.79	99.39
221	42.44	2462	2419	2419	0	40	40	1.62	98.37	100.00	98.37	99.18
222	45.57	2634	2475	2466	9	155	164	6.23	94.09	99.64	94.09	96.78
223	43.05	2643	2590	2590	0	53	53	2.01	97.99	100.00	97.99	98.99
228	44.79	2141	2060	2047	13	91	104	4.86	95.74	99.37	95.74	97.52
230	40.27	2466	2252	2252	0	213	213	8.64	91.36	100.00	91.36	95.48
231	36.80	2011	1568	1568	0	443	443	22.03	77.97	100.00	77.97	87.62
232	45.92	1816	1779	1778	1	33	34	1.87	98.18	99.94	98.18	99.05
233	51.65	3152	3068	3068	0	82	82	2.60	97.40	100.00	97.40	98.68
234	38.54	2764	2744	2744	0	19	19	0.69	99.31	100.00	99.31	99.65
Totals	**1897.67**	**103724**	**100132**	**99783**	**349**	**3720**	**4069**	**3.92**	**96.36**	**99.66**	**96.36**	**97.91**

Table 3.A2. Processing time per ten seconds of ECG data and correctness of the AMPT algorithm for the Arrhythmias dataset (B2) by sample.

Sample	Processing time (ms)	Total (Annotated Beats)	Peaks Detected	True Positives	False Positives	False Negatives	Failed Detection (Beats)	Total Error Rate (%)	Sensitivity (%)	Positive Predictive Value (%)	Accuracy (%)	F1 (%)
100	2.69	2274	2271	2271	0	3	3	0.13	99.87	100.00	99.87	99.93
101	1.91	1874	1865	1863	2	10	12	0.64	99.47	99.89	99.36	99.68
103	2.00	2091	2084	2084	0	7	7	0.33	99.67	100.00	99.67	99.83
105	1.91	2691	2577	2555	22	114	136	5.05	95.73	99.15	94.95	97.41
106	2.26	2098	2026	2026	0	72	72	3.43	96.57	100.00	96.57	98.25
108	2.17	1824	1762	1682	80	134	214	11.73	92.62	95.46	88.71	94.02
109	2.00	2535	2530	2530	0	5	5	0.20	99.80	100.00	99.80	99.90
111	2.26	2133	2123	2123	0	9	9	0.42	99.58	100.00	99.58	99.79
112	2.26	2550	2539	2539	0	10	10	0.39	99.61	100.00	99.61	99.80
113	1.82	1796	1794	1794	0	2	2	0.11	99.89	100.00	99.89	99.94
114	3.56	1890	1855	1849	6	41	47	2.49	97.83	99.68	97.52	98.74
115	1.82	1962	1952	1952	0	8	8	0.41	99.59	100.00	99.59	99.80
116	2.60	2421	2391	2389	2	32	34	1.40	98.68	99.92	98.60	99.29
117	2.00	1539	1534	1534	0	5	5	0.32	99.68	100.00	99.68	99.84
118	2.60	2301	2277	2277	0	21	21	0.91	99.09	100.00	99.09	99.54
119	2.08	2094	1987	1987	0	107	107	5.11	94.89	100.00	94.89	97.38
121	1.91	1876	1862	1862	0	11	11	0.59	99.41	100.00	99.41	99.71
122	2.00	2479	2475	2475	0	3	3	0.12	99.88	100.00	99.88	99.94
123	2.17	1519	1514	1514	0	5	5	0.33	99.67	100.00	99.67	99.84
124	1.91	1634	1619	1619	0	15	15	0.92	99.08	100.00	99.08	99.54
200	2.17	2792	2597	2596	1	192	193	6.91	93.11	99.96	93.08	96.42
201	3.12	2039	1908	1908	0	131	131	6.42	93.58	100.00	93.58	96.68
202	2.17	2146	2131	2131	0	14	14	0.65	99.35	100.00	99.35	99.67
203	3.65	3108	2708	2703	5	376	381	12.26	87.79	99.82	87.65	93.42
205	2.00	2672	2636	2636	0	32	32	1.20	98.80	100.00	98.80	99.40
207	3.47	2385	2101	2093	8	278	286	11.99	88.27	99.62	87.98	93.60
208	3.73	3040	2908	2904	4	130	134	4.41	95.72	99.86	95.59	97.74
209	2.00	3052	2986	2986	0	56	56	1.83	98.16	100.00	98.16	99.07
210	2.08	2685	2580	2579	1	103	104	3.87	96.16	99.96	96.12	98.02
212	2.08	2763	2747	2747	0	14	14	0.51	99.49	100.00	99.49	99.75
213	2.43	3294	3246	3246	0	48	48	1.46	98.54	100.00	98.54	99.27
214	1.91	2297	2257	2257	0	39	39	1.70	98.30	100.00	98.30	99.14
215	2.26	3400	3342	3342	0	49	49	1.44	98.55	100.00	98.55	99.27
219	2.43	2312	2147	2147	0	115	115	4.97	94.92	100.00	94.92	97.39
220	2.00	2069	2045	2045	0	24	24	1.16	98.84	100.00	98.84	99.42
221	2.34	2462	2409	2409	0	49	49	1.99	98.01	100.00	98.01	98.99
222	4.60	2634	2422	2414	8	205	213	8.09	92.17	99.67	91.89	95.77
223	2.17	2643	2602	2602	0	41	41	1.55	98.45	100.00	98.45	99.22
228	2.78	2141	2046	2045	1	89	90	4.20	95.83	99.95	95.78	97.85
230	2.43	2466	2255	2255	0	210	210	8.52	91.48	100.00	91.48	95.55
231	2.26	2011	1571	1571	0	440	440	21.88	78.12	100.00	78.12	87.72
232	18.23	1816	1781	1777	4	33	37	2.04	98.18	99.78	97.96	98.97
233	2.08	3152	3065	3065	0	87	87	2.76	97.24	100.00	97.24	98.60
234	1.82	2764	2752	2752	0	11	11	0.40	99.60	100.00	99.60	99.80
Totals	**120.13**	**103724**	**100279**	**100135**	**144**	**3380**	**3524**	**3.40**	**96.80**	**99.83**	**96.66**	**98.25**

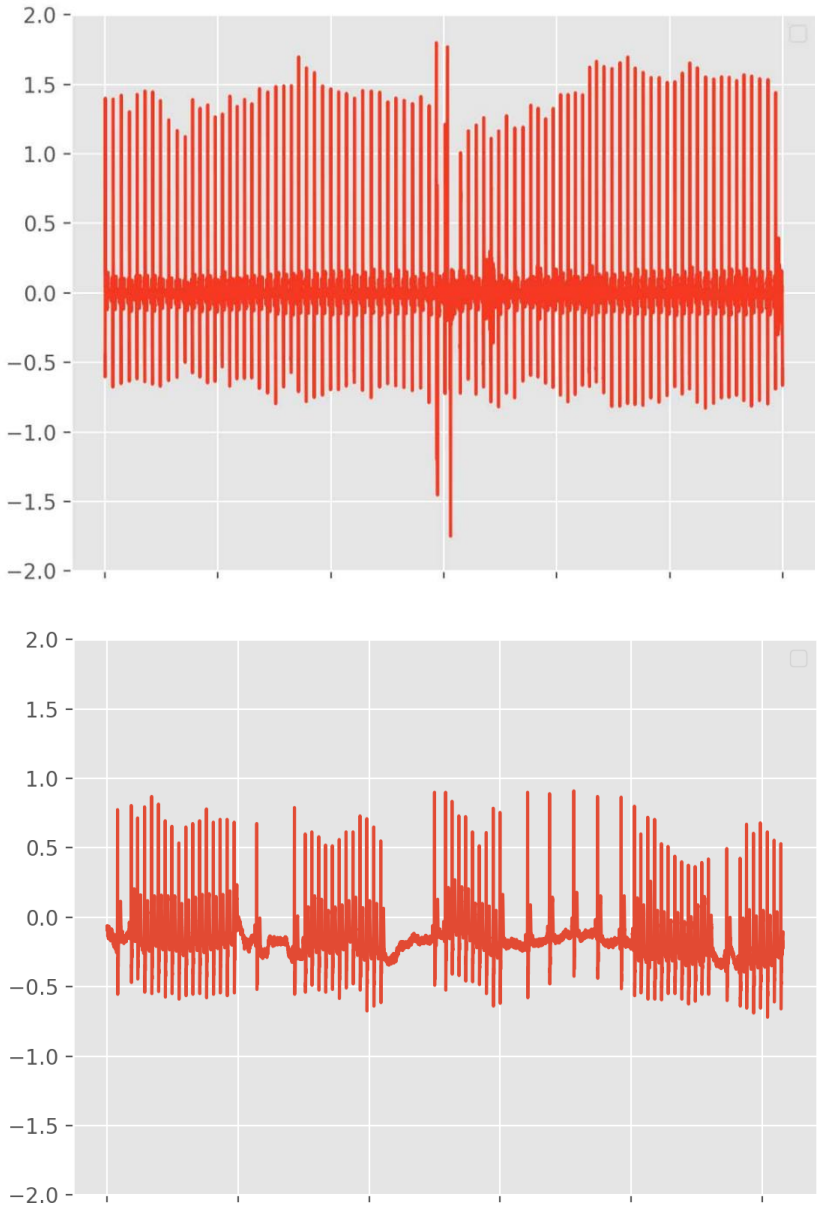

Figure 3.A1. Representative raw ECG signals for samples 101 (top) and 232 (bottom) of the Arrythmias dataset (B2) visually demonstrating differences in amplitude variability and the number of arrythmias.

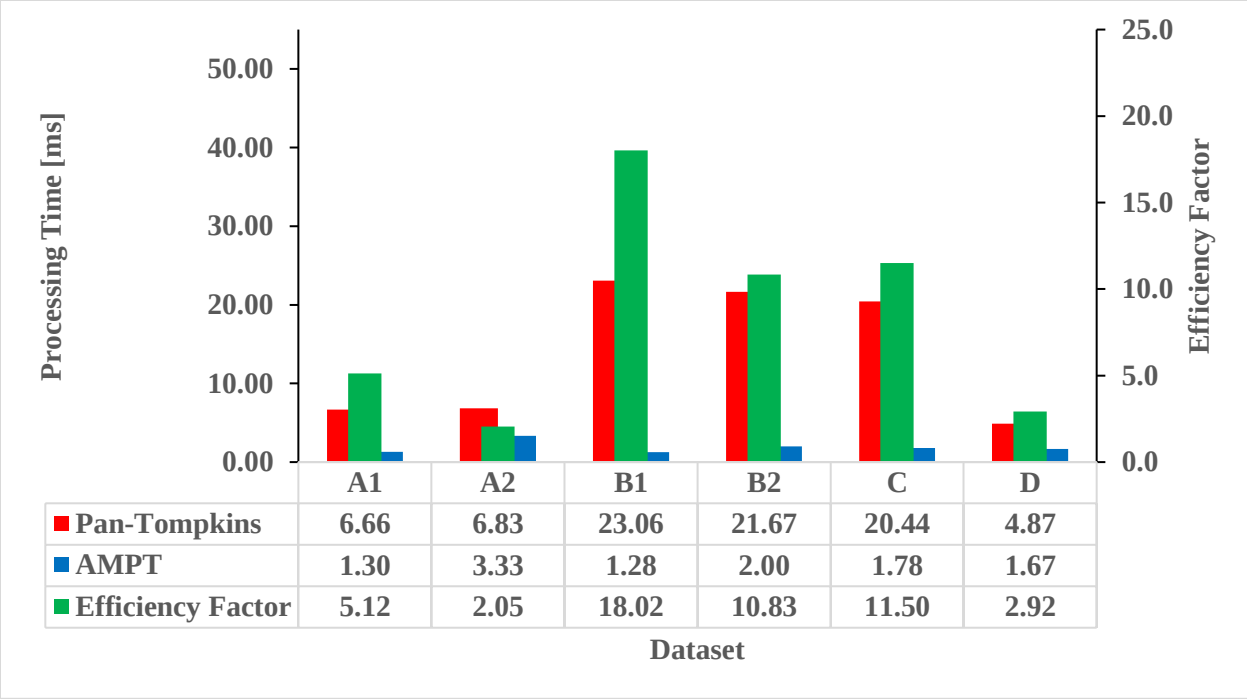

Figure 3.A2. Processing time per ten seconds of ECG data for the Pan-Tompkins (red) and AMPT (blue) algorithms with their efficiency factors (green) by dataset. A1 = High-Quality, A2 = Low-Quality, B2 = Arrhythmias, C = Paced Rhythm, and D = Telehealth datasets after resampling to 200 Hz.

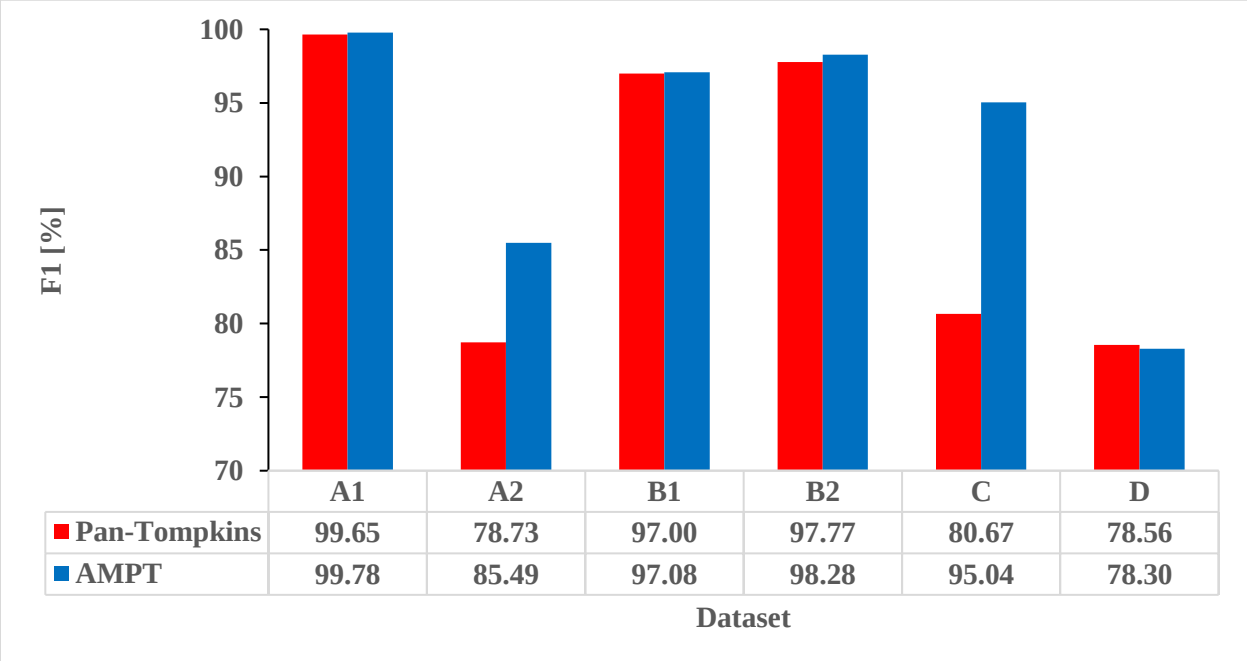

Figure 3.A3. F1 correctness for the Pan-Tompkins (red) and AMPT (blue) algorithms by dataset. A1 = High-Quality, A2 = Low-Quality, B2 = Arrhythmias, C = Paced Rhythm, and D = Telehealth datasets after resampling to 200 Hz.

4. Sudden Cardiac Arrest Prediction via Deep Learning Electrocardiogram Analysis

from the manuscript:

Sudden Cardiac Arrest Prediction via Deep Learning Electrocardiogram Analysis

L. Neri, M. T. Oberdier, A. Orro, R. T. Carrick, M. S. Nobile, S. Jaipalli, S. Diciotti, C. Borghi, H. R. Halperin

Paper in preparation for submission to *Circulation: Arrhythmia and Electrophysiology*

4.1 Abstract

Sudden Cardiac Arrest (SCA) is a potentially fatal event that can affect people of all ages, many times occurring without warning. Development of clinical tools to detect those individuals at risk for such events before they occur would save lives. The electrocardiogram, combined with recent advancements in artificial intelligence algorithms are showing promising results for SCA prediction. This research aims to develop a tool to identify the possible risk of SCA using electrocardiograms recorded prior to the event processed with deep learning model. This was a case-control analysis of patients who had electrocardiogram obtained between the same day to one year prior to SCA. We developed a novel deep-learning model that process the inputs, i.e., the patient electrocardiogram along with age and sex, and predicts the likelihood of subsequent SCA. The model was developed, validated, and tested using data from a publicly-available dataset, with 80% (n=1013 individuals) used for model training, 10% (n=127) for validation, and 10% (n=127) for testing. The model demonstrated good performance in identifying those patients at risk for SCA (AUC 0.774). At a sensitivity of 95%, model specificity was 31.1%. Thus, our study shows the potential of deep learning to predict SCA. Further development requiring larger datasets and external validation is needed.

4.2 Introduction

Sudden cardiac arrest (SCA) affects about 650,000 people per year in the United States [91] with successful cardiopulmonary resuscitation (CPR) rates only around 10% [165]. A major limitation in the prevention of SCA is that 20-25% of events involve individuals who have no risk factors [166–168], and over 50% of cardiac arrests occur in patients with undiagnosed heart disease [169–171]. That is, many of those who are most likely to need emergent care are the most unlikely to expect such an event or to be aware of the need to take precautionary or preventative measures. In addition, 60% of SCA's occur outside the hospital where immediate intervention is not available [172–174].

Towards improving outcomes and enabling proactions, risk factor (e.g. age, sex, race) analysis has been used to predict SCA, but this approach is only able to explain a small portion of SCA's [175]. Further, age and sex are among the most strongly predictive SCA factors; however, age and sex

are generic cardiovascular risk factors and are thus not valuable in distinguishing SCA from other potential cardiovascular events. Beyond risk factors, the electrocardiogram (ECG) has strong potential to predict SCA because it is inexpensive, non-invasive, provides real-time data, and is particularly valuable for detecting cardiac anomalies [133]. Summary features extracted from the ECG (e.g. QRS duration, QT interval) have been investigated for predicting SCA but were found to have limited utility [176,177].

Instead, an emerging opportunity exists to use artificial intelligence as a tool to predict SCA via ECG because of its potential to utilize all ECG data and their relations, not just small clusters such as with the summary feature extraction approach. Machine learning analysis of ECG data has produced strong SCA predictions; however, deep learning has even more profound potential beyond machine learning because of its ability to use large datasets, learn independently, determine complex and non-linear relationships, and be more accurate [178,179]. Therefore, it was hypothesized that ECG data could be used in conjunction with deep learning algorithms to predict imminent SCA's.

4.3 Methods

4.3.1 Dataset

This study was performed with the Nightingale Open Science - Subtyping Cardiac Arrest dataset [180,181]. The data consists of individuals who had their ECG's recorded between one day and ten years prior to having a cardiac arrest and who upon having SCA, presented in the Emergency Department (ED). A control group of patients consisted of individuals who visited the ED on the same day as a case from the SCA group but who did not have a cardiac arrest. For all arrest and control patients, ECG recordings consisted of ten second recordings at a sampling rate of 500 Hz across twelve leads.

There were 221 cardiac arrest cases and 1046 controls used in the analysis (Table 4.1). The main analysis uses ECG data acquired one day prior to arrest; however, supplemental analyses were performed with varying ranges of time between ECG data recording and arrest events. (Figures 4.1 and 4.A1). The control group used in the analysis were subjects who had an ECG

recorded within 1 month and 2 years (Figure 4.A2) . The controls were selected to be age and sex balanced with the SCA patients, and age and sex data were used in the main analysis.

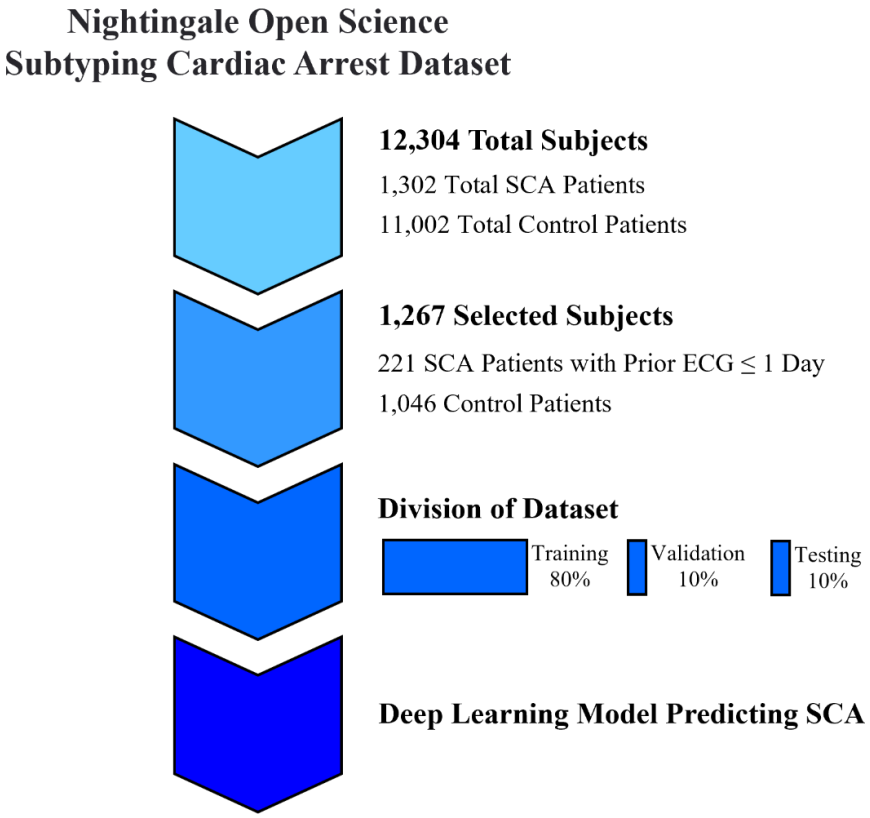

Figure 4.1. Overview of the selection of subjects and dataset division for the base deep learning model.

Table 4.1. Characteristics of the subjects used as input for the base model. Values are mean (standard deviation).

Variable	Controls [n=1046]	Cardiac Arrest [n=221]
Age [Years]	69.7 (12.3)	68.5 (15.5)
Sex [Men]	549	146

4.3.2 Preprocessing

Each signal was separated into segments (about 10 per signal depending on the heart rate) that were centered around the R waves via high-quality detectors [133,182]. Intervals of 720 milliseconds (360 milliseconds on either side of the R-wave) were used for the base analysis. Therefore, for each individual, ECG data consisting of twelve leads and approximately ten cardiac

cycles were provided as independent inputs to the deep learning model while assuring that there was no overlap of individuals in the data partitions (training, validation, and testing).

4.3.3 Deep Learning Model

The deep learning model was implemented in Python (version 3.10) with TensorFlow (version 2.12.0) [183] and other libraries (biosppy 1.0.0, matplotlib 3.7.1, neurokit2 0.2.4, numpy 1.23.5, pandas 2.0.1, and scikit-learn 1.2.2). The model consisted of three modules: ECG, age, and sex data were processed separately, and a final layer concatenated the three outputs (Figure 4.2). The ECG module is a sequence of four one-dimensional convolutional blocks followed by max pooling. The four blocks used 64, 128, 256, and 512 filters while the kernel size and max pooling size were maintained at 7 and 2, respectively.

The modules for sex and age used binary and normalized values, respectively, and processed them through a dense layer with sixteen outputs. We adopted an Adam optimizer, a cross-entropy loss function, and a 0.001 learning rate.

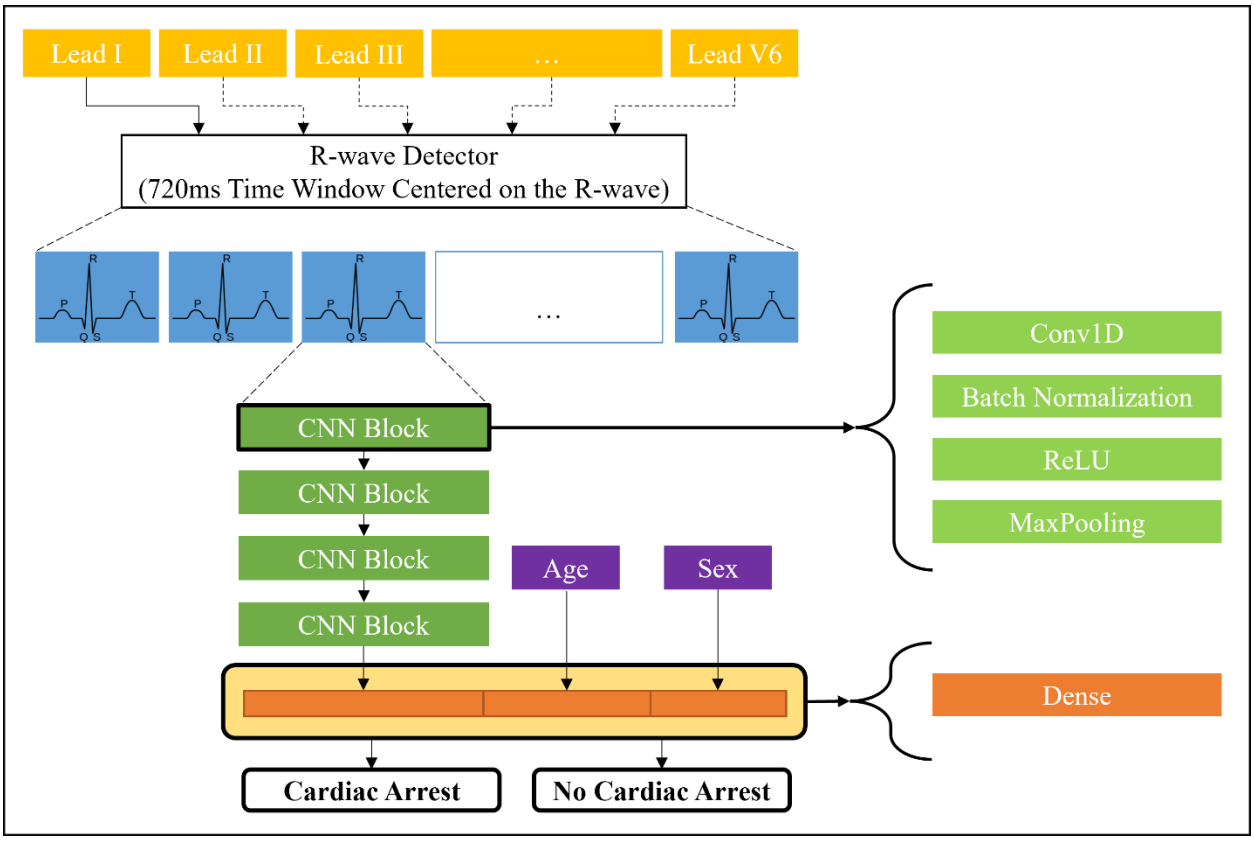

Figure 4.2. Architecture of the base deep learning model.

4.3.4 Training

The dataset was randomly split into training (80%), validation (10%), and testing (10%) sets while ensuring there was not an overlap of individuals among the groups. Model training was performed separately for each lead, and overall results are presented as the average for each lead. Cross validation was performed by repeating the experiment nine times. For each experiment, accuracy, specificity, F1, positive predictive value (PPV), and negative predictive value (NPV) were computed while setting the level of sensitivity at 95% and area under the receiver operating characteristic curve (AUROC) for both training and validation set.

4.3.5 Testing and Post-Processing

Among fifty epochs, the best performing experiment on the validation set was selected based on the highest area under the receiver operating characteristic curve (AUC). Additional computed measures of performance include accuracy, F1, PPV, NPV, and specificity. Each experiment was repeated nine times and performance metrics reported as average and standard deviation.

To gain a visual understanding of the deep learning model's decision strategy when analyzing the temporal evolution ECG signal, we employed GRAD-CAM (Gradient-weighted Class Activation Mapping) [184].

For each lead and each SCA of the test set, activation maps were taken for each of the four CNN layers and summed together, and a final image is obtained by overlapping the map and the ECG. One hundred GRAD-CAM images were then randomly selected, and for each lead, subjective tallies were made corresponding to the region of the ECG (i.e., P wave, P-Q interval, QRS complex, S-T interval, and T wave) that were most influential in determining SCA.

4.3.6 Models Generated with Varying Inputs

The base model (X) was generated with inputs including age and sex, ECG’s recorded within one day of arrests, all types of arrests (regardless of presenting rhythm), and ECG data within a window of 720 milliseconds around the R wave (Figure 4.3). However, additional models were created in which these inputs were varied. Specifically, a model was created in which age and sex were not inputs (A1). Another series of models were generated in which the times between ECG recording and SCA were varied from less than one week, less than one month, between one day and one

month, and between one month and one year (B1-B4, respectively). A third group of models were created by limiting the presenting rhythms to those that were non-shockable (C1) or only pulseless electrical activity (C2) (Figure 4.A3). A final set of models were generated with input data obtained when the window around the R wave was 600 or 500 milliseconds (D1 and D2, respectively).

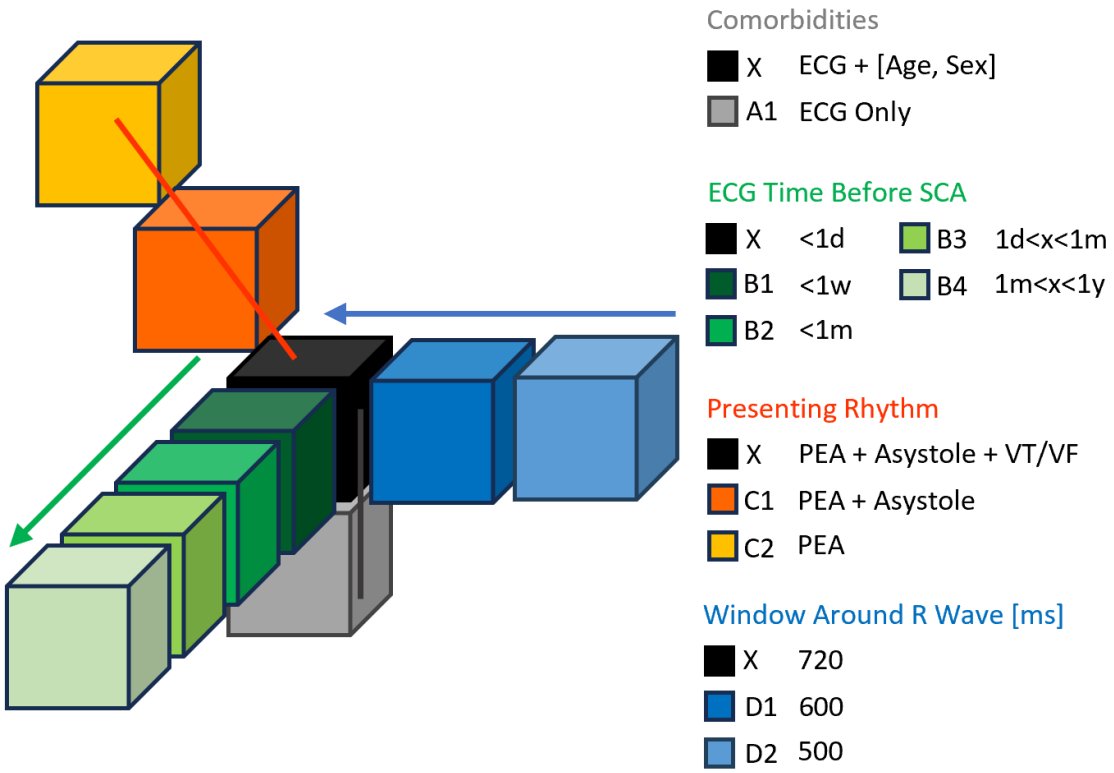

Figure 4.3. The base model consisting of age and sex with ECG data less than one day prior to arrest and a window around the R wave of 720 milliseconds (X). Variations of the base model were explored to determine the influence of variations of input data. d is day, w is week, m is month, y is year, ECG is electrocardiogram, SCA is sudden cardiac arrest, PEA is pulseless electrical activity, VT = ventricular tachycardia, VF = ventricular fibrillation)

4.4 Results

The ROC curves computed for training, validation, and testing set resulted in AUCs of 0.98, 0.91, and 0.85, respectively (Figure 4.4).

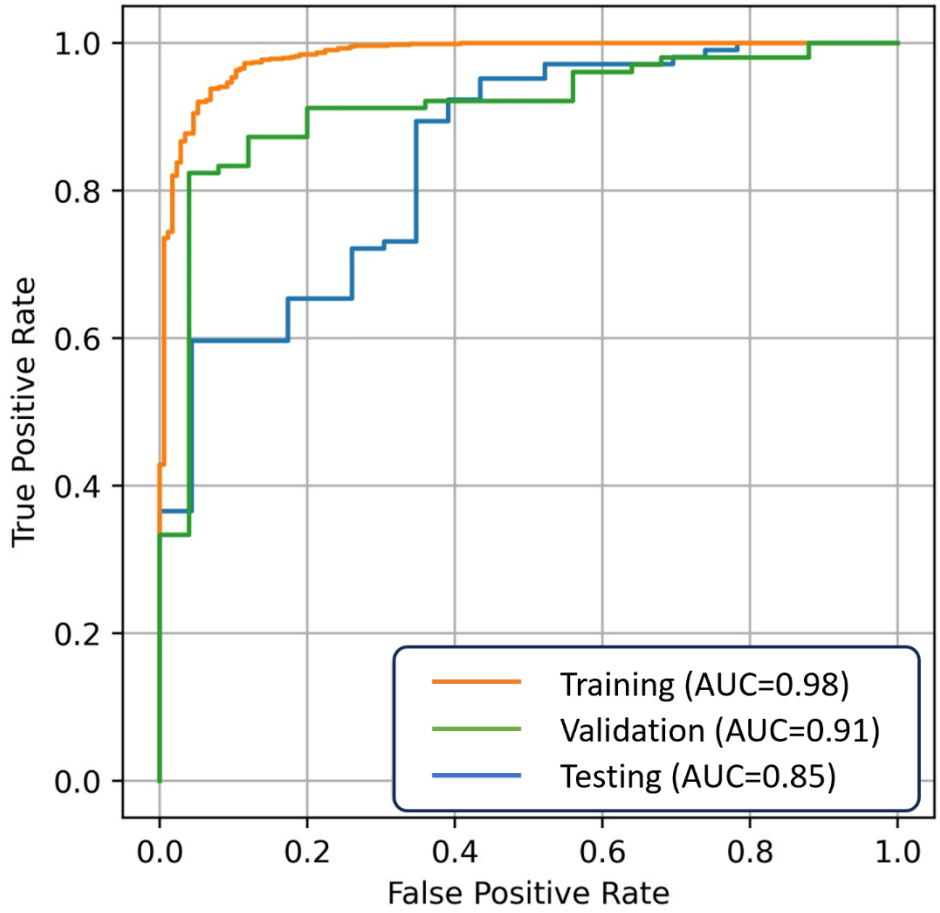

Figure 4.4. Receiver operating characteristic curve for one replicate experiment of the base deep learning model during training, validation, and testing.

With sensitivity fixed at 95% and across nine experiments, the base deep learning model had an average AUROC of 0.774, which was 84.8% accurate and 31.1% specific. Other obtained values of performance include 91.3% F1, 87.8% PPV, and 52.2% NPV (Table 4.2, Figure 4.4). When age and sex were not included as model input data, the AUC was 0.775. When the time between ECG recording and SCA was increased, AUC was 0.76 for data gathered within one week of arrest and 0.574 for data collected between one month and one year prior to arrest. Reducing the input data to only include non-shockable presenting rhythms resulted in an AUC of 0.769, and further reducing the input data to include only pulseless electrical activity (PEA arrests led to an AUC of 0.773. When the window around the R wave was reduced, the AUC's were 0.766 and 0.753 for 600 and 500 millisecond window widths, respectively.

Table 4.2. Measures of overall performance in the test set with sensitivity fixed at 95% for the base model, X, and its variations (A1, B1, B2, B3, B4, C1, C2, D1, D2). Metric values are reported as mean (standard deviation) of 9 randomized experiments.

Color	Model Input	AUC	Accuracy [%]	F1 [%]	PPV [%]	NPV [%]	Specificity [%]
	X	0.774 (0.046)	84.8 (3.1)	91.3 (1.7)	87.8 (3.1)	52.2 (12.8)	31.1 (10.8)
	A1	0.775 (0.048)	85.1 (2.8)	91.5 (1.5)	88.2 (2.8)	53.5 (13.3)	33.0 (11.4)
	B1	0.760 (0.049)	82.2 (3.0)	89.6 (1.6)	84.7 (3.0)	54.7 (13.0)	27.9 (10.0)
	B2	0.734 (0.042)	79.2 (2.8)	87.6 (1.6)	81.2 (2.8)	57.9 (11.3)	25.4 (8.7)
	B3	0.654 (0.072)	87.6 (2.4)	93.3 (1.2)	91.6 (2.4)	21.7 (14.1)	14.5 (9.9)
	B4	0.574 (0.069)	83.3 (2.4)	90.7 (1.3)	86.7 (2.4)	24.1 (15.4)	11.1 (8.1)
	C1	0.769 (0.053)	87.4 (3.0)	93.0 (1.5)	91.0 (3.0)	46.2 (12.7)	33.1 (11.5)
	C2	0.773 (0.067)	89.6 (2.7)	94.3 (1.4)	93.6 (2.7)	38.5 (12.4)	34.8 (14.0)
	D1	0.766 (0.052)	84.7 (3.4)	91.2 (1.8)	87.7 (3.4)	51.4 (14.0)	30.8 (11.5)
	D2	0.753 (0.056)	84.4 (3.2)	91.0 (1.7)	87.4 (3.2)	50.0 (13.0)	28.5 (10.4)

When individual ECG leads were used as model input to the base model, the AUC varied between 0.716 and 0.809 (III and V5, respectively), accuracy was between 83.6 and 86.2% (aVF and V5, respectively), F1 was between 90.6 and 92% (aVF and V5, respectively), PPV was between 86.7 and 89.2% (aVF, and V5, respectively), NPV was between 45.2 and 59% (aVF and V5, respectively), and specificity was between 23.4 and 40.1% (aVF and V5, respectively) (Table 4.A1). When the modified models were generated with their single leads as input, measures of performance varied but were generally consistent with averages obtained when all twelve leads were simultaneously used. (Tables 4.A1-A10)

Grad-CAM visual analysis revealed a general emphasis on the QRS complex via all lead configurations. (Figure 4.5).

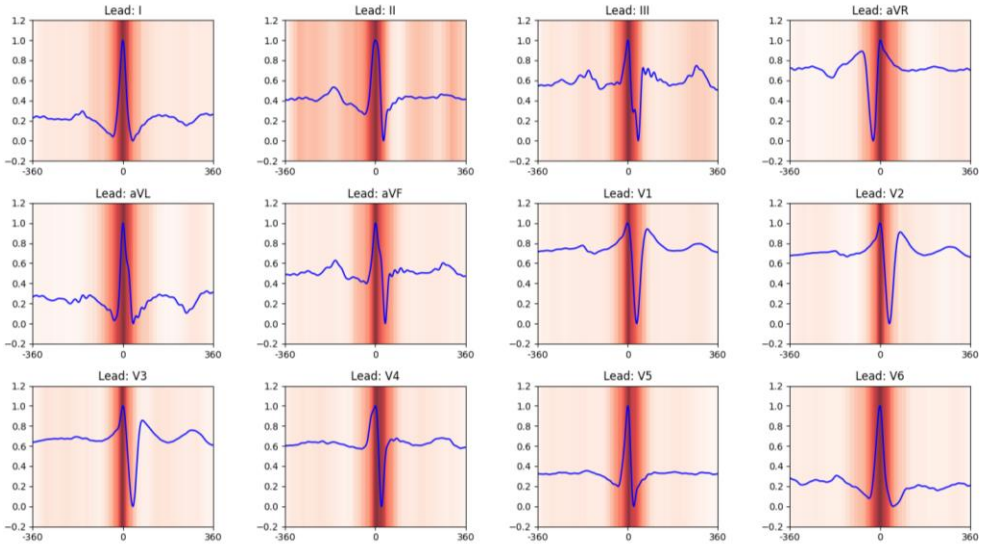

Figure 4.5. Representative GRAD-CAM images from the base case, X, in which only the QRS complex was highlighted. The color map is white (no activation) to red (full activation).

Tallies from one hundred randomly selected GRAD-CAM images (Table 4.3) showed that all but two leads (V3 and V6) had P wave contributions and there were as many as 14 from another lead (V1). All leads had T wave contributions with as few as 3 (AVR) and as many as 22 (V1 and V4) while all leads involved the QRS complex from as few as 94 (AVL) cases to as many as 99 (V3 and V4). The P-Q interval and S-T interval were generally not influential in determining SCA.

Table 4.3. Tallies of the major contributing segments of the ECG to SCA determination from one hundred randomly selected GRAD-CAM images from the base case, X.

	P Wave	P-Q Interval	QRS Complex	S-T Interval	T Wave
I	5	1	96	0	18
II	6	2	96	0	12
III	3	0	96	0	5
AVR	1	0	96	0	3
AVL	5	0	94	0	8
AVF	4	1	96	0	5
V1	14	0	95	0	22
V2	5	1	99	1	17
V3	0	0	99	0	16
V4	2	0	99	1	22
V5	4	0	98	0	20
V6	0	0	98	1	11

4.5 Discussion

This is the first study to utilize the Nightingale Open Science - Subtyping Cardiac Arrest dataset to predict SCA with deep learning. This is also the first deep learning application of ECG data to predict SCA in which determinations were made about the relative contributions of: 1) risk factors such as age and sex, 2) shockable versus non-shockable rhythms, 3) ECG data collected beyond twenty-four hours prior to SCA, 4) ECG data in varying temporal widths around the R wave, and 5) regions of the ECG beyond the QRS complex.

The findings suggest that the value of age and sex in predicting SCA were mostly explained by changes in the ECG. The exclusion of age and sex resulted in only a marginal decrease in SCA prediction performance, and this finding opposes a multi-dimensional “axes of risk” paradigm in

which age, sex, and race were depicted as most influential in predicting SCA while ECG summary parameters were shown to be among the least [175]. Such discrepancy highlights the value of ECG analysis with deep learning for SCA prediction because when unsupervised, the model can utilize characteristics that are beyond the threshold of human perception whereas the "axes of risk" paradigm presumably references ECG summary features that are discernable by a cardiologist.

The analyses were not able to discern differences among the arrythmias associated with SCA. Removing the shockable rhythm arrests from the analysis had negligible influence on the model's performance. This was also true when further removal excluded the asystole cases and left only PEA arrests for analysis. Nonetheless, the sample sizes of excluded analyses in the Nightingale dataset may not have been large enough to capture subtle differences attributable to classifications of presenting rhythm.

Physiologic changes indicative of an SCA are evident up to a year in advance of an event suggesting a more chronic than acute pathologic process leading to arrest in a large number of individuals. ECG data collected beyond twenty-four hours prior to SCA decreased model performance when it was included in the original analysis. However, when viewed in isolation, data from both one day to one month and one month to one year had value in predicting SCA, albeit with diminishing model performance over longer time.

Model performance also diminished with decreasing width around the QRS complex. The finding implies that ECG data relationships beyond the QRS complex confer information about an impending SCA. It is further suggested by the varying width data that as much of the ECG should be included for deep learning analysis with the entirety of the signal being ideal.

The GRAD-CAM data emphasizes, in order of influence, the QRS complex followed by the T wave and then the P wave, suggesting that changes during ventricular depolarization and repolarization predict SCA and that atrial depolarization may also play a role. Whether this influence is due to electrical or mechanical dysfunction, or both is yet to be determined. GRAD-CAM data in conjunction with analyses that isolate presenting rhythms could give prospective insight into pathologic mechanisms and anatomic sources of dysfunction that lead to SCA.

The only other similar study utilizing deep learning with ECG input to predict SCA was performed by Kwon et al [185]. Consistent with our study, ECG data was collected twenty-four hours prior to arrest. However, beyond our scope, Kwon et al. performed both internal and external validation and reported AUC's of 0.91 and 0.95, respectively. While these levels of performance

are notably higher than ours, the data utilized for training and validation by this group are unbalanced, featuring relatively few cardiac arrests, which we believe facilitates the high AUC and simultaneously results in their PPV of only around 8%.

The use of deep learning to screen for SCA via ECG data could be highly impactful because 25% of SCA cases have no previously identified heart disease [167], and over 60% of arrests occur outside the hospital [186] where delays in initiating CPR and defibrillation are common, bystander CPR is suboptimal [187], and there is a lack of epinephrine until paramedics arrive. Also, the proliferation of ECG recording wearable devices makes such an application readily available to the population at-large as a potentially inexpensive yet practical SCA screening tool. Widespread adoption could improve outcomes and decrease dependency on paramedics for emergency transport and resuscitation.

In our study, sensitivity was set at 95% while all other performance metrics were dependent. In general, sensitivity and specificity are negatively correlated, and therefore, the lower the sensitivity, the higher the specificity. However, it is uncertain as to whether decreasing sensitivity to increase specificity could result in a combination that is clinically significant because such thresholds have not been defined. Nonetheless, prior to being implemented on a large scale, the specificity needs to be improved because having more than half false positives (as shown in the current model) would create a combination of apathy among users and an unrealistic and unnecessary burden on ED's.

This study was limited in that all data was provided via the National Taiwan University Hospital; thus, the study population is not diverse enough to make conclusions that are generalizable to western populations. A second limitation is that this was a retrospective, case-control study in which the incidence of SCA is greatly inflated relative to the general population. Along those same lines, the SCA group here had a disproportionately large number of men. Thus, a more sex-balanced prospective cohort study is necessary to allow more confidence in the findings. Third, other deep learning models were not explored and as a result, there may be alternative methods available that are more predictive of SCA. Fourth, comorbidity data is not available for the control group, thus preventing the use of that information in the overall model. Finally, deep learning is highly dependent on large datasets, and a few hundred cases may not be enough to reveal the full potential of algorithms to predict SCA exclusively from ECG waveforms. Overcoming these issues is necessary to create a generalized screening tool for SCA.

4.6 Conclusions

This study shows that ten seconds of twelve-lead ECG data enables the prediction of an impending sudden cardiac arrest within twenty-four hours with 95% sensitivity and 36% specificity. Analyses with single leads showed similar results. Therefore, ECG data in conjunction with deep learning analyses may serve as a screening tool for cardiac arrest, and single-lead wearable devices may be amenable to such an approach. Studies with larger datasets and more diverse patients are necessary to confirm these findings and to potentially increase specificity.

4.7 Appendix

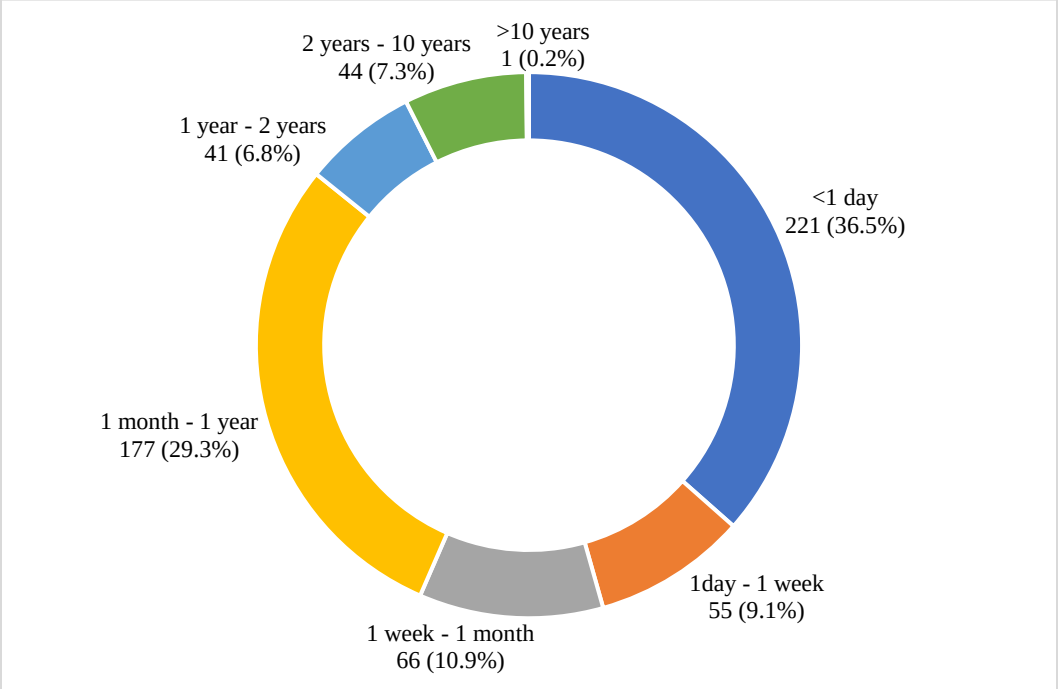

Figure 4.A1. Proportion of ECG's, in the original dataset, recorded at various times prior to their presenting SCA event.

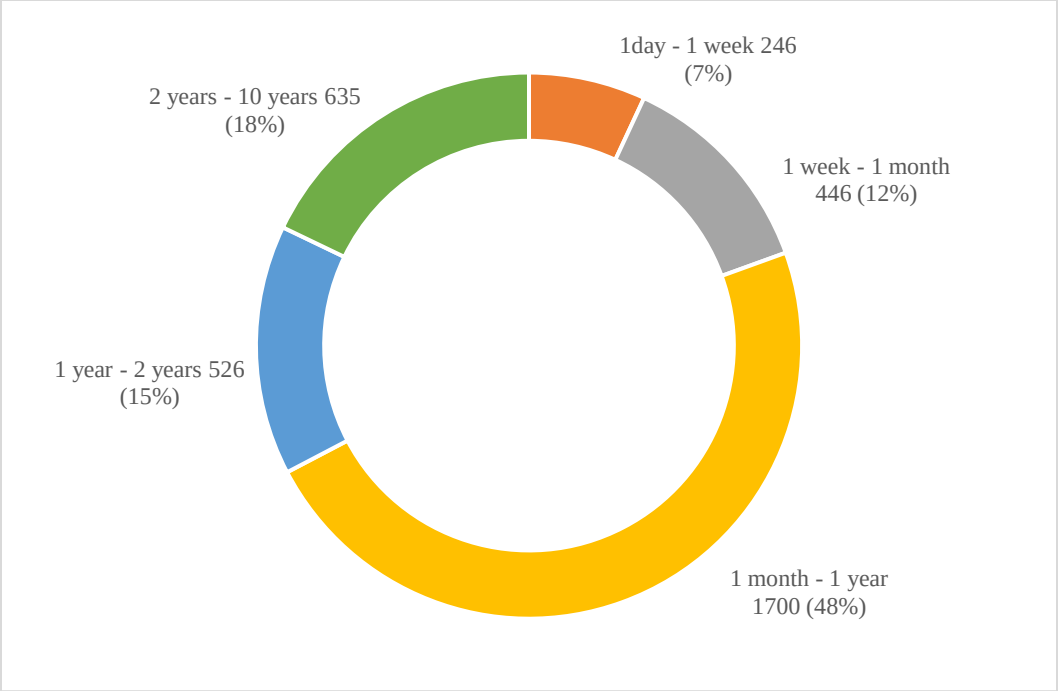

Figure 4.A2. Time from ECG acquisition to ED visit for controls with an ECG recorded before the visit.

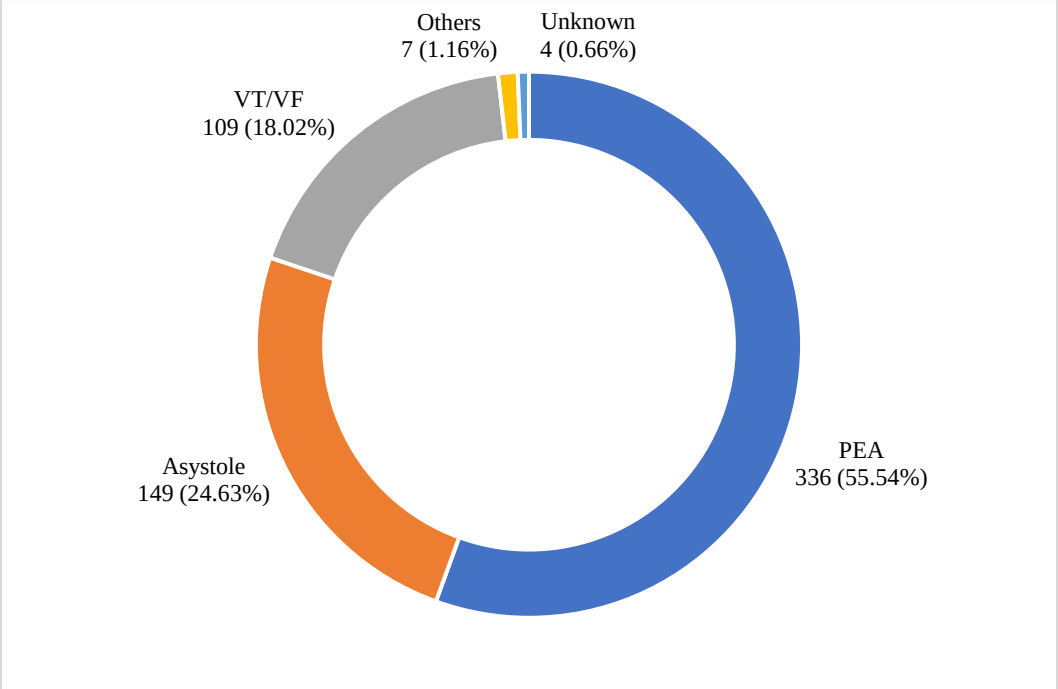

Figure 4.A3. Proportion of presenting SCA rhythms.

Table 4.A1. Measures of performance in the test set for the base case for each lead for the base model, X, with sensitivity fixed at 95%. Values are reported as mean (standard deviation) and are from nine repeated, randomized experiments.

	Lead	AUC	Accuracy [%]	F1 [%]	PPV [%]	NPV [%]	Specificity [%]
X	I	0.786 (0.047)	85.4 (3.0)	91.6 (1.8)	88.4 (3.4)	55.6 (13.8)	35.6 (13.4)
	II	0.790 (0.042)	84.9 (2.6)	91.3 (1.7)	87.9 (3.2)	56.2 (6.8)	33.7 (6.3)
	III	0.716 (0.061)	84.8 (1.6)	91.3 (1.1)	87.9 (2.0)	50.9 (16.0)	29.6 (11.2)
	aVR	0.767 (0.054)	84.4 (2.8)	91.0 (1.8)	87.4 (3.2)	52.9 (10.0)	30.1 (7.8)
	aVL	0.778 (0.033)	84.5 (1.4)	91.1 (1.0)	87.5 (1.9)	50.9 (15.1)	28.7 (9.8)
	aVF	0.741 (0.029)	83.6 (2.2)	90.6 (1.4)	86.7 (2.6)	45.2 (15.2)	23.4 (10.5)
	V1	0.732 (0.041)	84.0 (2.3)	90.9 (1.5)	87.1 (2.9)	48.5 (11.5)	25.7 (6.1)
	V2	0.771 (0.067)	84.5 (2.8)	91.1 (1.8)	87.6 (3.3)	50.0 (14.2)	28.6 (11.8)
	V3	0.817 (0.069)	85.6 (4.2)	91.7 (2.5)	88.7 (4.6)	55.0 (12.0)	36.9 (18.3)
	V4	0.803 (0.031)	84.7 (3.3)	91.3 (2.0)	87.8 (3.7)	51.4 (12.4)	30.8 (10.7)
	V5	0.809 (0.049)	86.2 (3.1)	92.0 (1.9)	89.2 (3.5)	59.0 (9.7)	40.1 (12.8)
	V6	0.775 (0.030)	84.6 (2.3)	91.2 (1.5)	87.6 (2.7)	50.8 (16.6)	29.4 (11.3)

Table 4.A2. Measures of performance in the test set for each lead for patients with ECG within one day prior to arrest and without age and sex, with sensitivity fixed at 95%. Values are reported as mean (standard deviation) and are from nine repeated, randomized experiments.

	Lead	AUC	Accuracy [%]	F1 [%]	PPV [%]	NPV [%]	Specificity [%]
A1	I	0.788 (0.051)	86.0 (2.8)	91.9 (1.8)	89.1 (3.2)	57.6 (12.6)	39.6 (13.8)
	II	0.793 (0.031)	85.6 (1.4)	91.7 (1.0)	88.5 (1.9)	57.0 (12.5)	36.1 (10.4)
	III	0.742 (0.040)	84.2 (1.9)	91.0 (1.3)	87.2 (2.5)	47.5 (17.3)	26.0 (10.6)
	aVR	0.767 (0.058)	84.8 (2.8)	91.3 (1.7)	87.9 (3.0)	52.3 (15.3)	31.4 (14.9)
	aVL	0.748 (0.051)	85.5 (1.3)	91.6 (0.9)	88.5 (1.7)	54.7 (16.9)	34.5 (12.6)
	aVF	0.752 (0.049)	84.2 (2.2)	90.9 (1.5)	87.2 (2.7)	50.3 (12.3)	27.5 (8.6)
	V1	0.747 (0.056)	84.3 (1.7)	91.0 (1.2)	87.4 (2.3)	49.2 (13.7)	27.0 (8.4)
	V2	0.757 (0.062)	84.4 (2.9)	91.1 (1.8)	87.5 (3.3)	49.6 (14.1)	28.1 (11.9)
	V3	0.808 (0.056)	86.1 (2.9)	92.0 (1.8)	89.1 (3.4)	58.3 (9.4)	39.1 (11.5)
	V4	0.801 (0.050)	85.9 (3.0)	91.9 (1.9)	89.0 (3.6)	57.5 (8.6)	38.1 (11.5)
	V5	0.815 (0.031)	86.5 (2.7)	92.2 (1.7)	89.5 (3.1)	59.6 (12.5)	41.7 (13.7)
	V6	0.782 (0.037)	84.0 (2.7)	90.9 (1.7)	87.1 (3.2)	48.9 (14.3)	26.8 (9.4)

Table 4.A3. Measures of performance in the test set for each lead for patients with ECG within one week of arrest**,** with sensitivity fixed at 95%. Values are reported as mean (standard deviation) and are from nine repeated, randomized experiments.

	Lead	AUC	Accuracy [%]	F1 [%]	PPV [%]	NPV [%]	Specificity [%]
B1	I	0.787 (0.041)	82.7 (2.6)	89.9 (1.6)	85.2 (2.9)	57 (15.6)	30.8 (12.2)
	II	0.763 (0.039)	82.5 (2.2)	89.7 (1.5)	85.0 (2.8)	59.7 (6.5)	31.0 (4.3)
	III	0.726 (0.061)	81.5 (1.1)	89.3 (0.7)	84.2 (1.4)	48.2 (22.4)	23.0 (12.1)
	aVR	0.759 (0.045)	82.1 (2.9)	89.5 (1.8)	84.6 (3.2)	56.4 (10.7)	28.5 (9.7)
	aVL	0.759 (0.051)	81.5 (1.5)	89.2 (1.0)	84.1 (1.9)	50.7 (17.2)	23.9 (10.9)
	aVF	0.717 (0.038)	81.0 (2.3)	88.9 (1.5)	83.6 (2.7)	49.4 (14.6)	22.2 (9.4)
	V1	0.696 (0.045)	81.1 (2.0)	89.0 (1.4)	83.7 (2.6)	50.6 (8.3)	21.9 (3.3)
	V2	0.766 (0.079)	82.1 (2.2)	89.6 (1.5)	84.7 (2.7)	54.7 (11.4)	26.9 (7.4)
	V3	0.798 (0.061)	83.1 (3.7)	90.1 (2.2)	85.7 (4.0)	58.6 (9.9)	32.8 (12.4)

	V4	0.789 (0.037)	82.6 (3.5)	89.8 (2.1)	85.2 (3.9)	57.0 (9.9)	30.4 (9.9)
	V5	0.795 (0.053)	83.7 (3.7)	90.4 (2.2)	86.3 (4.0)	60.8 (12.6)	36.4 (15.6)
	V6	0.767 (0.033)	82.0 (3.2)	89.5 (2.0)	84.6 (3.5)	53.3 (16.6)	27.2 (12.9)

Table 4.A4. Measures of performance in the test set for each lead for patients with ECG within one month of arrest, with sensitivity fixed at 95%. Values are reported as mean (standard deviation) and are from nine repeated, randomized experiments.

	Lead	**AUC**	**Accuracy [%]**	**F1 [%]**	**PPV [%]**	**NPV [%]**	**Specificity [%]**
B2	**I**	0.763 (0.035)	79.8 (1.9)	87.9 (1.2)	81.7 (2.1)	60.4 (13.3)	27.9 (9.4)
	II	0.722 (0.039)	78.6 (2.7)	87.2 (1.8)	80.6 (3.1)	58.5 (5.8)	24.0 (4.6)
	III	0.705 (0.063)	79.0 (1.2)	87.5 (0.9)	81.0 (1.6)	56.3 (14.5)	23.7 (8.5)
	aVR	0.736 (0.047)	79.2 (2.5)	87.5 (1.6)	81.2 (2.7)	59.4 (10.3)	26.1 (8.2)
	aVL	0.730 (0.037)	78.6 (2.5)	87.3 (1.7)	80.3 (2.3)	49.3 (23.8)	20.4 (12.5)
	aVF	0.695 (0.037)	78.2 (2.4)	87.0 (1.6)	80.3 (2.9)	55.5 (7.7)	21.6 (5.4)
	V1	0.696 (0.038)	77.9 (2.5)	86.9 (1.7)	80.1 (3.0)	53.0 (9.6)	19.9 (5.6)
	V2	0.747 (0.048)	79.3 (3.4)	87.7 (2.1)	81.4 (3.6)	58.2 (10.8)	25.8 (10.3)
	V3	0.776 (0.040)	80.4 (2.9)	88.2 (1.7)	82.3 (3.0)	61.2 (12.1)	29.9 (11.9)
	V4	0.752 (0.046)	80.2 (2.9)	88.1 (1.7)	82.2 (3.1)	60.8 (12.6)	29.4 (11.2)
	V5	0.753 (0.034)	79.9 (3.1)	87.9 (2.0)	81.8 (3.6)	62.2 (6.7)	29.0 (8.7)
	V6	0.737 (0.037)	79.5 (2.5)	87.7 (1.6)	81.4 (3.0)	60.3 (8.7)	26.9 (7.8)

Table 4.A5. Measures of performance in the test set for each lead for patients with ECG between one day and one month of arrest, with sensitivity fixed at 95%. Values are reported as mean (standard deviation) and are from nine repeated, randomized experiments.

	Lead	**AUC**	**Accuracy [%]**	**F1 [%]**	**PPV [%]**	**NPV [%]**	**Specificity [%]**
B3	**I**	0.698 (0.048)	87.8 (1.6)	93.4 (1.0)	91.8 (1.9)	25.4 (13.6)	16.7 (8.1)
	II	0.651 (0.055)	87.3 (2.3)	93.1 (1.4)	91.3 (2.7)	19.0 (12.3)	12.5 (9.3)
	III	0.630 (0.084)	87.2 (1.8)	93.1 (1.1)	91.2 (2.0)	16.5 (16.5)	9.8 (9.5)
	aVR	0.665 (0.069)	88.0 (1.6)	93.5 (1.0)	92.0 (1.9)	26.9 (14.8)	18.5 (9.3)
	aVL	0.662 (0.034)	87.5 (3.3)	93.2 (1.9)	91.0 (2.9)	13.6 (14.5)	9.2 (9.8)
	aVF	0.585 (0.068)	87.2 (1.7)	93.1 (1.0)	91.2 (2.0)	16.9 (16.3)	9.8 (8.5)
	V1	0.595 (0.099)	87.3 (2.5)	93.1 (1.4)	91.3 (2.8)	17.2 (14.5)	11.8 (12.8)
	V2	0.640 (0.094)	87.8 (2.0)	93.3 (1.2)	91.7 (2.3)	24.7 (13.9)	16.6 (9.2)
	V3	0.674 (0.094)	87.6 (2.0)	93.2 (1.2)	91.5 (2.4)	22.8 (11.2)	14.6 (7.3)
	V4	0.704 (0.079)	87.9 (1.9)	93.4 (1.1)	91.9 (2.2)	25.6 (14.9)	17.9 (12.0)
	V5	0.685 (0.060)	87.8 (2.4)	93.4 (1.4)	91.8 (2.7)	25.1 (13.1)	18.1 (11.8)
	V6	0.660 (0.084)	87.9 (2.1)	93.4 (1.2)	91.9 (2.4)	26.4 (13.5)	18.5 (10.6)

Table 4.A6. Measures of performance in the test set for each lead for patients with ECG between one month and one year of arrest**,** with sensitivity fixed at 95%. Values are reported as mean (standard deviation) and are from nine repeated, randomized experiments.

	Lead	**AUC**	**Accuracy [%]**	**F1 [%]**	**PPV [%]**	**NPV [%]**	**Specificity [%]**
B4	**I**	0.590 (0.044)	83.6 (2.6)	90.9 (1.6)	86.7 (2.8)	22.1 (18.7)	10.9 (9.8)
	II	0.573 (0.071)	83.2 (1.8)	90.7 (1.1)	86.4 (2.4)	19.0 (15.4)	8.3 (7.2)
	III	0.588 (0.053)	83.4 (2.6)	90.8 (1.5)	86.9 (2.9)	27.4 (15.2)	13.4 (8.3)
	aVR	0.597 (0.069)	83.1 (1.7)	90.6 (1.1)	86.5 (2.1)	24.8 (10.8)	9.9 (4.0)
	aVL	0.593 (0.057)	83.9 (1.5)	91.0 (0.9)	86.9 (2.0)	26.3 (18.6)	12.2 (9.4)
	aVF	0.532 (0.085)	82.5 (1.9)	90.3 (1.2)	86.0 (2.3)	15.7 (14.2)	6.3 (5.8)
	V1	0.542 (0.075)	82.6 (2.7)	90.4 (1.6)	86.2 (3.0)	16.9 (12.5)	7.8 (7.1)
	V2	0.551 (0.074)	83.5 (2.0)	90.8 (1.2)	86.9 (2.3)	27.5 (17.5)	12.9 (10.2)
	V3	0.543 (0.069)	83.2 (1.3)	90.7 (0.8)	86.7 (1.7)	25.1 (16.4)	10.6 (7.2)
	V4	0.575 (0.071)	83.4 (2.6)	90.7 (1.5)	86.8 (2.8)	26.9 (15.6)	12.8 (9.9)
	V5	0.625 (0.069)	84.1 (2.0)	91.1 (1.2)	87.5 (2.3)	34.2 (15.0)	17.2 (9.4)
	V6	0.574 (0.088)	83.1 (2.2)	90.6 (1.3)	86.6 (2.5)	23.3 (14.6)	10.5 (9.0)

Table 4.A7. Measures of performance in the test set for each lead for patients with ECG within one day of PEA and asystole arrests, with sensitivity fixed at 95%. Values are reported as mean (standard deviation) and are from nine repeated, randomized experiments.

	Lead	AUC	Accuracy [%]	F1 [%]	PPV [%]	NPV [%]	Specificity [%]
C1	I	0.781 (0.039)	88.1 (2.2)	93.3 (1.4)	91.7 (2.6)	49.2 (15.4)	37.7 (15.3)
	II	0.783 (0.046)	87.6 (2.1)	93.0 (1.4)	91.1 (2.7)	48.4 (9.1)	34.4 (6.0)
	III	0.739 (0.053)	87.3 (1.8)	92.9 (1.2)	90.9 (2.3)	46.0 (13.0)	31.5 (8.0)
	aVR	0.756 (0.068)	87.5 (3.4)	93.0 (2.0)	91.1 (3.8)	46.6 (16.3)	35.1 (17.0)
	aVL	0.789 (0.044)	87.7 (1.5)	93.1 (1.0)	91.3 (2.0)	48.1 (13.9)	34.6 (9.5)
	aVF	0.732 (0.034)	86.6 (2.0)	92.5 (1.3)	90.2 (2.6)	40.3 (12.7)	25.4 (8.5)
	V1	0.723 (0.059)	86.7 (2.5)	92.6 (1.5)	90.3 (3.0)	41.5 (13.4)	26.8 (9.4)
	V2	0.764 (0.075)	86.8 (3.2)	92.6 (1.9)	90.4 (3.6)	42.2 (11.7)	28.3 (14.0)
	V3	0.813 (0.058)	87.7 (3.4)	93.1 (2.0)	91.3 (3.9)	47.5 (12.1)	35.9 (18.0)
	V4	0.791 (0.033)	87.7 (2.2)	93.1 (1.4)	91.3 (2.8)	49.2 (9.0)	35.6 (4.8)
	V5	0.777 (0.079)	87.6 (3.1)	93.0 (1.9)	91.2 (3.6)	47.3 (10.7)	35.1 (14.1)
	V6	0.781 (0.050)	87.9 (2.3)	93.2 (1.5)	91.5 (2.8)	48.5 (15.1)	36.6 (12.8)

Table 4.A8. Measures of performance in the test set for each lead for patients with ECG within one day of PEA arrests**,** with sensitivity fixed at 95%. Values are reported as mean (standard deviation) and are from nine repeated, randomized experiments.

	Lead	AUC	Accuracy [%]	F1 [%]	PPV [%]	NPV [%]	Specificity [%]
C2	I	0.802 (0.048)	90.1 (2.1)	94.6 (1.3)	94.1 (2.5)	42.9 (10.6)	40.5 (12.9)
	II	0.741 (0.054)	89.5 (1.9)	94.3 (1.1)	93.5 (2.3)	38.8 (9.8)	33.4 (6.3)
	III	0.751 (0.087)	89.1 (1.6)	94.1 (1.0)	93.2 (2.0)	31.5 (22.3)	26.1 (18.6)
	aVR	0.804 (0.073)	90.1 (3.3)	94.5 (1.9)	94.1 (3.7)	43.0 (9.7)	43.6 (19.7)
	aVL	0.798 (0.065)	89.9 (1.6)	94.5 (1.0)	93.9 (2.0)	40.3 (13.7)	36.3 (11.2)
	aVF	0.751 (0.060)	89.1 (2.4)	94.1 (1.4)	93.2 (2.8)	35.3 (11.3)	29.9 (11.0)
	V1	0.719 (0.079)	89.1 (2.4)	94.0 (1.4)	93.1 (2.8)	34.9 (11.5)	29.1 (12.1)
	V2	0.743 (0.094)	88.8 (2.6)	93.9 (1.5)	92.8 (2.9)	31.6 (14.2)	25.9 (15.0)
	V3	0.799 (0.057)	89.8 (2.8)	94.4 (1.6)	93.8 (3.2)	41.2 (8.4)	39.4 (18.3)
	V4	0.777 (0.073)	89.7 (2.5)	94.4 (1.5)	93.7 (2.9)	40.0 (12.2)	37.1 (14.0)
	V5	0.798 (0.061)	89.8 (2.6)	94.4 (1.5)	93.8 (3.1)	40.5 (10.6)	38.0 (15.1)
	V6	0.793 (0.052)	90.0 (2.0)	94.5 (1.2)	94.0 (2.4)	41.4 (13.9)	38.5 (14.0)

Table 4.A9. Measures of performance in the test set for each lead for patients with ECG within one day of arrest and a 600ms time window around the R wave**,** with sensitivity fixed at 95%. Values are reported as mean (standard deviation) and are from nine repeated, randomized experiments.

	Lead	AUC	Accuracy [%]	F1 [%]	PPV [%]	NPV [%]	Specificity [%]
D1	I	0.779 (0.038)	84.1 (3.8)	90.9 (2.3)	87.2 (4.2)	50.1 (12)	28.8 (11.4)
	II	0.767 (0.047)	84.4 (2.1)	91.0 (1.4)	87.4 (2.6)	51.3 (16.5)	29.5 (11.4)
	III	0.708 (0.053)	83.3 (2.0)	90.5 (1.3)	86.4 (2.5)	40.5 (20.6)	20.1 (10.8)
	aVR	0.759 (0.075)	84.4 (4.0)	91.1 (2.3)	87.5 (4.3)	49.0 (19.3)	30.1 (19.9)
	aVL	0.750 (0.078)	84.9 (2.1)	91.3 (1.4)	87.9 (2.5)	52.8 (16.6)	31.5 (10.6)
	aVF	0.732 (0.054)	83.5 (2.7)	90.6 (1.8)	86.5 (3.2)	45.1 (18.1)	23.4 (10.3)

	V1	0.701 (0.052)	84.2 (3.6)	91.0 (2.2)	87.3 (4.1)	49.6 (11.4)	28.3 (11.4)
	V2	0.760 (0.041)	84.3 (2.7)	91.0 (1.7)	87.4 (3.2)	49.3 (12.7)	27.6 (10.3)
	V3	0.817 (0.059)	86.2 (4.3)	92.0 (2.5)	89.3 (4.7)	58.0 (10.4)	41.0 (15.9)
	V4	0.804 (0.029)	86.1 (2.2)	92.0 (1.4)	89.1 (2.7)	58.2 (9.1)	38.3 (7.6)
	V5	0.804 (0.060)	85.9 (2.6)	91.9 (1.7)	88.9 (3.2)	58.5 (9.5)	38.6 (9.7)
	V6	0.809 (0.039)	85.0 (2.6)	91.3 (1.6)	88.0 (3.0)	53.9 (11.4)	32.2 (9.2)

Table 4.A10. Measures of performance in the test set for each lead for patients with ECG within one day of arrest and a 500ms time window around the R wave**,** with sensitivity fixed at 95%. Values are reported as mean (standard deviation) and are from nine repeated, randomized experiments.

	Lead	**AUC**	**Accuracy [%]**	**F1 [%]**	**PPV [%]**	**NPV [%]**	**Specificity [%]**
	I	0.767 (0.036)	84.6 (2.7)	91.1 (1.7)	87.6 (3.2)	53.1 (9.4)	30.3 (6.6)
	II	0.766 (0.058)	83.9 (3.2)	90.8 (2.0)	86.9 (3.7)	50.3 (10.7)	27.6 (12.1)
	III	0.684 (0.082)	82.7 (2.9)	90.2 (1.8)	85.9 (3.4)	37.3 (16.5)	17.7 (10.4)
	aVR	0.758 (0.059)	84.5 (2.9)	91.1 (1.8)	87.5 (3.4)	53.1 (10.4)	30.6 (9.7)
	aVL	0.737 (0.048)	84.1 (1.9)	90.9 (1.3)	87.1 (2.5)	49.2 (14.2)	26.6 (9.3)
D2	**aVF**	0.743 (0.059)	83.8 (2.9)	90.7 (1.9)	86.8 (3.4)	49.0 (8.4)	25.9 (7.0)
	V1	0.704 (0.077)	84.3 (2.9)	91.0 (1.8)	87.4 (3.3)	49.5 (13.0)	27.8 (10.4)
	V2	0.745 (0.048)	84.6 (2.5)	91.2 (1.6)	87.6 (3.0)	51.7 (8.9)	29.3 (6.3)
	V3	0.782 (0.052)	85.2 (3.1)	91.5 (1.9)	88.2 (3.6)	53.6 (13.5)	33.3 (13.2)
	V4	0.791 (0.046)	85.8 (1.9)	91.8 (1.2)	88.8 (2.3)	55.3 (14.7)	35.7 (11.9)
	V5	0.783 (0.057)	84.8 (2.1)	91.3 (1.3)	87.8 (2.4)	50.8 (17.1)	29.8 (13.3)
	V6	0.778 (0.052)	84.1 (3.3)	90.9 (2.0)	87.2 (3.8)	47.5 (19.5)	27.5 (15.1)

5. Comparison between a Single-Lead ECG Garment Device and a Holter Monitor: A Signal Quality Assessment

from the manuscript:

Comparison between a Single-Lead ECG Garment Device and a Holter Monitor: A Signal Quality Assessment

L. Neri, I. Corazza, M. T. Oberdier, J. Lago, I. Gallelli, A. F. G. Cicero, I. Diemberger, A. Orro, A. Beker, N. Paolocci, H. R. Halperin, C. Borghi

Paper submitted to the *Journal of Medical Systems*

5.1 Abstract

Wearable electronics are increasingly common and useful as health monitoring devices, many of which feature the ability to record a single-lead electrocardiogram (ECG). However, recording the ECG commonly requires the user to touch the device to complete the lead circuit, which prevents continuous data acquisition. An alternative approach to enable continuous monitoring without user initiation is to embed the leads in a garment. This study assessed ECG data obtained from the YouCare device (a novel sensorized garment) via comparison with a conventional Holter monitor. A cohort of thirty patients (age range: 20-82 years; 16 females and 14 males) were enrolled and monitored for twenty-four hours with both the YouCare device and a Holter monitor. ECG data from both devices were qualitatively assessed by a panel of three expert cardiologists and quantitatively analyzed using specialized software. Patients also responded to a survey about the comfort of the YouCare device as compared to the Holter monitor. The YouCare device was assessed to have 70% of its ECG signals as “Good”, 12% as “Acceptable”, and 18% as “Not Readable”. The R-wave, independently recorded by the YouCare device and Holter monitor, were synchronized within measurement error during 99.4% of cardiac cycles. In addition, patients found the YouCare device more comfortable than the Holter monitor (comfortable 22 vs. 5 and uncomfortable 1 vs. 18, respectively). Therefore, the quality of ECG data collected from the garment-based device was comparable to a Holter monitor when the signal was sufficiently acquired, and the garment was also comfortable.

5.2 Introduction

Wearable electronics have advanced to the point of being comprehensive health monitoring devices [3,7] and are being combined with other technologies to enhance their capabilities. Current wearable devices are capable of simultaneously recording multiple biosignals such as oxygen saturation, heart rate, and heart rate variability [5,33,188–191]. Some models are even able to capture single-lead electrocardiogram (ECG) recordings. However, this function requires that the subject completes the lead circuit by holding the smartwatch case with their opposite hand, thus making the measurement dependent on inconvenient operator action for signal acquisition.

As an alternative, the YouCare device (AccYouRate Group S.p.A., L'Aquila, Italy), a garment with embedded polymer-based electrodes and Bluetooth connectivity, provides the opportunity for continuous single-lead ECG acquisition. Towards establishing the YouCare device as a reliable option for ECG acquisition, its performance was compared to that of a Holter monitor, the clinical standard for wearable ECG monitoring. It was hypothesized that the quality of the signals captured by the YouCare device and Holter monitor are similar.

5.3 Methods

5.3.1 Overview

Thirty ambulatory patients were subject to 24-hour cardiac rhythm monitoring with the YouCare device and a 3-lead Holter monitor, simultaneously. During the study, the patients performed activities of daily living. All subjects who met the inclusion/exclusion criteria (Table 5.1) were equipped with the YouCare device, its associated smartphone, and a Holter monitor for 24 hours.

Table 5.1. Eligibility criteria.

Inclusion criteria
• Subjects aged ≥ 18 years and ≤ 90 years old, • Subjects with heart rhythm diseases or under screening for the assessment of possible arrhythmias or other heart diseases. • Subjects who have the capability to communicate, to make themselves understood, and to comply with the study's requirements, • Subjects agree to participate in the study and having dated and signed the informed consent form,
Exclusion criteria
• Subjects who have difficulties in wearing the garment such as movements impairments or dermatological reactions to fabric or other materials, • Any medical or surgical condition that would limit the patient's adherence to the study protocol, • Extreme body habitus, • Subjects who are not able to understand the scope of the study.

The protocol and overall study were approved by an ethics committee (Internal code: 156/2022/Disp/AOUBo by the Comitato Etico Area Vasta Emilia Centro - CE-AVEC – Bologna, Italy), registered on the Italian Ministry of Health website, and on clinicaltrials.gov (Identifier NCT05771142). The study was conducted in accordance with the Declaration of Helsinki, and each participant provided written informed consent.

5.3.2 Youcare System

The YouCare device (AccYouRate Group S.p.A.; L'Aquila, Italy; Figure 5.1) is a crop top garment made of cotton and ceramic with integrated polymer-based electrodes and an acquisition module for data recording and processing. The garment contains 3 polymer-based electrodes that, when in contact with the skin, allow the acquisition of a single-lead ECG. Two of the electrodes are located close to the diaphragm just below the major pectoral muscles (Figure 5.1 F). A third electrode is positioned on the back of the chest belt, and it has the function of the right leg lead used to reduce the noise and artifacts present on the other two electrodes. The control unit, anchored to the garment via four metal snap fasteners (Figure 5.1 D-E), has an ECG sampling rate of 246 Hz and collects and sends the data to a smartphone via Bluetooth for storage.

In addition to the one-lead ECG, the garment is paired with a control unit (Figure 5.1 C) that has an accelerometer, a gyroscope, and body temperature sensor. A respiration waveform is derived from the ECG. YouCare garments are offered in varied sizes for women and men (Figure 5.1 A-B). Garment size is important to ensure continuous sensor contact with the skin, leading to the best signal quality.

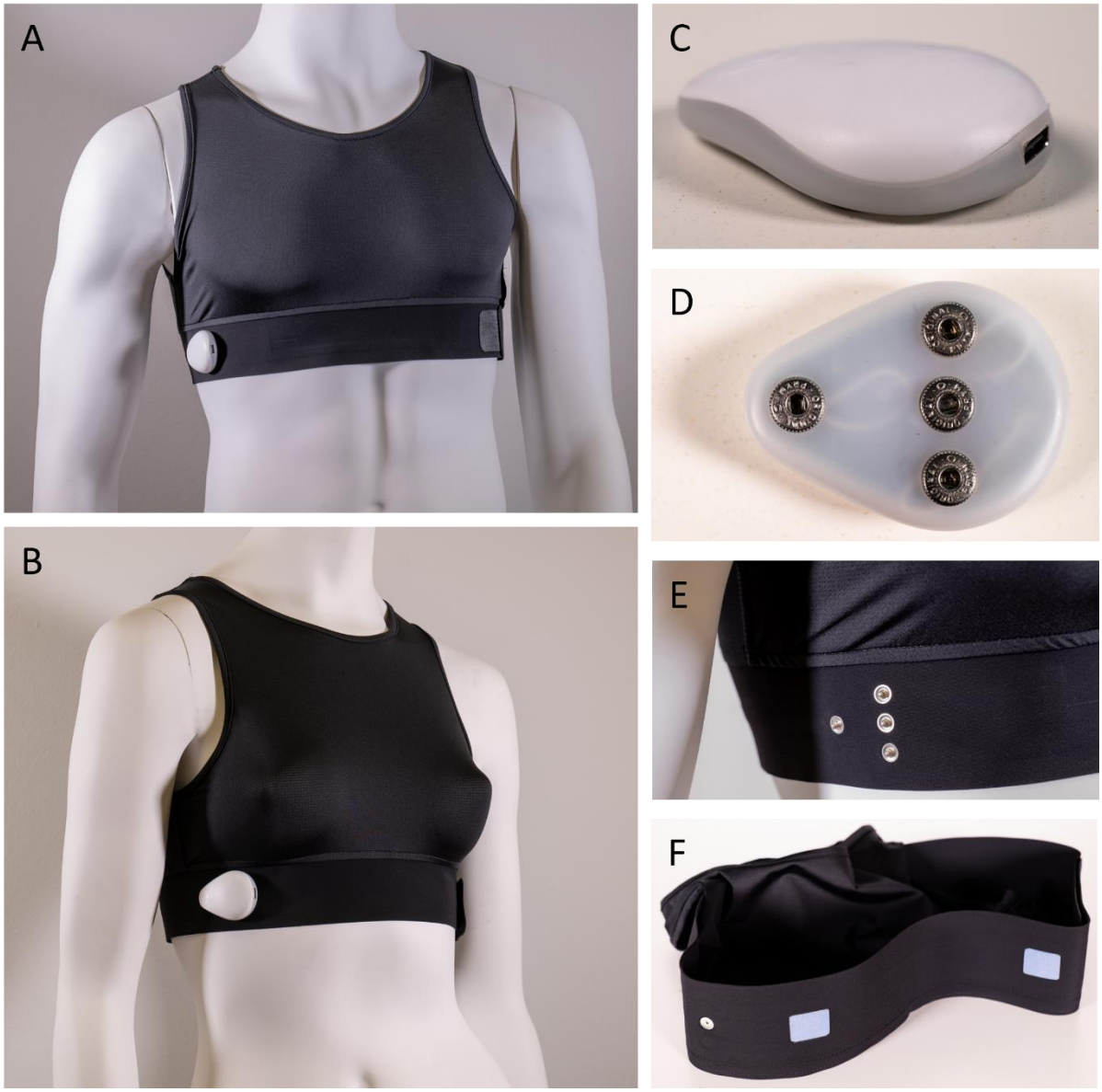

Figure 5.1. The YouCare device is a garment with polymer-based sensors directly integrated in the garment fabric. When in direct contact with the skin, the device can record a single-lead ECG through sensors in the belt around and below the chest. There are two versions, one for men (A) and one for women (B) with different sizes. The garment is connected to the control unit, that works as an acquisition and transmission module, (C, D) through four snaps (E). Polymer-based sensors provide contact with the skin (F).

5.3.3 ECG Holter Monitor

The Holter recording system (SEER 1000 GE Healthcare, Chicago, Illinois) features three leads with an ECG sampling rate of 256 Hz, 0.05 - 70 Hz response, and 12-bit resolution. The system uses standard disposable silver/silver chloride (Ag/AgCl)–gelled electrodes. The electrode-skin connection was reinforced with medical tape to ensure stable contact.

5.3.4 Assessment and Validation of Signal Quality

ECG signal qualities from both devices were evaluated according to two independent approaches:

1) Qualitative Assessment: ECG signal quality was evaluated by a team of three expert cardiologists and classified according to three categories: “Good” (all major ECG features - P, QRS, and T - are visible for diagnostic purposes), “Acceptable” (the QRS is visible), and “Not Readable” (mostly noise with no ECG waveforms clearly visible).
2) Quantitative Validation: R-R interval comparison between the YouCare device and the Holter monitor were performed after extracting 30 consecutive minutes of data where the quality was at least “Acceptable”. The time distances between corresponding R waves of each device were classified as either within the measurement error (of 8 milliseconds, as determined from error propagation rules [192]), or over the measurement error. The R-R interval comparison was not performed for two patients (#’s 2 and 25) because thirty consecutive minutes of stable signals were not available. Only the longest, uninterrupted recordings were analyzed, and the corresponding segments of the Holter ECG were isolated for comparison. The analysis was performed with Python and its libraries (i.e.: Numpy v.1.17.3, Pandas v1.3.4, Neurokit2 v0.1.7 [193]) in conjunction with ANScovery (SparkBio S.r.l., San Lazzaro di Savena, Bologna, Italy) [194].

5.3.5 Patient Surveys

A survey of the patients in the study was performed via follow-up phone interview in which patients were asked to rate both the YouCare and Holter devices on a scale of four levels of comfort: very comfortable, comfortable, uncomfortable, very uncomfortable. Four patients were unreachable via the telephone and three did not participate due to a language barrier.

5.4 Results

The thirty patients studied had a mean age of 55 years (range 20-82) and sixteen were women. (Table 5.2). The average patient was 167 centimeters tall and 70 kilograms with a body mass index

of 25 and a waist circumference of 92 centimeters. The mean heart rate was 75 beats per minute and average blood pressure was 128 over 79 millimeters of mercury. Twelve patients had a history of transient ischemic attack or stroke, twelve patients had a history of palpitations, tachycardia, or extrasystole, six had other cardiac pathologies including mitral insufficiency, and eighteen had a history of chronotropic drug therapy.

Table 5.2. Baseline characteristics of the study population. Values are average (standard deviation).

	Patients (N = 30)
Age [years]	55.3 (20.2); Range 20-82
Females [n [%]]	16 [53.3%]
Height [centimeter]	166.7 (7.6)
Weight [kilograms]	69.6 (14.4)
Body Mass Index [kilograms/meter^2]	24.9 (4.2)
Waist circumference [centimeter]	91.7 (13.7)
Resting Heart Rate [beats per minute]	74.6 (16.1)
Systolic Blood Pressure [millimeters of mercury]	127.5 (13.4)
Diastolic blood pressure [millimeters of mercury]	78.5 (8.7)
Transient Ischemic Event or Stroke (# of patients)	12
Palpitations, Tachycardia, or Extrasystole (# of patients)	12
Other cardiac pathologies (e.g., mitral insufficiency) (# of patients)	6
Chronotropic Drug Therapy (# of patients)	18

5.4.1 Assessment and Validation of Signal Quality

Connectivity issues between the control unit and smartphone led to data loss. In 17 cases, lost data was less than 1 hour, in 5 cases lost data was between 1 and 10 hours, and in 8 cases lost data was between 10 and 20 hours.

Experts' assessments determined that signal quality from the YouCare device was "Good" 70% of the time, "Acceptable" 12% of the time, and "Not Readable" 18% of the time (Figure 5.2). For four patients, the signal was "Good" at least 90% of the time, and for twenty-four patients, the signal was "Good" at least 60% of the time. Signals from the Holter monitor were "Good" 99% of the time, "Acceptable" 1% of the time, and "Not Readable" 0% of the time. Representative ECG signals for the YouCare device and based on the three categories are shown in Figure 5.3.

There was an R wave overlap between the devices that occurred within the measurement error (≤ 8ms) during 99.4% of cardiac cycles, and outside the measurement error (> 8ms) during 0.6% of cardiac cycles (Table 5.3). An example of the tachogram is shown in Figure 5.4, and representative arrhythmic beats as recorded by each device are shown in Figure 5.5.

Patient	Good [%]	Acceptable [%]	Not readable [%]
1	41	10	49
2	38	27	35
3	96	2	2
4	55	21	24
5	88	2	10
6	60	12	28
7	83	11	6
8	79	12	9
9	41	14	45
10	89	8	3
11	67	27	6
12	67	13	20
13	63	9	28
14	75	1	24
15	87	7	6
16	92	4	4
17	80	18	2
18	95	4	1
19	80	13	7
20	99	1	0
21	73	15	12
22	35	22	43
23	85	9	6
24	64	20	16
25	3	10	87
26	77	13	10
27	84	9	7
28	69	12	19
29	67	19	14
30	79	9	12
Average	70	12	18
Standard Deviation	22	7	19

Figure 5.2. ECG quality assessment for each patient.

Table 5.3. Temporal distances between YouCare and Holter devices' R waves. Patients 2 and 25 were not analyzed because they did not have thirty consecutive minutes of stable signals. ms is milliseconds.

	R wave sync [%]	
Patient	**<= 8 ms**	**> 8 ms**
1	98,7	1,3
3	99,9	0,1
4	99,0	1,0
5	100	0
6	100	0
7	99,9	0,1
8	100	0
9	99,9	0,1
10	98,9	1,1
11	99,6	0,4
12	100	0
13	98,4	1,6
14	99,4	0,6
15	99,6	0,4
16	99,9	0,1
17	98,4	1,6
18	99,9	0,1
19	100	0
20	99,9	0,1
21	99,5	0,5
22	98.7	1.3
23	100	0
24	100	0
26	99,9	0,1
27	100	0
28	99,5	0,5
29	92,8	7,2
30	100	0

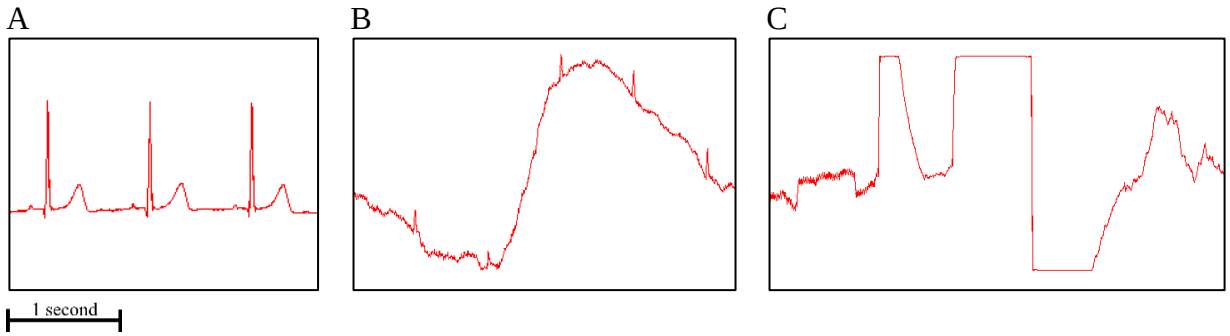

Figure 5.3. Representative ECG signals recorded with the YouCare classified as: A. "Good" – all ECG waveform features (P, QRS, and T) are visible; B. "Acceptable" – the QRS is visible; C. "Not Readable" – mostly noise with no ECG waveforms clearly visible.

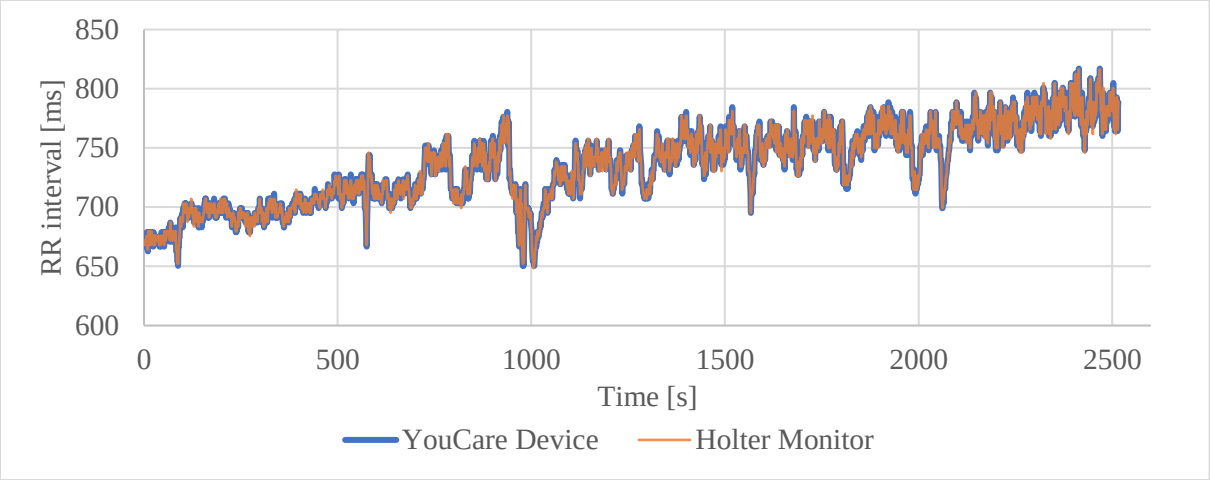

Figure 5.4. Example of overlapped tachograms from the YouCare device and the Holter monitor.

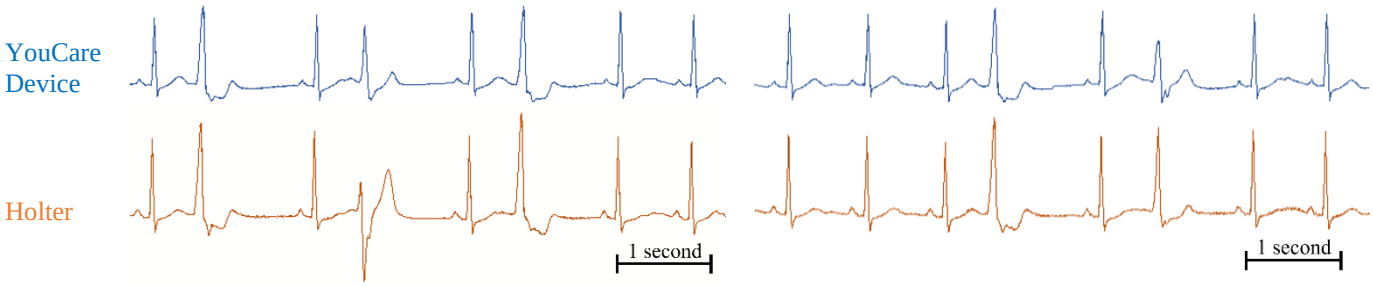

Figure 5.5. Representative ECG signals with arrhythmias from the YouCare device (above, in blue) and Holter monitor (below, in orange).

5.4.2 Patient Surveys

The YouCare device was classified as very comfortable by 9 patients, comfortable by 13 patients, uncomfortable by 1 patient, and none considered it very uncomfortable (Figure 5.6). On the other hand, the Holter monitor was classified as very comfortable by 1 patient, comfortable by 4 patients, uncomfortable by 17 patients, and 1 considered it very uncomfortable.

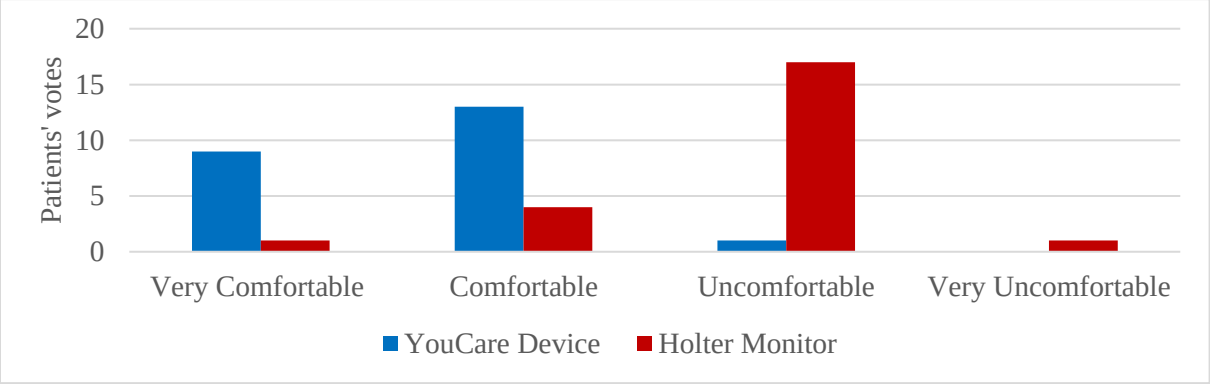

Figure 5.6. Comfort comparison between the YouCare and Holter devices.

5.5 Discussion

This is the first study to evaluate the YouCare device relative to a Holter monitor on patients during their activities of daily living. Data show the potential of the garment system as a tool for long-term monitoring due to its high comfort and general ability to capture major ECG features. However, data collection interruptions were frequent and prolonged, primarily because of Bluetooth disconnections but also due to intermittent electrode-skin contact. It is important to note that signal acquisition issues related to electrode-skin contact arise, in part, due to a necessary compromise between usability and comfort [195]. When the signal was captured without noise, there was an exceptionally reliable overlap of R-waves with most differences being attributed to unique filters and lead configurations between the devices.

Two other studies have evaluated the performance of ECG recording garments relative to Holter monitors. The trial with the OMshirt involved twenty-four hour monitoring of the garment in parallel with the Holter and reported an agreement of around 60% for detecting the QRS complex, and 47% of recordings had some intermittent noise [188]. These findings are consistent with ours in that major ECG features could be detected when noise was minimal, but the continuity of quality signals remains an issue. Another study involving the “hitoe” electrode embedded in a garment showed significant differences between the experimental device and the Holter’s signal-to-noise ratio during the four activities of living that were studied with torso twisting being the least favorable [196]. The study highlights the difficulty in collecting reliable signals during the complex movements that may be experienced during activities of daily living.

This study has several limitations. First, the devices were worn simultaneously, potentially resulting in the Holter leads and cables interfering with electrode-skin contact of the YouCare device. Therefore, it is expected that the YouCare device would have less noise and connectivity issues if it were tested in isolation. Second, it was not possible to determine why Bluetooth disconnections occurred or what activity was going on when electrode-skin contacts were not sufficient to maintain a quality signal. Such findings are crucial for improving future iterations of the YouCare device. Third, although individuals with cardiac irregularities were included in the study population, this study did not evaluate device performance in the context of detecting disease. A future study is necessary to quantify disease detection and enable certification of the garment system as a medical device in the United States. Fourth, the R-wave was the only major

landmark that was investigated. That is, it has not yet been quantified what capability the YouCare device has in capturing more subtle ECG features such as the P- and T-waves and ST-segment magnitude.

Future development is necessary to improve the continuity of high-quality signal acquisition. Such development may include improved communication between the controller and smartphone or better contacting electrodes. Together, such a device in conjunction with improved ECG analysis techniques [133], including artificial intelligence, have the potential to revolutionize the detection of cardiac arrhythmias and disease in the general population [197] and may even enable the detection of subclinical conditions [5].

5.6 Conclusion

The quality of single-lead ECG data collected from a novel garment-based device was shown to be comparable to a Holter monitor during periods when there was adequate signal acquisition. The garment was also found to be comfortable. Therefore, the garment performs similarly to a Holter monitor and may be a practical means of collecting single-lead ECGs without user actuation. However, improvements are necessary to ensure signal acquisition is uninterrupted.

6. Limitations and Studies in Perspective

In this Ph.D. project, we performed research applied to the electrocardiogram in combination with AI and wearable to contribute to the development of a novel smart t-shirt, the YouCare device. The first stint of the work was a literature review of the electrocardiogram use in monitoring wearable devices in combination with AI algorithms for disease detection and prediction. The evaluation of the vast research manuscript highlighted the opportunities and current interest for AI and wearable for medical applications, that is spreading from Cardiology to several other medical areas. However, the review showed the present limitations of this application, from wearable usability, through data processing, to AI reliability. To contribute to this field of studies our research has focused on three directions improving ECG signal processing, developing an AI model for prediction of cardiac arrest and comparing our prototype of smart t-shirt with a Holter monitor.

A well-known QRS detection algorithm was modified to improve computational efficiency and accuracy. The algorithm was tested with different ECG datasets and compared with the original gold standard reference. The results showed algorithm capabilities to improve the accuracy and time performances, and thus enhance the ECG signal processing in particular for wearable and mobile applications.

One limitation stems from the database's limited population, potentially deviating from the broader demographic. To assess the AMPT algorithm's real-time performance across a more diverse patient pool, a comprehensive study is necessary. Another constraint is the reliance on a desktop computer for consistent conditions in efficiency comparison. Future assessments should include mobile devices with various operating systems and concurrent applications for a more practical evaluation in real-world scenarios.

An AI model for prediction of cardiac arrest was developed using a novel public dataset on sudden cardiac arrest. The application of DL on the ECG of sudden cardiac arrest patients and a control group showed the potential of AI to be used as a screening tool to predict who is more prone to develop a cardiac arrest in the following days, weeks, months, and years.

A limitation arises from its exclusive reliance on data from the database of one hospital only, leading to a lack of diversity that limits the generalizability of conclusions to worldwide populations. In fact, limited datasets may not fully unlock the potential of deep learning algorithms

in predicting SCA exclusively from ECG waveforms. Another constraint is the retrospective, case-control design, exaggerating the incidence of SCA compared to the general population. To enhance confidence in findings, a wider and more balanced prospective cohort study is essential. Lastly, the absence of comorbidity data for the control group hinders its incorporation into the overall model.

A clinical test was executed to compare the signal quality of the YouCare device with a standard Holter monitor. The results showed the potential of the YouCare device, that could be used as an additional tool to monitor the patients that are under control for possible cardiac diseases.

This study has several limitations. Firstly, simultaneous use of devices may have caused interference, impacting the YouCare device's signal quality. Testing the YouCare device alone could reduce noise and connectivity issues. Secondly, reasons for Bluetooth disconnections and inadequate electrode-skin contact were unclear. Understanding these factors is vital for enhancing future YouCare iterations. Thirdly, though individuals with cardiac irregularities were studied, the device's performance in disease detection wasn't assessed. Fourthly, only the R-wave was analyzed, and the YouCare device's capability for capturing subtle ECG features remains unquantified. To enhance signal continuity, future development should focus on improved communication and electrode contact. Combining such advancements with enhanced ECG analysis, including artificial intelligence, holds potential for revolutionizing cardiac arrhythmia and disease detection in the general population, even enabling the detection of subclinical conditions.

7. Conclusions

This research project contributed to the enhancement of the electrocardiogram capabilities through the development and improvements of wearable and AI applications. In the next years, additional research contributions should focus on: (i) developing more reliable wearable devices with attention to usability; (ii) exploring new and larger ECG datasets promoting data standardization; (iii) developing more efficient and explainable AI algorithms; (iv) improving the sensors and the techniques to improve the ECG signal-noise ratio.

The evolution and exploration of wearable devices and biosignal analysis represent transformative forces in reshaping the healthcare landscape. However, it is crucial to exercise meticulous attention to ensure that the solutions developed not only keep pace with technological advancements but also actively contribute to the enhancement of patient care and the trajectory of healthcare in the future.

Bibliography

1. Guyton and Hall Textbook of Medical Physiology - 14th Edition Available online: https://shop.elsevier.com/books/guyton-and-hall-textbook-of-medical-physiology/hall/978-0-323-59712-8 (accessed on 27 December 2023).
2. *Essential Cardiology: Principles and Practice*; Rosendorff, C., Ed.; Humana Press: Totowa, NJ, 2006; ISBN 978-1-58829-370-1.
3. Dagher, L.; Shi, H.; Zhao, Y.; Marrouche, N.F. Wearables in Cardiology: Here to Stay. *Heart Rhythm* **2020**, *17*, 889–895, doi:10.1016/j.hrthm.2020.02.023.
4. Lu, L.; Zhang, J.; Xie, Y.; Gao, F.; Xu, S.; Wu, X.; Ye, Z. Wearable Health Devices in Health Care: Narrative Systematic Review. *JMIR Mhealth Uhealth* **2020**, *8*, e18907, doi:10.2196/18907.
5. Duncker, D.; Ding, W.Y.; Etheridge, S.; Noseworthy, P.A.; Veltmann, C.; Yao, X.; Bunch, T.J.; Gupta, D. Smart Wearables for Cardiac Monitoring-Real-World Use beyond Atrial Fibrillation. *Sensors (Basel)* **2021**, *21*, 2539, doi:10.3390/s21072539.
6. Kumari, P.; Mathew, L.; Syal, P. Increasing Trend of Wearables and Multimodal Interface for Human Activity Monitoring: A Review. *Biosensors and Bioelectronics* **2017**, *90*, 298–307, doi:10.1016/j.bios.2016.12.001.
7. *Wearable/Personal Monitoring Devices Present to Future*; Gargiulo, G.D., Naik, G.R., Eds.; Springer Singapore: Singapore, 2022; ISBN 9789811653230.
8. Rajpurkar, P.; Chen, E.; Banerjee, O.; Topol, E.J. AI in Health and Medicine. *Nat Med* **2022**, *28*, 31–38, doi:10.1038/s41591-021-01614-0.
9. Rajkomar, A.; Dean, J.; Kohane, I. Machine Learning in Medicine. *N Engl J Med* **2019**, *380*, 1347–1358, doi:10.1056/NEJMra1814259.
10. Koulaouzidis, G.; Jadczyk, T.; Iakovidis, D.K.; Koulaouzidis, A.; Bisnaire, M.; Charisopoulou, D. Artificial Intelligence in Cardiology-A Narrative Review of Current Status. *J Clin Med* **2022**, *11*, 3910, doi:10.3390/jcm11133910.
11. Witvliet, M.P.; Karregat, E.P.M.; Himmelreich, J.C.L.; de Jong, J.S.S.G.; Lucassen, W.A.M.; Harskamp, R.E. Usefulness, Pitfalls and Interpretation of Handheld Single-lead Electrocardiograms. *Journal of Electrocardiology* **2021**, *66*, 33–37, doi:10.1016/j.jelectrocard.2021.02.011.
12. Attia, Z.I.; Harmon, D.M.; Behr, E.R.; Friedman, P.A. Application of Artificial Intelligence to the Electrocardiogram. *Eur Heart J* **2021**, *42*, 4717–4730, doi:10.1093/eurheartj/ehab649.
13. Feeny, A.K.; Chung, M.K.; Madabhushi, A.; Attia, Z.I.; Cikes, M.; Firouznia, M.; Friedman, P.A.; Kalscheur, M.M.; Kapa, S.; Narayan, S.M.; et al. Artificial Intelligence and Machine Learning in Arrhythmias and Cardiac Electrophysiology. *Circulation: Arrhythmia and Electrophysiology* **2020**, *13*, e007952, doi:10.1161/CIRCEP.119.007952.
14. Hamet, P.; Tremblay, J. Artificial Intelligence in Medicine. *Metabolism* **2017**, *69S*, S36–S40, doi:10.1016/j.metabol.2017.01.011.
15. Health, C. for D. and R. Artificial Intelligence and Machine Learning (AI/ML)-Enabled Medical Devices. *FDA* **2022**.
16. Gibson, C.M.; Mehta, S.; Ceschim, M.R.S.; Frauenfelder, A.; Vieira, D.; Botelho, R.; Fernandez, F.; Villagran, C.; Niklitschek, S.; Matheus, C.I.; et al. Evolution of Single-Lead ECG for STEMI Detection Using a Deep Learning Approach. *International Journal of Cardiology* **2022**, *346*, 47–52, doi:10.1016/j.ijcard.2021.11.039.
17. Shao, M.; Zhou, Z.; Bin, G.; Bai, Y.; Wu, S. A Wearable Electrocardiogram Telemonitoring System for Atrial Fibrillation Detection. *Sensors* **2020**, *20*, 606, doi:10.3390/s20030606.
18. Fu, Z.; Hong, S.; Zhang, R.; Du, S. Artificial-Intelligence-Enhanced Mobile System for Cardiovascular Health Management. *Sensors (Basel)* **2021**, *21*, 773, doi:10.3390/s21030773.

19. Cai, W.; Chen, Y.; Guo, J.; Han, B.; Shi, Y.; Ji, L.; Wang, J.; Zhang, G.; Luo, J. Accurate Detection of Atrial Fibrillation from 12-Lead ECG Using Deep Neural Network. *Computers in Biology and Medicine* **2020**, *116*, 103378, doi:10.1016/j.compbiomed.2019.103378.
20. Baloglu, U.B.; Talo, M.; Yildirim, O.; Tan, R.S.; Acharya, U.R. Classification of Myocardial Infarction with Multi-Lead ECG Signals and Deep CNN. *Pattern Recognition Letters* **2019**, *122*, 23–30, doi:10.1016/j.patrec.2019.02.016.
21. Meng, L.; Tan, W.; Ma, J.; Wang, R.; Yin, X.; Zhang, Y. Enhancing Dynamic ECG Heartbeat Classification with Lightweight Transformer Model. *Artificial Intelligence in Medicine* **2022**, *124*, 102236, doi:10.1016/j.artmed.2022.102236.
22. Yu, J.; Wang, X.; Chen, X.; Guo, J. Automatic Premature Ventricular Contraction Detection Using Deep Metric Learning and KNN. *Biosensors (Basel)* **2021**, *11*, 69, doi:10.3390/bios11030069.
23. Ellenbogen, K.A. Josephson's Clinical Cardiac Electrophysiology. *JACC: Clinical Electrophysiology* **2021**, *7*, 957–958, doi:10.1016/j.jacep.2021.05.007.
24. Lip, G.Y.H.; Nieuwlaat, R.; Pisters, R.; Lane, D.A.; Crijns, H.J.G.M. Refining Clinical Risk Stratification for Predicting Stroke and Thromboembolism in Atrial Fibrillation Using a Novel Risk Factor-Based Approach: The Euro Heart Survey on Atrial Fibrillation. *Chest* **2010**, *137*, 263–272, doi:10.1378/chest.09-1584.
25. Gopinathannair, R.; Sullivan, R.; Olshansky, B. Tachycardia-Mediated Cardiomyopathy: Recognition and Management. *Curr Heart Fail Rep* **2009**, *6*, 257–264, doi:10.1007/s11897-009-0035-3.
26. Epidemiology of Atrial Fibrillation in the 21st Century Available online: https://www.ahajournals.org/doi/epub/10.1161/CIRCRESAHA.120.316340 (accessed on 18 April 2023).
27. Bashar, S.K.; Han, D.; Zieneddin, F.; Ding, E.; Fitzgibbons, T.P.; Walkey, A.J.; McManus, D.D.; Javidi, B.; Chon, K.H. Novel Density Poincaré Plot Based Machine Learning Method to Detect Atrial Fibrillation From Premature Atrial/Ventricular Contractions. *IEEE Trans Biomed Eng* **2021**, *68*, 448–460, doi:10.1109/TBME.2020.3004310.
28. Wang, J. Automated Detection of Premature Ventricular Contraction Based on the Improved Gated Recurrent Unit Network. *Comput Methods Programs Biomed* **2021**, *208*, 106284, doi:10.1016/j.cmpb.2021.106284.
29. Zipes, D.P.; Wellens, H.J. Sudden Cardiac Death. *Circulation* **1998**, *98*, 2334–2351, doi:10.1161/01.cir.98.21.2334.
30. Malakar, A.Kr.; Choudhury, D.; Halder, B.; Paul, P.; Uddin, A.; Chakraborty, S. A Review on Coronary Artery Disease, Its Risk Factors, and Therapeutics. *Journal of Cellular Physiology* **2019**, *234*, 16812–16823, doi:10.1002/jcp.28350.
31. Heart Disease and Stroke Statistics—2022 Update: A Report From the American Heart Association | Circulation Available online: https://www.ahajournals.org/doi/10.1161/CIR.0000000000001052 (accessed on 28 November 2022).
32. Zipes, M. *Braunwald's Heart Disease: A Textbook of Cardiovascular Medicine, 2019*;
33. Mannhart, D.; Lischer, M.; Knecht, S.; du Fay de Lavallaz, J.; Strebel, I.; Serban, T.; Vögeli, D.; Schaer, B.; Osswald, S.; Mueller, C.; et al. Clinical Validation of 5 Direct-to-Consumer Wearable Smart Devices to Detect Atrial Fibrillation: BASEL Wearable Study. *JACC: Clinical Electrophysiology* **2023**, doi:10.1016/j.jacep.2022.09.011.
34. Chen, E.; Jiang, J.; Su, R.; Gao, M.; Zhu, S.; Zhou, J.; Huo, Y. A New Smart Wristband Equipped with an Artificial Intelligence Algorithm to Detect Atrial Fibrillation. *Heart Rhythm* **2020**, *17*, 847–853, doi:10.1016/j.hrthm.2020.01.034.
35. Panganiban, E.B.; Paglinawan, A.C.; Chung, W.Y.; Paa, G.L.S. ECG Diagnostic Support System (EDSS): A Deep Learning Neural Network Based Classification System for Detecting ECG Abnormal Rhythms from a Low-Powered Wearable Biosensors. *Sensing and Bio-Sensing Research* **2021**, *31*, 100398, doi:10.1016/j.sbsr.2021.100398.

36. Lown, M.; Brown, M.; Brown, C.; Yue, A.M.; Shah, B.N.; Corbett, S.J.; Lewith, G.; Stuart, B.; Moore, M.; Little, P. Machine Learning Detection of Atrial Fibrillation Using Wearable Technology. *PLoS One* **2020**, *15*, e0227401, doi:10.1371/journal.pone.0227401.
37. Khan, M.; Abbas, S.; Atta, A.; Ditta, A.; Alquhayz, H.; Khan, M.; Atta-ur-Rahman; Naqvi, R. Intelligent Cloud Based Heart Disease Prediction System Empowered with Supervised Machine Learning. *cmc* **2020**, *65*, 139–151, doi:10.32604/cmc.2020.011416.
38. Wasimuddin, M.; Elleithy, K.; Abuzneid, A.; Faezipour, M.; Abuzaghleh, O. Multiclass ECG Signal Analysis Using Global Average-Based 2-D Convolutional Neural Network Modeling. *Electronics* **2021**, *10*, 170, doi:10.3390/electronics10020170.
39. Chowdhury, M.E.H.; Alzoubi, K.; Khandakar, A.; Khallifa, R.; Abouhasera, R.; Koubaa, S.; Ahmed, R.; Hasan, M.A. Wearable Real-Time Heart Attack Detection and Warning System to Reduce Road Accidents. *Sensors (Basel)* **2019**, *19*, E2780, doi:10.3390/s19122780.
40. Perez, M.V.; Mahaffey, K.W.; Hedlin, H.; Rumsfeld, J.S.; Garcia, A.; Ferris, T.; Balasubramanian, V.; Russo, A.M.; Rajmane, A.; Cheung, L.; et al. Large-Scale Assessment of a Smartwatch to Identify Atrial Fibrillation. *New England Journal of Medicine* **2019**, *381*, 1909–1917, doi:10.1056/NEJMoa1901183.
41. Fu, W.; Li, R. Diagnostic Performance of a Wearing Dynamic ECG Recorder for Atrial Fibrillation Screening: The HUAMI Heart Study. *BMC Cardiovasc Disord* **2021**, *21*, 558, doi:10.1186/s12872-021-02363-1.
42. Santala, O.E.; Halonen, J.; Martikainen, S.; Jäntti, H.; Rissanen, T.T.; Tarvainen, M.P.; Laitinen, T.P.; Laitinen, T.M.; Väliaho, E.-S.; Hartikainen, J.E.K.; et al. Automatic Mobile Health Arrhythmia Monitoring for the Detection of Atrial Fibrillation: Prospective Feasibility, Accuracy, and User Experience Study. *JMIR Mhealth Uhealth* **2021**, *9*, e29933, doi:10.2196/29933.
43. Jeon, E.; Oh, K.; Kwon, S.; Son, H.; Yun, Y.; Jung, E.-S.; Kim, M.S. A Lightweight Deep Learning Model for Fast Electrocardiographic Beats Classification With a Wearable Cardiac Monitor: Development and Validation Study. *JMIR Med Inform* **2020**, *8*, e17037, doi:10.2196/17037.
44. Bazi, Y.; Al Rahhal, M.M.; AlHichri, H.; Ammour, N.; Alajlan, N.; Zuair, M. Real-Time Mobile-Based Electrocardiogram System for Remote Monitoring of Patients with Cardiac Arrhythmias. *Int. J. Patt. Recogn. Artif. Intell.* **2020**, *34*, 2058013, doi:10.1142/S0218001420580136.
45. Ma, C.; Wei, S.; Chen, T.; Zhong, J.; Liu, Z.; Liu, C. Integration of Results From Convolutional Neural Network in a Support Vector Machine for the Detection of Atrial Fibrillation. *IEEE Transactions on Instrumentation and Measurement* **2021**, *70*, 1–10, doi:10.1109/TIM.2020.3044718.
46. Goldberger, A.L.; Amaral, L.A.; Glass, L.; Hausdorff, J.M.; Ivanov, P.C.; Mark, R.G.; Mietus, J.E.; Moody, G.B.; Peng, C.K.; Stanley, H.E. PhysioBank, PhysioToolkit, and PhysioNet: Components of a New Research Resource for Complex Physiologic Signals. *Circulation* **2000**, *101*, E215-220, doi:10.1161/01.cir.101.23.e215.
47. Moody, G.B.; Mark, R.G. The Impact of the MIT-BIH Arrhythmia Database. *IEEE Engineering in Medicine and Biology Magazine* **2001**, *20*, 45–50, doi:10.1109/51.932724.
48. Lee, K.-S.; Park, H.-J.; Kim, J.E.; Kim, H.J.; Chon, S.; Kim, S.; Jang, J.; Kim, J.-K.; Jang, S.; Gil, Y.; et al. Compressed Deep Learning to Classify Arrhythmia in an Embedded Wearable Device. *Sensors (Basel)* **2022**, *22*, 1776, doi:10.3390/s22051776.
49. Wu, X.; Zheng, Y.; Chu, C.-H.; He, Z. Extracting Deep Features from Short ECG Signals for Early Atrial Fibrillation Detection. *Artificial Intelligence in Medicine* **2020**, *109*, 101896, doi:10.1016/j.artmed.2020.101896.
50. Ben Itzhak, S.; Ricon, S.S.; Biton, S.; Behar, J.A.; Sobel, J.A. Effect of Temporal Resolution on the Detection of Cardiac Arrhythmias Using HRV Features and Machine Learning. *Physiol Meas* **2022**, *43*, doi:10.1088/1361-6579/ac6561.
51. Mei, Z.; Gu, X.; Chen, H.; Chen, W. Automatic Atrial Fibrillation Detection Based on Heart Rate Variability and Spectral Features. *IEEE Access* **2018**, *6*, 53566–53575, doi:10.1109/ACCESS.2018.2871220.

52. Smisek, R.; Hejc, J.; Ronzhina, M.; Nemcova, A.; Marsanova, L.; Kolarova, J.; Smital, L.; Vitek, M. Multi-Stage SVM Approach for Cardiac Arrhythmias Detection in Short Single-Lead ECG Recorded by a Wearable Device. *Physiol Meas* **2018**, *39*, 094003, doi:10.1088/1361-6579/aad9e7.
53. Tang, X.; Ma, Z.; Hu, Q.; Tang, W. A Real-Time Arrhythmia Heartbeats Classification Algorithm Using Parallel Delta Modulations and Rotated Linear-Kernel Support Vector Machines. *IEEE Transactions on Biomedical Engineering* **2020**, *67*, 978–986, doi:10.1109/TBME.2019.2926104.
54. Hua, J.; Zhang, H.; Liu, J.; Xu, Y.; Guo, F. Direct Arrhythmia Classification from Compressive ECG Signals in Wearable Health Monitoring System. *J CIRCUIT SYST COMP* **2018**, *27*, 1850088, doi:10.1142/S0218126618500883.
55. Pławiak, P.; Acharya, U.R. Novel Deep Genetic Ensemble of Classifiers for Arrhythmia Detection Using ECG Signals. *Neural Comput & Applic* **2020**, *32*, 11137–11161, doi:10.1007/s00521-018-03980-2.
56. Yıldırım, Ö.; Pławiak, P.; Tan, R.-S.; Acharya, U.R. Arrhythmia Detection Using Deep Convolutional Neural Network with Long Duration ECG Signals. *Computers in Biology and Medicine* **2018**, *102*, 411–420, doi:10.1016/j.compbiomed.2018.09.009.
57. Karthiga, S.; Abirami, A. Deep Learning Convolutional Neural Network for ECG Signal Classification Aggregated Using IoT. *csse* **2022**, *42*, 851–866, doi:10.32604/csse.2022.021935.
58. Zhang, Y.; Liu, S.; He, Z.; Zhang, Y.; Wang, C. A CNN Model for Cardiac Arrhythmias Classification Based on Individual ECG Signals. *Cardiovasc Eng Technol* **2022**, *13*, 548–557, doi:10.1007/s13239-021-00599-8.
59. Ramesh, J.; Solatidehkordi, Z.; Aburukba, R.; Sagahyroon, A. Atrial Fibrillation Classification with Smart Wearables Using Short-Term Heart Rate Variability and Deep Convolutional Neural Networks. *Sensors (Basel)* **2021**, *21*, 7233, doi:10.3390/s21217233.
60. Chen, Y.; Zhang, C.; Liu, C.; Wang, Y.; Wan, X. Atrial Fibrillation Detection Using a Feedforward Neural Network. *J. Med. Biol. Eng.* **2022**, *42*, 63–73, doi:10.1007/s40846-022-00681-z.
61. Huang, Y.; Li, H.; Yu, X. A Multiview Feature Fusion Model for Heartbeat Classification. *Physiol Meas* **2021**, *42*, doi:10.1088/1361-6579/ac010f.
62. Shin, S.; Kang, M.; Zhang, G.; Jung, J.; Kim, Y.T. Lightweight Ensemble Network for Detecting Heart Disease Using ECG Signals. *Applied Sciences* **2022**, *12*, 3291, doi:10.3390/app12073291.
63. Mazumder, O.; Banerjee, R.; Roy, D.; Mukherjee, A.; Ghose, A.; Khandelwal, S.; Sinha, A. Computational Model for Therapy Optimization of Wearable Cardioverter Defibrillator: Shockable Rhythm Detection and Optimal Electrotherapy. *Front Physiol* **2021**, *12*, 787180, doi:10.3389/fphys.2021.787180.
64. Tan, L.; Yu, K.; Bashir, A.K.; Cheng, X.; Ming, F.; Zhao, L.; Zhou, X. Toward Real-Time and Efficient Cardiovascular Monitoring for COVID-19 Patients by 5G-Enabled Wearable Medical Devices: A Deep Learning Approach. *Neural Comput Appl* **2021**, 1–14, doi:10.1007/s00521-021-06219-9.
65. Li, Y.; Pang, Y.; Wang, J.; Li, X. Patient-Specific ECG Classification by Deeper CNN from Generic to Dedicated. *Neurocomputing* **2018**, *314*, 336–346, doi:10.1016/j.neucom.2018.06.068.
66. Fan, X.; Yao, Q.; Cai, Y.; Miao, F.; Sun, F.; Li, Y. Multiscaled Fusion of Deep Convolutional Neural Networks for Screening Atrial Fibrillation From Single Lead Short ECG Recordings. *IEEE J Biomed Health Inform* **2018**, *22*, 1744–1753, doi:10.1109/JBHI.2018.2858789.
67. Zhang, P.; Ma, C.; Sun, Y.; Fan, G.; Song, F.; Feng, Y.; Zhang, G. Global Hybrid Multi-Scale Convolutional Network for Accurate and Robust Detection of Atrial Fibrillation Using Single-Lead ECG Recordings. *Computers in Biology and Medicine* **2021**, *139*, 104880, doi:10.1016/j.compbiomed.2021.104880.
68. Sakib, S.; Fouda, M.M.; Fadlullah, Z.Md.; Nasser, N.; Alasmary, W. A Proof-of-Concept of Ultra-Edge Smart IoT Sensor: A Continuous and Lightweight Arrhythmia Monitoring Approach. *IEEE Access* **2021**, *9*, 26093–26106, doi:10.1109/ACCESS.2021.3056509.
69. De Melo Ribeiro, H.; Arnold, A.; Howard, J.P.; Shun-Shin, M.J.; Zhang, Y.; Francis, D.P.; Lim, P.B.; Whinnett, Z.; Zolgharni, M. ECG-Based Real-Time Arrhythmia Monitoring Using Quantized Deep

Neural Networks: A Feasibility Study. *Computers in Biology and Medicine* **2022**, *143*, 105249, doi:10.1016/j.compbiomed.2022.105249.
70. Ran, S.; Yang, X.; Liu, M.; Zhang, Y.; Cheng, C.; Zhu, H.; Yuan, Y. Homecare-Oriented ECG Diagnosis With Large-Scale Deep Neural Network for Continuous Monitoring on Embedded Devices. *IEEE Transactions on Instrumentation and Measurement* **2022**, *71*, 1–13, doi:10.1109/TIM.2022.3147328.
71. Mian Qaisar, S.; Fawad Hussain, S. Arrhythmia Diagnosis by Using Level-Crossing ECG Sampling and Sub-Bands Features Extraction for Mobile Healthcare. *Sensors (Basel)* **2020**, *20*, E2252, doi:10.3390/s20082252.
72. Mian Qaisar, S.; Subasi, A. Cloud-Based ECG Monitoring Using Event-Driven ECG Acquisition and Machine Learning Techniques. *Phys Eng Sci Med* **2020**, *43*, 623–634, doi:10.1007/s13246-020-00863-6.
73. Qaisar, S.M.; Mihoub, A.; Krichen, M.; Nisar, H. Multirate Processing with Selective Subbands and Machine Learning for Efficient Arrhythmia Classification. *Sensors* **2021**, *21*, 1511, doi:10.3390/s21041511.
74. Cheng, Y.; Hu, Y.; Hou, M.; Pan, T.; He, W.; Ye, Y. Atrial Fibrillation Detection Directly from Compressed ECG with the Prior of Measurement Matrix. *Information* **2020**, *11*, 436, doi:10.3390/info11090436.
75. Zhang, H.; Dong, Z.; Gao, J.; Lu, P.; Wang, Z. Automatic Screening Method for Atrial Fibrillation Based on Lossy Compression of the Electrocardiogram Signal. *Physiol Meas* **2020**, *41*, 075005, doi:10.1088/1361-6579/ab979f.
76. Alqudah, A.M.; Alqudah, A. Deep Learning for Single-Lead ECG Beat Arrhythmia-Type Detection Using Novel Iris Spectrogram Representation. *Soft Comput* **2022**, *26*, 1123–1139, doi:10.1007/s00500-021-06555-x.
77. Lee, H.; Shin, M. Learning Explainable Time-Morphology Patterns for Automatic Arrhythmia Classification from Short Single-Lead ECGs. *Sensors (Basel)* **2021**, *21*, 4331, doi:10.3390/s21134331.
78. Seo, W.; Kim, N.; Kim, S.; Lee, C.; Park, S.-M. Deep ECG-Respiration Network (DeepER Net) for Recognizing Mental Stress. *Sensors (Basel)* **2019**, *19*, E3021, doi:10.3390/s19133021.
79. Alqudah, A.M.; Qazan, S.; Al-Ebbini, L.; Alquran, H.; Qasmieh, I.A. ECG Heartbeat Arrhythmias Classification: A Comparison Study between Different Types of Spectrum Representation and Convolutional Neural Networks Architectures. *J Ambient Intell Human Comput* **2022**, *13*, 4877–4907, doi:10.1007/s12652-021-03247-0.
80. Dami, S.; Yahaghizadeh, M. Predicting Cardiovascular Events with Deep Learning Approach in the Context of the Internet of Things. *Neural Comput & Applic* **2021**, *33*, 7979–7996, doi:10.1007/s00521-020-05542-x.
81. Khan, M.A. An IoT Framework for Heart Disease Prediction Based on MDCNN Classifier. *IEEE Access* **2020**, *8*, 34717–34727, doi:10.1109/ACCESS.2020.2974687.
82. Sopic, D.; Aminifar, A.; Aminifar, A.; Atienza, D. Real-Time Event-Driven Classification Technique for Early Detection and Prevention of Myocardial Infarction on Wearable Systems. *IEEE Trans Biomed Circuits Syst* **2018**, doi:10.1109/TBCAS.2018.2848477.
83. Shahnawaz, M.B.; Dawood, H. An Effective Deep Learning Model for Automated Detection of Myocardial Infarction Based on Ultrashort-Term Heart Rate Variability Analysis. *Mathematical Problems in Engineering* **2021**, *2021*, e6455053, doi:10.1155/2021/6455053.
84. Martin, H.; Morar, U.; Izquierdo, W.; Cabrerizo, M.; Cabrera, A.; Adjouadi, M. Real-Time Frequency-Independent Single-Lead and Single-Beat Myocardial Infarction Detection. *Artificial Intelligence in Medicine* **2021**, *121*, 102179, doi:10.1016/j.artmed.2021.102179.
85. Cao, Y.; Wei, T.; Zhang, B.; Lin, N.; Rodrigues, J.J.P.C.; Li, J.; Zhang, D. ML-Net: Multi-Channel Lightweight Network for Detecting Myocardial Infarction. *IEEE J Biomed Health Inform* **2021**, *25*, 3721–3731, doi:10.1109/JBHI.2021.3060433.

86. Cho, J.; Lee, B.; Kwon, J.-M.; Lee, Y.; Park, H.; Oh, B.-H.; Jeon, K.-H.; Park, J.; Kim, K.-H. Artificial Intelligence Algorithm for Screening Heart Failure with Reduced Ejection Fraction Using Electrocardiography. *ASAIO J* **2021**, *67*, 314–321, doi:10.1097/MAT.0000000000001218.
87. Cowie, M.R. Sleep Apnea: State of the Art. *Trends Cardiovasc Med* **2017**, *27*, 280–289, doi:10.1016/j.tcm.2016.12.005.
88. Roberts, E.G.; Raphelson, J.R.; Orr, J.E.; LaBuzetta, J.N.; Malhotra, A. The Pathogenesis of Central and Complex Sleep Apnea. *Curr Neurol Neurosci Rep* **2022**, *22*, 405–412, doi:10.1007/s11910-022-01199-2.
89. Pham, L.V.; Jun, J.; Polotsky, V.Y. Chapter 6 - Obstructive Sleep Apnea. In *Handbook of Clinical Neurology*; Chen, R., Guyenet, P.G., Eds.; Respiratory Neurobiology: Physiology and Clinical Disorders, Part II; Elsevier, 2022; Vol. 189, pp. 105–136.
90. Malhotra, A.; Ayappa, I.; Ayas, N.; Collop, N.; Kirsch, D.; Mcardle, N.; Mehra, R.; Pack, A.I.; Punjabi, N.; White, D.P.; et al. Metrics of Sleep Apnea Severity: Beyond the Apnea-Hypopnea Index. *Sleep* **2021**, *44*, zsab030, doi:10.1093/sleep/zsab030.
91. Benjamin, E.J.; Muntner, P.; Alonso, A.; Bittencourt, M.S.; Callaway, C.W.; Carson, A.P.; Chamberlain, A.M.; Chang, A.R.; Cheng, S.; Das, S.R.; et al. Heart Disease and Stroke Statistics—2019 Update: A Report From the American Heart Association. *Circulation* **2019**, *139*, e56–e528, doi:10.1161/CIR.0000000000000659.
92. de Zambotti, M.; Menghini, L.; Grandner, M.A.; Redline, S.; Zhang, Y.; Wallace, M.L.; Buxton, O.M. Rigorous Performance Evaluation (Previously, "Validation") for Informed Use of New Technologies for Sleep Health Measurement. *Sleep Health* **2022**, *8*, 263–269, doi:10.1016/j.sleh.2022.02.006.
93. Penzel, T.; Moody, G.B.; Mark, R.G.; Goldberger, A.L.; Peter, J.H. The Apnea-ECG Database. In Proceedings of the Computers in Cardiology 2000. Vol.27 (Cat. 00CH37163); September 2000; pp. 255–258.
94. Wang, T.; Lu, C.; Shen, G.; Hong, F. Sleep Apnea Detection from a Single-Lead ECG Signal with Automatic Feature-Extraction through a Modified LeNet-5 Convolutional Neural Network. *PeerJ* **2019**, *7*, e7731, doi:10.7717/peerj.7731.
95. Urtnasan, E.; Park, J.U.; Joo, E.Y.; Lee, K.J. Identification of Sleep Apnea Severity Based on Deep Learning from a Short-Term Normal ECG. *J Korean Med Sci* **2020**, *35*, e399, doi:10.3346/jkms.2020.35.e399.
96. Shen, Q.; Qin, H.; Wei, K.; Liu, G. Multiscale Deep Neural Network for Obstructive Sleep Apnea Detection Using RR Interval From Single-Lead ECG Signal. *IEEE Transactions on Instrumentation and Measurement* **2021**, *70*, 1–13, doi:10.1109/TIM.2021.3062414.
97. Almutairi, H.; Hassan, G.M.; Datta, A. Classification of Obstructive Sleep Apnoea from Single-Lead ECG Signals Using Convolutional Neural and Long Short Term Memory Networks. *Biomedical Signal Processing and Control* **2021**, *69*, 102906, doi:10.1016/j.bspc.2021.102906.
98. Bahrami, M.; Forouzanfar, M. Deep Learning Forecasts the Occurrence of Sleep Apnea from Single-Lead ECG. *Cardiovasc Eng Tech* **2022**, doi:10.1007/s13239-022-00615-5.
99. Qin, H.; Liu, G. A Dual-Model Deep Learning Method for Sleep Apnea Detection Based on Representation Learning and Temporal Dependence. *Neurocomputing* **2022**, *473*, 24–36, doi:10.1016/j.neucom.2021.12.001.
100. Yang, Q.; Zou, L.; Wei, K.; Liu, G. Obstructive Sleep Apnea Detection from Single-Lead Electrocardiogram Signals Using One-Dimensional Squeeze-and-Excitation Residual Group Network. *Comput Biol Med* **2021**, *140*, 105124, doi:10.1016/j.compbiomed.2021.105124.
101. Cacioppo, J.T.; Tassinary, L.G.; Berntson, G.G. Psychophysiological Science: Interdisciplinary Approaches to Classic Questions About the Mind. In *Handbook of Psychophysiology*; Cacioppo, J.T., Tassinary, L.G., Berntson, G., Eds.; Cambridge University Press: Cambridge, 2007; pp. 1–16 ISBN 978-0-511-54639-6.
102. O'Connor, D.B.; Thayer, J.F.; Vedhara, K. Stress and Health: A Review of Psychobiological Processes. *Annu Rev Psychol* **2021**, *72*, 663–688, doi:10.1146/annurev-psych-062520-122331.

103. Krantz, D.S.; Manuck, S.B. Acute Psychophysiologic Reactivity and Risk of Cardiovascular Disease: A Review and Methodologic Critique. *Psychol Bull* **1984**, *96*, 435–464.
104. Schwartz, A.R.; Gerin, W.; Davidson, K.W.; Pickering, T.G.; Brosschot, J.F.; Thayer, J.F.; Christenfeld, N.; Linden, W. Toward a Causal Model of Cardiovascular Responses to Stress and the Development of Cardiovascular Disease. *Psychosom Med* **2003**, *65*, 22–35, doi:10.1097/01.psy.0000046075.79922.61.
105. Dedovic, K.; Ngiam, J. The Cortisol Awakening Response and Major Depression: Examining the Evidence. *Neuropsychiatr Dis Treat* **2015**, *11*, 1181–1189, doi:10.2147/NDT.S62289.
106. Chida, Y.; Hamer, M. Chronic Psychosocial Factors and Acute Physiological Responses to Laboratory-Induced Stress in Healthy Populations: A Quantitative Review of 30 Years of Investigations. *Psychol Bull* **2008**, *134*, 829–885, doi:10.1037/a0013342.
107. Chauvet-Gelinier, J.-C.; Bonin, B. Stress, Anxiety and Depression in Heart Disease Patients: A Major Challenge for Cardiac Rehabilitation. *Ann Phys Rehabil Med* **2017**, *60*, 6–12, doi:10.1016/j.rehab.2016.09.002.
108. Castaldo, R.; Melillo, P.; Bracale, U.; Caserta, M.; Triassi, M.; Pecchia, L. Acute Mental Stress Assessment via Short Term HRV Analysis in Healthy Adults: A Systematic Review with Meta-Analysis. *Biomedical Signal Processing and Control* **2015**, *18*, 370–377, doi:10.1016/j.bspc.2015.02.012.
109. Parlak, O. Portable and Wearable Real-Time Stress Monitoring: A Critical Review. *Sensors and Actuators Reports* **2021**, *3*, 100036, doi:10.1016/j.snr.2021.100036.
110. Bali, A.; Jaggi, A.S. Clinical Experimental Stress Studies: Methods and Assessment. *Rev Neurosci* **2015**, *26*, 555–579, doi:10.1515/revneuro-2015-0004.
111. Shiban, Y.; Diemer, J.; Brandl, S.; Zack, R.; Mühlberger, A.; Wüst, S. Trier Social Stress Test in Vivo and in Virtual Reality: Dissociation of Response Domains. *Int J Psychophysiol* **2016**, *110*, 47–55, doi:10.1016/j.ijpsycho.2016.10.008.
112. Wilhelm, F.H.; Grossman, P. Emotions beyond the Laboratory: Theoretical Fundaments, Study Design, and Analytic Strategies for Advanced Ambulatory Assessment. *Biological Psychology* **2010**, *84*, 552–569, doi:10.1016/j.biopsycho.2010.01.017.
113. Shaffer, F.; McCraty, R.; Zerr, C.L. A Healthy Heart Is Not a Metronome: An Integrative Review of the Heart's Anatomy and Heart Rate Variability. *Front Psychol* **2014**, *5*, 1040, doi:10.3389/fpsyg.2014.01040.
114. Thayer, J.F.; Hansen, A.L.; Saus-Rose, E.; Johnsen, B.H. Heart Rate Variability, Prefrontal Neural Function, and Cognitive Performance: The Neurovisceral Integration Perspective on Self-Regulation, Adaptation, and Health. *Ann Behav Med* **2009**, *37*, 141–153, doi:10.1007/s12160-009-9101-z.
115. Berntson, G.G.; Bigger, J.T.; Eckberg, D.L.; Grossman, P.; Kaufmann, P.G.; Malik, M.; Nagaraja, H.N.; Porges, S.W.; Saul, J.P.; Stone, P.H.; et al. Heart Rate Variability: Origins, Methods, and Interpretive Caveats. *Psychophysiology* **1997**, *34*, 623–648, doi:10.1111/j.1469-8986.1997.tb02140.x.
116. Schulze-Bonhage, A.; Sales, F.; Wagner, K.; Teotonio, R.; Carius, A.; Schelle, A.; Ihle, M. Views of Patients with Epilepsy on Seizure Prediction Devices. *Epilepsy Behav* **2010**, *18*, 388–396, doi:10.1016/j.yebeh.2010.05.008.
117. Lotufo, P.A.; Valiengo, L.; Benseñor, I.M.; Brunoni, A.R. A Systematic Review and Meta-Analysis of Heart Rate Variability in Epilepsy and Antiepileptic Drugs. *Epilepsia* **2012**, *53*, 272–282, doi:10.1111/j.1528-1167.2011.03361.x.
118. Eggleston, K.S.; Olin, B.D.; Fisher, R.S. Ictal Tachycardia: The Head-Heart Connection. *Seizure* **2014**, *23*, 496–505, doi:10.1016/j.seizure.2014.02.012.
119. Betti, S.; Lova, R.M.; Rovini, E.; Acerbi, G.; Santarelli, L.; Cabiati, M.; Del Ry, S.; Cavallo, F. Evaluation of an Integrated System of Wearable Physiological Sensors for Stress Monitoring in Working Environments by Using Biological Markers. *IEEE Trans Biomed Eng* **2018**, *65*, 1748–1758, doi:10.1109/TBME.2017.2764507.

120. Cho, H.-M.; Park, H.; Dong, S.-Y.; Youn, I. Ambulatory and Laboratory Stress Detection Based on Raw Electrocardiogram Signals Using a Convolutional Neural Network. *Sensors (Basel)* **2019**, *19*, E4408, doi:10.3390/s19204408.
121. Huang, S.; Li, J.; Zhang, P.; Zhang, W. Detection of Mental Fatigue State with Wearable ECG Devices. *Int J Med Inform* **2018**, *119*, 39–46, doi:10.1016/j.ijmedinf.2018.08.010.
122. Healey, J.A.; Picard, R.W. Detecting Stress during Real-World Driving Tasks Using Physiological Sensors. *IEEE Transactions on Intelligent Transportation Systems* **2005**, *6*, 156–166, doi:10.1109/TITS.2005.848368.
123. Sepúlveda, A.; Castillo, F.; Palma, C.; Rodriguez-Fernandez, M. Emotion Recognition from ECG Signals Using Wavelet Scattering and Machine Learning. *Applied Sciences* **2021**, *11*, 4945, doi:10.3390/app11114945.
124. Yamakawa, T.; Miyajima, M.; Fujiwara, K.; Kano, M.; Suzuki, Y.; Watanabe, Y.; Watanabe, S.; Hoshida, T.; Inaji, M.; Maehara, T. Wearable Epileptic Seizure Prediction System with Machine-Learning-Based Anomaly Detection of Heart Rate Variability. *Sensors (Basel)* **2020**, *20*, E3987, doi:10.3390/s20143987.
125. Vandecasteele, K.; De Cooman, T.; Chatzichristos, C.; Cleeren, E.; Swinnen, L.; Macea Ortiz, J.; Van Huffel, S.; Dümpelmann, M.; Schulze-Bonhage, A.; De Vos, M.; et al. The Power of ECG in Multimodal Patient-Specific Seizure Monitoring: Added Value to an EEG-Based Detector Using Limited Channels. *Epilepsia* **2021**, *62*, 2333–2343, doi:10.1111/epi.16990.
126. Ihle, M.; Feldwisch-Drentrup, H.; Teixeira, C.A.; Witon, A.; Schelter, B.; Timmer, J.; Schulze-Bonhage, A. EPILEPSIAE - a European Epilepsy Database. *Comput Methods Programs Biomed* **2012**, *106*, 127–138, doi:10.1016/j.cmpb.2010.08.011.
127. Beniczky, S.; Ryvlin, P. Standards for Testing and Clinical Validation of Seizure Detection Devices. *Epilepsia* **2018**, *59 Suppl 1*, 9–13, doi:10.1111/epi.14049.
128. Malik, M.; Bigger, J.T.; Camm, A.J.; Kleiger, R.E.; Malliani, A.; Moss, A.J.; Schwartz, P.J. Heart Rate Variability: Standards of Measurement, Physiological Interpretation, and Clinical Use. *European Heart Journal* **1996**, *17*, 354–381, doi:10.1093/oxfordjournals.eurheartj.a014868.
129. Porumb, M.; Stranges, S.; Pescapè, A.; Pecchia, L. Precision Medicine and Artificial Intelligence: A Pilot Study on Deep Learning for Hypoglycemic Events Detection Based on ECG. *Sci Rep* **2020**, *10*, 170, doi:10.1038/s41598-019-56927-5.
130. Cordeiro, R.; Karimian, N.; Park, Y. Hyperglycemia Identification Using ECG in Deep Learning Era. *Sensors (Basel)* **2021**, *21*, 6263, doi:10.3390/s21186263.
131. Luo, X. ECG Signal Analysis for Fatigue and Abnormal Event Detection during Sport and Exercise. *Internet Technology Letters* **2021**, *4*, e262, doi:10.1002/itl2.262.
132. Meskó, B.; Görög, M. A Short Guide for Medical Professionals in the Era of Artificial Intelligence. *npj Digit. Med.* **2020**, *3*, 1–8, doi:10.1038/s41746-020-00333-z.
133. Neri, L.; Oberdier, M.T.; Augello, A.; Suzuki, M.; Tumarkin, E.; Jaipalli, S.; Geminiani, G.A.; Halperin, H.R.; Borghi, C. Algorithm for Mobile Platform-Based Real-Time QRS Detection. *Sensors* **2023**, *23*, 1625, doi:10.3390/s23031625.
134. Hossain, M.B.; Bashar, S.K.; Walkey, A.J.; McManus, D.D.; Chon, K.H. An Accurate QRS Complex and P Wave Detection in ECG Signals Using Complete Ensemble Empirical Mode Decomposition with Adaptive Noise Approach. *IEEE Access* **2019**, *7*, 128869–128880, doi:10.1109/ACCESS.2019.2939943.
135. Mück, J.E.; Ünal, B.; Butt, H.; Yetisen, A.K. Market and Patent Analyses of Wearables in Medicine. *Trends in Biotechnology* **2019**, *37*, 563–566, doi:10.1016/j.tibtech.2019.02.001.
136. Hong, Y.J.; Jeong, H.; Cho, K.W.; Lu, N.; Kim, D. Wearable and Implantable Devices for Cardiovascular Healthcare: From Monitoring to Therapy Based on Flexible and Stretchable Electronics. *Adv. Funct. Mater.* **2019**, *29*, 1808247, doi:10.1002/adfm.201808247.
137. Stehlik, J.; Schmalfuss, C.; Bozkurt, B.; Nativi-Nicolau, J.; Wohlfahrt, P.; Wegerich, S.; Rose, K.; Ray, R.; Schofield, R.; Deswal, A.; et al. Continuous Wearable Monitoring Analytics Predict Heart

Failure Hospitalization. *Circulation: Heart Failure* **2020**, *13*, e006513, doi:10.1161/CIRCHEARTFAILURE.119.006513.
138. Elgendi, M. Fast QRS Detection with an Optimized Knowledge-Based Method: Evaluation on 11 Standard ECG Databases. *PLoS One* **2013**, *8*, e73557, doi:10.1371/journal.pone.0073557.
139. Manikandan, M.S.; Soman, K.P. A Novel Method for Detecting R-Peaks in Electrocardiogram (ECG) Signal. *Biomedical Signal Processing and Control* **2012**, *7*, 118–128, doi:10.1016/j.bspc.2011.03.004.
140. Kim, J.; Shin, H. Simple and Robust Realtime QRS Detection Algorithm Based on Spatiotemporal Characteristic of the QRS Complex. *PLoS ONE* **2016**, *11*, e0150144, doi:10.1371/journal.pone.0150144.
141. Zalabarria, U.; Irigoyen, E.; Martinez, R.; Lowe, A. Online Robust R-Peaks Detection in Noisy Electrocardiograms Using a Novel Iterative Smart Processing Algorithm. *Applied Mathematics and Computation* **2020**, *369*, 124839, doi:10.1016/j.amc.2019.124839.
142. El Bouny, L.; Khalil, M.; Adib, A. A Wavelet Denoising and Teager Energy Operator-Based Method for Automatic QRS Complex Detection in ECG Signal. *Circuits Syst Signal Process* **2020**, *39*, 4943–4979, doi:10.1007/s00034-020-01397-8.
143. Farashi, S. A Multiresolution Time-Dependent Entropy Method for QRS Complex Detection. *Biomedical Signal Processing and Control* **2016**, *24*, 63–71, doi:10.1016/j.bspc.2015.09.008.
144. Cuiwei Li; Chongxun Zheng; Changfeng Tai Detection of ECG Characteristic Points Using Wavelet Transforms. *IEEE Trans. Biomed. Eng.* **1995**, *42*, 21–28, doi:10.1109/10.362922.
145. Romero Legarreta, I.; Addison, P.S.; Grubb, N.; Clegg, G.R.; Robertson, C.E.; Fox, K.A.A.; Watson, J.N. R-Wave Detection Using Continuous Wavelet Modulus Maxima. In Proceedings of the Computers in Cardiology, 2003; IEEE: Thessaloniki Chalkidiki, Greece, 2003; pp. 565–568.
146. Yeh, Y.-C.; Wang, W.-J. QRS Complexes Detection for ECG Signal: The Difference Operation Method. *Computer Methods and Programs in Biomedicine* **2008**, *91*, 245–254, doi:10.1016/j.cmpb.2008.04.006.
147. Madeiro, J.P.V.; Cortez, P.C.; Marques, J.A.L.; Seisdedos, C.R.V.; Sobrinho, C.R.M.R. An Innovative Approach of QRS Segmentation Based on First-Derivative, Hilbert and Wavelet Transforms. *Medical Engineering & Physics* **2012**, *34*, 1236–1246, doi:10.1016/j.medengphy.2011.12.011.
148. Poli, R.; Cagnoni, S.; Valli, G. Genetic Design of Optimum Linear and Nonlinear QRS Detectors. *IEEE Trans. Biomed. Eng.* **1995**, *42*, 1137–1141, doi:10.1109/10.469381.
149. Chen, A.; Zhang, Y.; Zhang, M.; Liu, W.; Chang, S.; Wang, H.; He, J.; Huang, Q. A Real Time QRS Detection Algorithm Based on ET and PD Controlled Threshold Strategy. *Sensors* **2020**, *20*, 4003, doi:10.3390/s20144003.
150. Raj, S.; Ray, K.C.; Shankar, O. Development of Robust, Fast and Efficient QRS Complex Detector: A Methodological Review. *Australas Phys Eng Sci Med* **2018**, *41*, 581–600, doi:10.1007/s13246-018-0670-7.
151. Kumar, A.; Komaragiri, R.; Kumar, M. From Pacemaker to Wearable: Techniques for ECG Detection Systems. *J Med Syst* **2018**, *42*, 34, doi:10.1007/s10916-017-0886-1.
152. Pan, J.; Tompkins, W.J. A Real-Time QRS Detection Algorithm. *IEEE Transactions on Biomedical Engineering* **1985**, *BME-32*, 230–236, doi:10.1109/TBME.1985.325532.
153. Shabaan, M.; Arshid, K.; Yaqub, M.; Jinchao, F.; Zia, M.S.; Bojja, G.R.; Iftikhar, M.; Ghani, U.; Ambati, L.S.; Munir, R. Survey: Smartphone-Based Assessment of Cardiovascular Diseases Using ECG and PPG Analysis. *BMC Med Inform Decis Mak* **2020**, *20*, 177, doi:10.1186/s12911-020-01199-7.
154. Elgendi, M.; Eskofier, B.; Dokos, S.; Abbott, D. Revisiting QRS Detection Methodologies for Portable, Wearable, Battery-Operated, and Wireless ECG Systems. *PLoS One* **2014**, *9*, e84018, doi:10.1371/journal.pone.0084018.

155. Liu, F.; Liu, C.; Jiang, X.; Zhang, Z.; Zhang, Y.; Li, J.; Wei, S. Performance Analysis of Ten Common QRS Detectors on Different ECG Application Cases. *J Healthc Eng* **2018**, *2018*, 9050812, doi:10.1155/2018/9050812.
156. Kim, H.; Yazicioglu, R.F.; Merken, P.; Van Hoof, C.; Yoo, H.-J. ECG Signal Compression and Classification Algorithm with Quad Level Vector for ECG Holter System. *IEEE Trans Inf Technol Biomed* **2010**, *14*, 93–100, doi:10.1109/TITB.2009.2031638.
157. Pickus, S. Pan-Tompkins.
158. Khamis, H.; Weiss, R.; Xie, Y.; Chang, C.-W.; Lovell, N.H.; Redmond, S.J. TELE ECG Database: 250 Telehealth ECG Records (Collected Using Dry Metal Electrodes) with Annotated QRS and Artifact Masks, and MATLAB Code for the UNSW Artifact Detection and UNSW QRS Detection Algorithms 2016.
159. Robust Detection of Heart Beats in Multimodal Data: The PhysioNet/Computing in Cardiology Challenge 2014 Available online: https://archive.physionet.org/challenge/2014/ (accessed on 3 May 2022).
160. The Beth Israel Deaconess Medical Center, T.A.L. The MIT-BIH Normal Sinus Rhythm Database 1990.
161. Moody, G.B.; Mark, R.G. MIT-BIH Arrhythmia Database 1992.
162. Association for the Advancement of Medical Instrumentation: Testing and Reporting Performance Results of Cardiac Rhythm and ST Segment Measurement Algorithms 2012.
163. Khundaqji, H.; Hing, W.; Furness, J.; Climstein, M. Smart Shirts for Monitoring Physiological Parameters: Scoping Review. *JMIR Mhealth Uhealth* **2020**, *8*, doi:10.2196/18092.
164. Gualandi, I.; Marzocchi, M.; Achilli, A.; Cavedale, D.; Bonfiglio, A.; Fraboni, B. Textile Organic Electrochemical Transistors as a Platform for Wearable Biosensors. *Sci Rep* **2016**, *6*, 33637, doi:10.1038/srep33637.
165. Meaney, P.A.; Bobrow, B.J.; Mancini, M.E.; Christenson, J.; De Caen, A.R.; Bhanji, F.; Abella, B.S.; Kleinman, M.E.; Edelson, D.P.; Berg, R.A.; et al. Cardiopulmonary Resuscitation Quality: Improving Cardiac Resuscitation Outcomes Both Inside and Outside the Hospital: A Consensus Statement From the American Heart Association. *Circulation* **2013**, *128*, 417–435, doi:10.1161/CIR.0b013e31829d8654.
166. Modi, S.; Krahn, A.D. Sudden Cardiac Arrest Without Overt Heart Disease. *Circulation* **2011**, *123*, 2994–3008, doi:10.1161/CIRCULATIONAHA.110.981381.
167. Myerburg, R.J.; Kessler, K.M.; Castellanos, A. Sudden Cardiac Death: Epidemiology, Transient Risk, and Intervention Assessment. *Ann Intern Med* **1993**, *119*, 1187–1197, doi:10.7326/0003-4819-119-12-199312150-00006.
168. Myerburg, R.J.; Interian, A.; Mitrani, R.M.; Kessler, K.M.; Castellanos, A. Frequency of Sudden Cardiac Death and Profiles of Risk. *The American Journal of Cardiology* **1997**, *80*, 10F-19F, doi:10.1016/S0002-9149(97)00477-3.
169. Kannel, W.B.; Doyle, J.T.; McNamara, P.M.; Quickenton, P.; Gordon, T. Precursors of Sudden Coronary Death. Factors Related to the Incidence of Sudden Death. *Circulation* **1975**, *51*, 606–613, doi:10.1161/01.CIR.51.4.606.
170. Stecker, E.C.; Vickers, C.; Waltz, J.; Socoteanu, C.; John, B.T.; Mariani, R.; McAnulty, J.H.; Gunson, K.; Jui, J.; Chugh, S.S. Population-Based Analysis of Sudden Cardiac Death with and without Left Ventricular Systolic Dysfunction: Two-Year Findings from the Oregon Sudden Unexpected Death Study. *J Am Coll Cardiol* **2006**, *47*, 1161–1166, doi:10.1016/j.jacc.2005.11.045.
171. Chiuve, S.E.; Fung, T.T.; Rexrode, K.M.; Spiegelman, D.; Manson, J.E.; Stampfer, M.J.; Albert, C.M. Adherence to a Low-Risk, Healthy Lifestyle and Risk of Sudden Cardiac Death among Women. *JAMA* **2011**, *306*, 62–69, doi:10.1001/jama.2011.907.
172. Berdowski, J.; Berg, R.A.; Tijssen, J.G.P.; Koster, R.W. Global Incidences of Out-of-Hospital Cardiac Arrest and Survival Rates: Systematic Review of 67 Prospective Studies. *Resuscitation* **2010**, *81*, 1479–1487, doi:10.1016/j.resuscitation.2010.08.006.

173. Andersson, A.; Arctaedius, I.; Cronberg, T.; Levin, H.; Nielsen, N.; Friberg, H.; Lybeck, A. In-Hospital versus out-of-Hospital Cardiac Arrest: Characteristics and Outcomes in Patients Admitted to Intensive Care after Return of Spontaneous Circulation. *Resuscitation* **2022**, *176*, 1–8, doi:10.1016/j.resuscitation.2022.04.023.
174. Merchant, R.M.; Topjian, A.A.; Panchal, A.R.; Cheng, A.; Aziz, K.; Berg, K.M.; Lavonas, E.J.; Magid, D.J.; null, null Part 1: Executive Summary: 2020 American Heart Association Guidelines for Cardiopulmonary Resuscitation and Emergency Cardiovascular Care. *Circulation* **2020**, *142*, S337–S357, doi:10.1161/CIR.0000000000000918.
175. Ha, A.C.T.; Doumouras, B.S.; Wang, C. (Nancy); Tranmer, J.; Lee, D.S. Prediction of Sudden Cardiac Arrest in the General Population: Review of Traditional and Emerging Risk Factors. *Canadian Journal of Cardiology* **2022**, *38*, 465–478, doi:10.1016/j.cjca.2022.01.007.
176. Holmstrom, L.; Bednarski, B.; Chugh, H.; Aziz, H.; Pham, H.N.; Sargsyan, A.; Uy-Evanado, A.; Dey, D.; Salvucci, A.; Jui, J.; et al. Artificial Intelligence Model Predicts Sudden Cardiac Arrest Manifesting With Pulseless Electric Activity Versus Ventricular Fibrillation. *Circ Arrhythm Electrophysiol* **2024**, e012338, doi:10.1161/CIRCEP.123.012338.
177. Abdelghani, S.A.; Rosenthal, T.M.; Morin, D.P. Surface Electrocardiogram Predictors of Sudden Cardiac Arrest. *Ochsner J* **2016**, *16*, 280–289.
178. Goodfellow, I.; Bengio, Y.; Courville, A. *Deep Learning*; The MIT Press, 2016; ISBN 978-0-262-03561-3.
179. Kwon, J.; Lee, Y.; Lee, Y.; Lee, S.; Park, J. An Algorithm Based on Deep Learning for Predicting In-Hospital Cardiac Arrest. *Journal of the American Heart Association* **2018**, *7*, e008678, doi:10.1161/JAHA.118.008678.
180. Huang, C.H.; Su, R.; Huang, H.C.; Lin, K.; Foster, N.; Juergens, N.; Risley, J.; Haynes, K.; Obermeyer, Z. Subtyping Cardiac Arrest with ECG Waveforms: A Nightingale Open Science Dataset Available online: https://doi.org/10.48815/N5WC7D (accessed on 7 June 2023).
181. Mullainathan, S.; Obermeyer, Z. Solving Medicine's Data Bottleneck: Nightingale Open Science. *Nat Med* **2022**, *28*, 897–899, doi:10.1038/s41591-022-01804-4.
182. Carreiras, C.; Alves, A.P.; Lourenço, A.; Canento, F.; Silva, H.; Fred, A. BioSPPy - Biosignal Processing in Python 2015.
183. Abadi, M.; Agarwal, A.; Barham, P.; Brevdo, E.; Chen, Z.; Citro, C.; Corrado, G.S.; Davis, A.; Dean, J.; Devin, M.; et al. TensorFlow: Large-Scale Machine Learning on Heterogeneous Distributed Systems.
184. Selvaraju, R.R.; Cogswell, M.; Das, A.; Vedantam, R.; Parikh, D.; Batra, D. Grad-CAM: Visual Explanations from Deep Networks via Gradient-Based Localization. In Proceedings of the 2017 IEEE International Conference on Computer Vision (ICCV); October 2017; pp. 618–626.
185. Kwon, J.-M.; Kim, K.-H.; Jeon, K.-H.; Lee, S.Y.; Park, J.; Oh, B.-H. Artificial Intelligence Algorithm for Predicting Cardiac Arrest Using Electrocardiography. *Scand J Trauma Resusc Emerg Med* **2020**, *28*, 98, doi:10.1186/s13049-020-00791-0.
186. Benjamin, E.J.; Virani, S.S.; Callaway, C.W.; Chamberlain, A.M.; Chang, A.R.; Cheng, S.; Chiuve, S.E.; Cushman, M.; Delling, F.N.; Deo, R.; et al. Heart Disease and Stroke Statistics—2018 Update: A Report From the American Heart Association. *Circulation* **2018**, *137*, e67–e492, doi:10.1161/CIR.0000000000000558.
187. Chocron, R.; Jobe, J.; Guan, S.; Kim, M.; Shigemura, M.; Fahrenbruch, C.; Rea, T. Bystander Cardiopulmonary Resuscitation Quality: Potential for Improvements in Cardiac Arrest Resuscitation. *Journal of the American Heart Association* **2021**, *10*, e017930, doi:10.1161/JAHA.120.017930.
188. Steinberg, C.; Philippon, F.; Sanchez, M.; Fortier-Poisson, P.; O'Hara, G.; Molin, F.; Sarrazin, J.-F.; Nault, I.; Blier, L.; Roy, K.; et al. A Novel Wearable Device for Continuous Ambulatory ECG Recording: Proof of Concept and Assessment of Signal Quality. *Biosensors* **2019**, *9*, 17, doi:10.3390/bios9010017.

189. Cao, R.; Azimi, I.; Sarhaddi, F.; Niela-Vilen, H.; Axelin, A.; Liljeberg, P.; Rahmani, A.M. Accuracy Assessment of Oura Ring Nocturnal Heart Rate and Heart Rate Variability in Comparison With Electrocardiography in Time and Frequency Domains: Comprehensive Analysis. *J Med Internet Res* **2022**, *24*, e27487, doi:10.2196/27487.
190. Huhn, S.; Axt, M.; Gunga, H.-C.; Maggioni, M.A.; Munga, S.; Obor, D.; Sié, A.; Boudo, V.; Bunker, A.; Sauerborn, R.; et al. The Impact of Wearable Technologies in Health Research: Scoping Review. *JMIR Mhealth Uhealth* **2022**, *10*, e34384, doi:10.2196/34384.
191. Basza, M.; Krzowski, B.; Balsam, P.; Grabowski, M.; Opolski, G.; Kołtowski, L. An Apple Watch a Day Keeps the Doctor Away? *Cardiol J* **2021**, *28*, 801–803, doi:10.5603/CJ.2021.0140.
192. Taylor, J.R. An Introduction to Error Analysis: The Study of Uncertainties in Physical Measurements, Second Edition. *University Science Books*.
193. Makowski, D.; Pham, T.; Lau, Z.J.; Brammer, J.C.; Lespinasse, F.; Pham, H.; Schölzel, C.; Chen, S.H.A. NeuroKit2: A Python Toolbox for Neurophysiological Signal Processing. *Behav Res* **2021**, *53*, 1689–1696, doi:10.3758/s13428-020-01516-y.
194. Corazza, I.; Barletta, G.; Guaraldi, P.; Cecere, A.; Calandra-Buonaura, G.; Altini, E.; Zannoli, R.; Cortelli, P. A New Integrated Instrumental Approach to Autonomic Nervous System Assessment. *Comput Methods Programs Biomed* **2014**, *117*, 267–276, doi:10.1016/j.cmpb.2014.08.002.
195. Nigusse, A.B.; Mengistie, D.A.; Malengier, B.; Tseghai, G.B.; Langenhove, L.V. Wearable Smart Textiles for Long-Term Electrocardiography Monitoring—A Review. *Sensors* **2021**, *21*, 4174, doi:10.3390/s21124174.
196. Tsukada, Y.T.; Tokita, M.; Murata, H.; Hirasawa, Y.; Yodogawa, K.; Iwasaki, Y.; Asai, K.; Shimizu, W.; Kasai, N.; Nakashima, H.; et al. Validation of Wearable Textile Electrodes for ECG Monitoring. *Heart Vessels* **2019**, *34*, 1203–1211, doi:10.1007/s00380-019-01347-8.
197. Neri, L.; Oberdier, M.T.; van Abeelen, K.C.J.; Menghini, L.; Tumarkin, E.; Tripathi, H.; Jaipalli, S.; Orro, A.; Paolocci, N.; Gallelli, I.; et al. Electrocardiogram Monitoring Wearable Devices and Artificial-Intelligence-Enabled Diagnostic Capabilities: A Review. *Sensors* **2023**, *23*, 4805, doi:10.3390/s23104805.

Acknowledgement

The three years of this PhD have been an incredible adventure that completes my education and pushes me toward new goals and discoveries. I would like to show my gratitude to all the people who followed my journey, providing help, support, and encouraging me to give my best.

First my family, my father Valerio, my mother Amedea, and my brother Marco, for the infinite love, support, and patience during my studies, career, and life. Thanks to you I had all I wanted in life, and I am reaching my dreams.

The three professors that have changed my life forever:

- Romano Zannoli, for understanding my interests, and giving the spark and boost to my life dreams and career path. I worked in your lab and from there, as a domino effect, several opportunities in research and industry that reached the top with my experiences at Johns Hopkins University and the PhD. Unique in your intelligence, generosity, and empathy prototype of the Romagna's people.
- Claudio Borghi, for constantly supporting my efforts to pursue my PhD and career in research. You are the architect behind this incredible PhD experience and my previous position as adjunct professor. Your extreme positivity, compassion, mentorship, and knowledge have guided me in the last thirteen years taking me beyond my dreams.
- Henry Halperin, for giving me lifetime opportunities in your lab where I am currently working and where all research dreams come true. The most skilled and knowledgeable professor I have ever seen. A great mentor, a visionary, and a friend who has taught and is still teaching me millions of new concepts and skills that are priceless.

Matt T. Oberdier, for having always been on my side during the last three years, and you taught me everything I need to know for my PhD, how to organize, conduct, and write research. My PhD would not be possible without you. Your intelligence, patience, empathy, and calm make a great mentor, scientist, co-worker, friend, soccer and tennis player….one in a million.

Nazareno Paolocci, for being always present to help me, and support me. You connected me and Prof. Zannoli with Prof. Halperin for my first experience at Johns Hopkins, and this opportunity has totally changed my life. Generous, empathic, and creative, a great Italian professor doing top-notch science in Baltimore.

Merat Bagha, for supporting and helping me to pursue my dream to move to the USA and get my PhD, without it I would be difficult to pass all the challenges I encountered. Generous, compassionate, intelligent, and in love with life, you are the best friend I have ever had.

Ivan Corazza, for always helping me on several occasions during my experiences with Prof. Zannoli e in particular for my PhD. A passionate and meticulous and expert physicist, scientist, and professor. I really appreciated your help and friendship during my journey in research.

My co-workers at Johns Hopkins: Sandra Assaf, Ehud Schmidt, Sarah Fink, and Ryan Baumgaertner. Extraordinary colleagues and friends, my family in USA. I really love to work with you all.

All co-authors and those supported me in my research projects. Prof. Gianni Brighetti, Alessandro Orro, Prof. Marco S. Nobile, Antonio Augello, Gian Angelo Geminiani, Franco Perone, Amir Beker and Arnaldo Usai.

My professors before and during my master's degree: it is important to have exceptional mentors during the educational journey, and I had some incredible teachers, professors, and human beings.

- Middle school - Prof.ssa Castoro, who understood the potential of a middle school boy who had a dream to become an engineer.
- Secondary school - Aurelio Centritto, who saw and released my potential; Mariagrazia Frani, who made math easy and fascinating and accompanied me with love and attention for all five years and beyond.
- University: Tullio Salmon Cinotti, Giulio Cesare Barozzi, Claudio Lamberti, Leonardo Calandrino, Guido Masetti, Massimo Rudan.

All the people who helped me without asking for anything in return and in particular all my friends and loved ones that are still present and the ones that got lost during the journey.

Eventually, I want to congratulate myself. It is important to recognize my own efforts and the vision of a young me in middle school who had the courage to dream big and feel the potential that few were able to see. First an engineer then a scientist, on an incredible journey through research and new discoveries, above and beyond. You did it and you are doing it.

Sincerely,